# Blood Brain Barrier Dysfunction in Chronic Cerebral Ischemia

**Hamidreza Edrissi**

Thesis submitted to the
Faculty of Graduate and Postdoctoral Studies
in partial fulfillment of the requirements
for the Doctorate in Philosophy degree in Neuroscience

Department of Cellular and Molecular Medicine

Faculty of medicine

University of Ottawa

**Authorization**

Authorization to reuse the figures in the journal article below is granted by the Copyright Clearance Center, Rightslink, in accordance with their copyright permission policy.

Schock SC, Edrissi H, Burger D, Cadonic R, Hakim A, Thompson C. 2014. Microparticles generated during chronic cerebral ischemia deliver proapoptotic signals to cultured endothelial cells. Biochem Biophys Res Commun. 450(1):912-7.

RightsLink

Copyright Clearance Center

**Thank You For Your Order!**

Dear Hamidreza Edrissi,

Thank you for placing your order through Copyright Clearance Center's RightsLink service. Elsevier has partnered with RightsLink to license its content. This notice is a confirmation that your order was successful.

Your order details and publisher terms and conditions are available by clicking the link below:
http://s100.copyright.com/CustomerAdmin/PLF.jsp?ref=fd0435fd-8f77-4c18-9ddb-fa896f2a1806

**Order Details**
Licensee: Hamidreza Edrissi
License Date: Apr 13, 2015
License Number: 3607171078261
Publication: Biochemical and Biophysical Research Communications
Title: Microparticles generated during chronic cerebral ischemia deliver proapoptotic signals to cultured endothelial cells
Type Of Use: reuse in a thesis/dissertation
Total: 0.00 CAD

To access your account, please visit https://myaccount.copyright.com.

Please note: Online payments are charged immediately after order confirmation; invoices are issued daily and are payable immediately upon receipt.

To ensure that we are continuously improving our services, please take a moment to complete our customer satisfaction survey.

**B.1:v4.2**

**Abstract**

Cerebral small vessel pathology is now known to be associated with the development of cognitive impairment and mild motor impairments such as gait disturbance in a variety of neurodegenerative diseases. This dissertation explores the hypothesis that blood brain barrier dysfunction is an early event in cerebral ischemia and contributes to the development of cerebral small vessel disease (CSVD). A common rodent model of CSVD is permanent bilateral common carotid artery occlusion in the rat. This model was used to study several aspects of the progression of CSVD including the timecourse of blood brain barrier permeability changes following the onset of ischemia, gait disturbance, the expression of tight junction proteins and cytokine expression. It was determined that BBB permeability was elevated for 2 weeks following BCCAO and ischemic rats displayed lower gait velocity. There was no change in expression of TJ proteins. However, ischemic rats had higher levels of some proinflammatory cytokines and chemokines in brain tissue with no obvious changes in plasma levels.

The mechanisms underlying the increase in BBB permeability were studied in vitro using artificial barriers made of confluent rat brain microvascular endothelial cells. Cerebral ischemia has been reported to cause an increase in plasma toxicity, likely by elevating the numbers of circulating microparticles (MPs). MPs isolated from the plasma of ischemic rats were applied to artificial barriers where it was found that they act mainly as vectors of TNF-α signaling. MPs induce activation of caspase-3 and the Rho/Rho kinase pathways. It is concluded that most of the increase in barrier permeability is due to apoptosis and disassembly of actin cytoskeleton and disruption of adherens junctions

and not an increase in transcellular transport.

The effects of treatment with the type III phosphodiesterase inhibitor cilostazol on dye extravasation in the brain, glial activation, white matter damage and motor performance were evaluated. It was determined that cilostazol could improve the increased BBB permeability and gait disturbance and microglial activation in optic tract following BCCAO. Also, the effects of treatment with cilostazol on plasma toxicity *in vivo* (24h and 14d following BCCAO) and artificial barriers (*in vitro*) were assessed. It was found that cilostazol could reduce plasma toxicity at 24h and improve increased endothelial barrier permeability that is induced by MP treatment respectively.

In summary BBB dysfunction occurs in the rat model of chronic cerebral hypoperfusion with no differences in expression of TJ proteins. There is a mild motor disturbance in the form of lower gait velocity following BCCAO. Cytokines released in brain tissue may be associated with pathological consequences following BCCAO while there is no significant difference in plasma levels and circulating MPs may play a role in BBB dysfunction.

**Table of Contents**

**List of Tables**

**List of Figures**

**List of Abbreviations**

2VO = two vessel occlusion

ANOVA = analysis of variance

BBB = blood brain barrier

BCCAO = bilateral common carotid artery occlusion

Bcl-2 = B-cell lymphoma 2

Cav-1 = caveolin-1

CCH = chronic cerebral hypoperfusion

CP = constricted pupil

CVD = cerebrovascular disease

CSVD = cerebral small vessel disease

DP = dilated pupil

EB = Evans Blue

FITC = fluorescein isothiocynate

EMPs = endothelial microparticles

GFAP = Glial fibrillary acidic protein

hCMEC/D3 = immortalized human brain endothelial cell line

HMEC-1 = microvascular endothelial cell line 1

H/R = hypoxia/reoxygenation

HUVEC = human umbilical vein endothelial cell

ICAM-1= intracellular adhesion molecule-1

IFN-γ = interferon-gamma

INF-α = interferon alpha

LDH = lactate deyhdrogenase

ILs = Interleukins

LPS = lipopolysaccharides

MAP kinase = mitogen-activated protein kinase

MCP-1 = monocyte chemoattractant protein-1

MID = multi-infarct dementia

MIP-1α = Macrophage Inflammatory Protein-1$\alpha$

MLC = light chain myosin

MLCK = myosin light chain kinase

MMPs = metalloproteinases

MPs = microparticles

OGD = oxygen glucose deprivation

OGD/R = oxygen glucose deprivation and re-oxygenation

p-CREB = cAMP-responsive element binding protein phosphorylation

PFA = paraformaldehyde

PBS = phosphate buffer saline

PI3 kinase = phosphatidylinositol 3-kinase

PMPs = platelet MPs

PPP = platelet poor plasma

PKC = protein kinase C

PVDF = Polyvinylidene Fluoride membrane

RBMVECs = rat brain microvascular endothelial cells

ROS = reactive oxygen species

SHRSP = stroke-prone spontaneously hypertensive rat

TACE = TNF-α converting enzyme/ADAM17

*TBST* = Tris-buffered saline with Tween

TEER = transendothelial electrical resistance

TJs = Tight junctions

TNF-α = Tumor necrosis factor alpha

TNFR1= Tumor necrosis factor receptor 1

TNFR2 = Tumor necrosis factor receptor 2

TRAIL = TNF-related apoptosis-inducing ligand

TUNEL = Terminal deoxynucleotidyl transferase dUTP nick end labeling

VaD = vascular dementia

VCAM-1 = vascular cell adhesion molecule-1

VCI = vascular cognitive impairment

WMH = white matter hyperintensity

WML = white matter lesion

ZO = Zonula occludens protein

**Acknowledgements**

Undertaking this PhD has been a truly life-changing experience for me and it would not have been possible to do without the support and guidance that I received from many people.

Foremost, I would like to express my sincere gratitude to my advisors, Dr. Antoine Hakim and Dr. Charlie Thompson for the continuous support of my PhD study and research, for their patience, motivation, enthusiasm, and immense knowledge. Dr. Thompson's guidance helped me tremendously with my research and the writing of this thesis. I would like to thank you for encouraging my research and for allowing me to grow as a research scientist. Your advice on both research as well as on my career have been invaluable. You also demonstrated me what a brilliant and hard-working scientist can accomplish. I could not have imagined having a better advisor and mentor for my PhD study.

Besides my advisors, I would like to thank my committee members: Dr. Diane Lagace, Dr. Steffany Bennett and Dr. Hsiao-Huei Chen for their encouragement, insightful comments, suggestions and hard questions. I take this opportunity to express gratitude to all of the Department faculty members for their help and support.

This research was supported by funding from The Heart and Stroke foundation Center for Stroke Recovery as well as the Canadian Stroke network.

A special thanks to my family. Words cannot express how grateful I am to my mother and mother-in law for all of the sacrifices that they made on my behalf. Your prayers for me were what sustained me thus far.

Last, but not least, I would like to dedicate this thesis to my family, my beloved wife and my dear sons for their love, patience, and understanding. They allowed me to spend most of my time on my research.

# Chapter 1

# General Introduction

### 1.1. Cerebral small vessel disease

Cerebrovascular disease (CVD) is one of the causes of cognitive impairment. It often exists in conjunction with Alzheimer and other pathologies and 25–80% of elderly demented show mixed pathologies (Jellinger, 2013). CVD is considered to be the second most common cause of dementia that causes a cognitive decline in neurodegenerative dementias (O'Brien et al., 2003). Dementia following vascular disorders, later termed multi-infarct dementia (MID), post-stroke dementia or vascular dementia (VaD), is now renamed vascular cognitive impairment (VCI) or vascular cognitive disorder (VCD) (Kalaria et al., 2004; Jellinger, 2008).

Demented patients display a variety of large and small vascular lesions in the brain. These pathologies are classified as large vessel dementia or small vessel disease/microangiopathic dementia, according the size of lesions. VCI results from systemic, cardiac and local large or small vessel disease (Jellinger, 2014). Cerebral small vessel disease (CSVD) or microangiopathy of the cerebral white and central grey matter (subcortical VCI) is the most common type of VCI and is responsible for more than 40% of all cases (Bowler, 2005). CSVD may also cause behavioral, neurological and psychological symptoms and is a consequence of hypoperfusion in the perforating arteries that supply the white matter and basal nuclei, resulting in ischemia (Markus, 2008). These small perforating arteries originate from the large pial arteries at the base of the skull. They are end arteries and have few branches or anastomosing vessels with no collateral supply. They supply the brainstem, the basal ganglia and the corona radiate and the surrounding white matter but not the cortex and its U fibers. Lacunes, or microinfarcts of the central grey matter, and diffuse lesions of the subcortical and

periventricular white matter or leukoaraiosis are characteristics of the microangiopathy induced by CSVD (Schmidtke and Hüll, 2005). SVD is an important cause of stroke and increases the future risk of stroke (Wardlaw et al., 2013). Lacunar stroke accounts for a quarter of ischemic strokes, is frequently asymptomatic and can occur with an incidence of up to ten-times that of large vessel stroke (Vermeer et al., 2007). Patients with subclinical strokes have symptoms such as changes in judgment, in intellectual ability, personality change and depression (Hachinski, 2008). CSVD may result in cognitive impairment and mild motor impairments such as gait disturbance (de Laat et al., 2010).

It has been suggested that there are two types of cerebral SVD. In those with single or a few larger lacunar infarcts, in the absence of leukoaraiosis, have vessels occluded by atheromatous plaques originating in the larger intracerebral arteries and occluding the origins of the perforating vessels, or the proximal regions of perforating arteries. The second type features multiple smaller lacunar infarcts and leukoaraiosis resulting from a diffuse arteriopathy affecting smaller perforating arteries (Fisher, 1968; Boiten et al., 1993; Lammie, 2000; Khan et al., 2007). There are significant risk factor differences between the two subtypes of SVD, suggesting that they represent different pathologies. Khan et al., (2007) have shown that age and hypertension were associated with smaller lacunar infarcts with leukoaraiosis, while hypercholesterolemia, diabetes and myocardial infarction were linked to larger lacunar subtype without leukoaraiosis.

Three vascular lesions have been described in CSVD including arteriosclerosis, lipohyalinosis and small vessel atherosclerosis (Fisher, 1968; Lammie, 2002). Arteriolosclerosis is featured by smooth muscle loss and collagenization of small arteries and arterioles (approximately 40–150 μm outer diameter) (Lammie, 2002). The larger-

diameter vessels are affected by lipohyalinosis (40–300 μm) and small vessel atherosclerosis (200–800 μm) (Lammie, 2002).

Arteriolosclerosis or hyaline arteriolosclerosis is the most common form of SVD and is associated with aging, hypertension and diabetes (Lammie, 2002; Pantoni, 2010). Arteriosclerosis has also referred to simple small vessel disease and associated with lacunar infarcts and the diffuse radiological changes in white matter known as leukoaraiosis (Lammie, 2002; Pantoni, 2010). In histology, this form of CSVD is characterized by wall thickening, collagen deposition, degeneration of smooth muscle cells and narrowing of lumen. It is often associated with localized BBB dysfunction (Lammie, 2002, Jellinger, 2008). The histological changes associated with leukoaraiosis are localized edema, damage to axons, myelin, and oligodendrocytes, and local activation of astrocytes and microglia (Fernando et al, 2006; Jellinger, 2008). Arteriosclerosis has been considered as the vascular contributor to cognitive impairment, gait disturbance and dementia (Gorelick et al., 2011, Smallwood et al., 2012).

Recent studies have greatly improved the understanding of the pathogenesis of CSVD, although many questions remain, such as how the proposed mechanisms are exactly involved in the induction of the disease. Acute, focal ischemia resulting from the occlusion of a single perforating artery results in lacunar infarction, while more chronic ischemia results in leukoaraiosis or white matter damage. Hypoperfusion affecting multiple arteries simultaneously causes the borderzone between two or more arteries to become chronically ischemic (Chui, 2007). Pantoni and Garcia (1997) have proposed that an initial step in the pathogenesis of CSVD might involve a failure of the arteriolar endothelium due to partial ischemia. The endothelium plays a crucial role in processes

such as the autoregulation of blood flow, reactive hyperemia and the formation and function of the blood-brain barrier. It has been proposed that endothelial dysfunction could cause the pathological symptoms of CSVD in two ways. The reduction in baseline cerebral blood flow and impaired autoregulation predispose small regions of the brain parenchyma served by single vessels to become ischemic (O'Sullivan et al, 2002; Farkas et al, 2006). Secondly, an increase in blood–brain barrier (BBB) permeability may result in leakage of plasma components into the vessel wall and brain parenchyma, causing inflammation, thickening of the vessel wall and a further reduction in blood flow and lesions in the parenchyma (Wardlaw, 2005; Wardlaw *et al.,* 2003, 2008, 2009).

### 1.2. Blood Brain barrier

The blood brain barrier (BBB) is composed of vascular endothelial cells and pericytes, which are surrounded by basal lamina and astrocytic end feet. Fluid and molecules move across this barrier either via a transcellular or a paracellular pathway. An example of transcellular pathway is the transport of plasma proteins such as albumin by caveolae and vesiculo-vascular organelles (Shen et al., 2009). Endothelial caveolae are membrane-bound vesicles that may shuttle between the luminal and abluminal surfaces of the endothelial cells to mediate transcytosis of proteins (Nag et al., 2011). Caveolin-1 (cav-1) is an integral caveolar membrane protein and an increase in the expression of cav-1 has been reported to accompany BBB breakdown in arterioles and veins (Nag et al., 2007). Knockout of the cav-1 gene results in defects in the uptake and transport of albumin in cav-1 gene knock-out mice (Schubert et al., 2001).

The paracellular pathway is responsible for the transport of small molecules and plasma fluids, and occurs through the junctions proteins. Endothelial cells have two junctional regions that include adherens junctions (AJs) and tight junctions (TJs) (Dejana et al., 2009). Tight junctions between endothelial cells are formed by the interaction between the transmembrane proteins claudins, occludins, and junctional adhesion molecules on adjacent endothelial cells. Zonula occludens proteins (ZO-1, ZO-2, and ZO-3) are intracellular anchoring proteins, which connect transmembrane proteins of tight junction to the actin cytoskeleton. Alterations in the phosphorylation state of some of these proteins are known to regulate their function (Stamatovic et al., 2006). AJs include cadherins (VE-cadherin and N-cadherins) which directly bind to β-catenin, and plakoglobin (Dejana et al., 2009).

The interendothelial junctions are responsible for paracellular permeability of the BBB, which is the product of a balance between the contractile force generated by the endothelial cytoskeleton and the adhesive force produced at endothelial cell-cell junctions and cell-matrix contacts (Yu et al, 2012). An imbalance between these forces by proinflammatory stimuli such as histamine, cytokines and reactive oxygen species causes alterations in paracellular permeability by inducing endothelial cell retraction (Abbott, 2000).

Some evidence indicates the important role of endothelial cell contractility in controlling microvascular permeability (Yuan, 2002). The contractility of endothelial cells is mainly through mechanical interaction between actin and myosin, and myosin activity is controlled through phosphorylation of regulatory myosin light chain (MLC) by myosin light chain kinase (MLCK, Shen et al., 2009). Phosphorylation of MLC leads to

a change in the myosin structure and its interaction with actin. The Rho family of small GTPases, especially RhoA and its downstream kinase ROCK can phosphorylate and inactivate MLC phosphatase, which promotes MLC phosphorylation and actomyosin contraction. ROCK can also enhance cell contractility directly by phosphorylation of MLC or indirectly by activating the MLCK (Totsukawa et al., 2000). It has been shown that hypoxia induced BBB disruption was prevented by inhibition of the MLCK (Kuhlmann et al., 2007). Also, several proinflammatory agents, such as thrombin, histamine, cytokines and oxygen radicals activate MLCK and RhoA/Rho kinase, and increase contractility and paracellular permeability of endothelial cells (Stamatovic et al., 2006).

Several kinases have been reported to modulate TJ protein phosphorylation and endothelial permeability such as protein kinase C (PKC; particularly PKCα and PKCβ), phosphatidylinositol 3-kinase, mitogen-activated protein kinases, and the nonreceptor tyrosine kinase Src family members (c-Src, Lyn, Fyn). These kinases can act as regulators of endothelial paracellular permeability (Stamatovic et al., 2006). It has been shown that PKC can induce MLC phosphorylation, which results in endothelial cytoskeleton contraction (Garcia et al., 1995).

Another element that contributes in BBB structure is basal lamina. The basal lamina is a part of the extracellular matrix that connects the endothelial cells to the adjacent cell layers and the smooth muscle layer of the media. The basal lamina loses its integrity early following ischemia by rapid degradation of laminin, fibronectin, and collagen type IV, the three main components of the basal lamina (Hamann et al., 1995; Hamann et al., 2002).

The matrix metalloproteinases (MMPs) are matrix-degrading enzymes that are involved in the disruption of the matrix of the basal lamina. They can degrade most of the extracellular matrix components including fibronectin, laminin, proteoglycans and type IV collagen (Yong et al., 2001; Rosenberg, 2002). They also play a role in disrupting the BBB by degradation of TJ proteins in neuroinflammatory conditions. MMPs are able to process other proMMPs and molecules including proforms of cytokines such as TNF-α and IL-1β (Cauwe et al., 2007). A large quantity of MMP-2 is present in the normal brain and is found in astrocytes and cerebrospinal fluid (CSF) (Candelario-Jalil et al., 2009). Increased expression and activity of MMP-2 following hypoxia/ischemia may disrupt basal lamina and tight junctions between ECs leading to BBB disruption. It has been shown that MMPs disrupt the basal lamina and degrade TJPs (occludin and claudin-5) after reperfusion in focal ischemia induced by middle cerebral artery occlusion (Yang et al, 2007). Endothelial cells contain MMP-9. MMP-3 and -9 are expressed in pericytes and MMP-2 and MT1-MMP are present in the astrocytic end feet surrounding the endothelial cells. Myelin is degraded by MMPs and MMP-2 can degrade myelin basic protein with more potency than MMP-9 (Chandler et al, 1995). Brain autopsy of vascular dementia cases indicates increased expression of MMP-2 in reactive astrocytes and MMP-3 in macrophages around blood vessels in demyelinated regions, and the presence of MMP-2 in white matter was suggested as a possible cause of BBB damage (Rosenberg et al, 2001). Regarding these facts, MMPs tend to have important roles in modulation of BBB during acute and chronic cerebral ischemia.

### 1.3. Cytokines

Cytokines are a group of proteins with low molecular weight (8–80 kDa) that regulate inflammatory processes and induce BBB leakage. The level of cytokines is very low in brain under physiological conditions (Angelopoulos et al., 2008). Cytokines have been classified as either pro-inflammatory agents such as tumor necrosis factor (TNF-α), IL-1β and IL-6 or anti-inflammatory agents such as interleukin-1 receptor antagonist (IL-1ra), IL-10 and transforming growth factor (TGF-β) (Johnston and Webster, 2009).

Ischemic brain damage is associated with inflammatory processes following activation of brain resident cells such as microglia localized within the ischemic region, and the rapid synthesis of cytokines (Zhu et al., 2006). Some evidence shows that the immune system contributes to the development and progression of CSVD. High serum levels of CRP, IL-6 (Hoshi et al., 2005) and TNF-α have been associated with lacunar stroke (Nakase et al., 2008) and the existence and progression of white matter damage (van Dijk et al., 2005). A recent experimental study has revealed the relevance of immune responses for the initiation and progression of CSVD as spontaneously hypertensive rats (SHR) had lower levels of IL-10 in the cerebrospinal fluid (Kaiser et al., 2014). In addition, it has been shown that some of the cytokines can increase BBB permeability by affecting TJs and the actin cytoskeleton and inducing MMPs production (Ahdieh et al., 2001, Oshima et al., 2001; Castillo and Rodríguez, 2004). Therefore, cytokines/ chemokines can induce direct effects on endothelial regulation of BBB components, as well as indirect effects through cytokine/chemokine-dependent immune system mediated injury.

### 1.4. Microparticles

Microparticles are another factor that may affect the blood brain barrier. MPs are small vesicles, 0.1 to 1.0 μm in size that bud off from plasma membrane of various cell types in response to shear stress, physiological agonists, and pro-apoptotic stimulation (Lovren and Verma, 2013). MPs may also be released spontaneously from cells under basal condition (Italiano et al., 2010). MPs contain membrane and cytoplasmic proteins of their cell of origin and their composition may depend on stimuli that lead to their generation. MPs transfer information from the cell of origin to target cells by cell-to-cell contact or through secretion of soluble mediators (Mause and Weber, 2010). It has been supposed that MPs play a role in pathogenesis of cerebral malaria and multiple sclerosis through induction of brain endothelial dysfunction and alterations in BBB permeability (Combes et al., 2006; Minagar and Alexander, 2003).

### 1.5. Rodent model of CSVD

Different pathological lesions are seen in CSVD including small vessel arteriopathy, white matter hyperintensities (leukoaraiosis), lacunar infarction and microbleeds. Therefore, animal models of SVD should be similar to these key features: (1) small, discrete infarcts; (2) small vessel arteriopathy; (3) diffuse white matter damage; (4) cognitive impairment. No model can represent all aspects of the disease. Experimental species that have been widely used are mice and rats. Hainsworth and Markus (2008) have identified 15 models that reflect different aspects of CSVD including embolic injuries (injected blood clot, photochemical, detergent-evoked), hypoperfusion/ischemic injury (bilateral common carotid occlusion/stenosis, striatal

endothelin-1 injection, striatal mitotoxin 3-NPA), hypertension-based injuries (surgical narrowing of the aorta, or genetic mutations, usually in the renin-angiotensin system) and blood vessel damage (injected proteases, endothelium targeting viral infection, or genetic mutations affecting vessel walls). In these models animals either reflect the arterial lesions of SVD or mimic the brain injury (leukoaraiosis, lacunar infarction).

Using experimental animals one can study pathological processes relevant to CSVD such as arterial fibrohyaline thickening, white matter ischemia and blood brain barrier dysfunction. Among the mentioned models stroke-prone spontaneously hypertensive rats (SHRSP) have the most features that resemble human CSVD although leukoariosis-like white matter changes have not determined untill 5-8 months of age (Maguire et al., 2004; Schreiber et al., 2012). In addition, these rats displayed local BBB breakdown that was determined with MRI (Lee et al., 2007). Another popular model of CSVD is Notch3 transgenic mice that mimic CADASIL. CADASIL (Cerebral Autosomal-Dominant Arteriopathy with Subcortical Infarcts and Leukoencephalopathy) is the most common form of monogenic stroke disorder in human which resembles age-related sporadic SVD but is earlier in onset and less hypertension-dependent than sporadic SVD (Chabriat et al., 2009). Although Notch3R169C mice develop diffuse white matter lesions in corpus callosum, internal capsule and striatal white matter bundles, no change in BBB function was detected (Joutel et al., 2010). Therefore, to study BBB dysfunction in white matter lesions a hypoperfusion model should be used. The animal model that is used in this study is permanent bilateral common carotid occlusion (BCCAO) or 2 vessel occlusion (2VO). This is the most widely used model for the study of vascular cognitive impairment (Jiwa et al., 2010). BCCAO in rats induces a

chronic reduction in cerebral blood flow by 50% to 70% in forebrain that lasts 8 weeks to 3 months after surgery (Ohta et al., 1997; Ueno et al., 2002; Farkas et al., 2007). Lesions are mainly in white matter (WM), and are characterized by vacuolation of myelin, axonal damage, and demyelination in corpus callosum, internal capsule, and caudate putamen. WM Lesions appear 7 days after occlusion and are persistent (Wakita et al., 1995, 2002; Farkas et al., 2004), and are preceded by temporary BBB opening in white matter areas with collagen deposition in vessel walls (Ueno et al., 2002). Permanent BCCAO in rats does not induce focal infarcts because of presence of a complete circle of Willis, which allows the frontal part of the brain receives blood supply by way of the vertebral and spinal arteries through compensatory mechanisms. These compensatory mechanisms include enlargement of the arteries at the base of the brain (basilar artery, posterior cerebral artery, posterior communicating artery, Choy et al, 2006). Collagen fibrils proliferated in the thickened basal lamina on days 7 and 14 can be detected with electron microscopy (Ueno et al., 2002). Collagen deposition resembles collagenization of small arteries and arterioles that have been observed in arteriosclerosis, one of distinctive vascular lesions in human CSVD. Behavioral disturbances such as cognitive and memory impairments that are demonstrated in these rats permit us to estimate the effect of chronic cerebral hypoperfusion (Farkas et al., 2007). In our opinion permanent BCCCAO in rat mimics chronic hypoperfusion of small vessel disease and arteriosclerosis. Although there are no multiple, small infarcts, there are diffuse white matter changes and temporary BBB opening within white matter areas. Therefore, permanent BCCAO appears to be an appropriate model to study the role of BBB dysfunction in pathogenesis of CSVD.

### 1.6. Objectives

The main hypothesis of this study is that early dysfunction in BBB is involved in pathogenesis of CSVD and protection of BBB will improve the outcome. A rodent model of CSVD, permanent BCCAO, was used to assess BBB permeability and describe the pathological consequences is this setting of chronic cerebral hypoperfusion. Proof that blood brain barrier dysfunction contributes to the progression of CSVD could provide a target for new therapeutic interventions to reduce the impact of disease on the brain and to improve outcome.

The specific objectives are:

1) To characterize the extent and time course of change in BBB permeability following BCCAO;

2) To assess motor impairment, specifically through examination of gait disturbance at different time points following BCCAO;

3) To evaluate the role of transcellular and paracellular endothelial pathways in BBB disruption following BCCAO. Specifically, the expression of junctional proteins involved in paracellular transport, caveolar proteins involved in transcellular transport, basal laminar proteins and mediators involved in BBB alteration are examined;

4) To assess if potential factors such as cytokines and circulating MPs are involved in BBB permeability alteration;

(a) To assess cytokine expression in plasma and brain tissue of rats receiving BCCAO at different time points;

(b) To determine the role of circulating MPs in BBB dysfunction following BCCAO using an *in vitro* model of BBB and to explore the signaling pathways involved in this process;

(c) To evaluate the effect of cilostazol, a type III phosphodiesterase inhibitor in the BCCAO model to determine if it can protect the BBB against ischemic injury *in vivo*, alter plasma toxicity (as a marker of MPs number) or change BBB permeability induced by MPs *in vitro*.

# Chapter 2

## Impact of BCCAO on BBB permeability, TJs and motor performance

**Collaborator Contribution**

**Hamidreza Edrissi: S**urgeries, Evans Blue quantification, Western blot and immunohistochemistry were performed by author under supervision of Dr. Antoine Hakim and Dr. Charlie Thomson.

**Sarah C. Schock:** Dr. Sarah Schock helped with Evans Blue quantification.

**Robert Cadonic:** The tapered beam test was performed by Robert Cadonic (research technician).

**Antione M Hakim:** Dr. Antoine Hakim supervised the work and provided financial support.

**Charlie S. Thompson:** Dr. Charlie Thompson helped in collecting tissue and immunohistochemistry and supervised the project.

**Abstract**

Blood brain barrier dysfunction has been proposed as a mechanism in the progression cerebral small vessel disease. Some patients with CSVD have mild motor impairments such as gait disturbance. BCCAO in rats that induces a chronic cerebral hypoperfusion is a rodent model commonly used to study some aspects of CSVD. It was determined that BBB permeability increased following BCCAO through measurement of Evans Blue dye extravasation in brain tissue at different time points. Rats subjected to BCCAO were examined for gait disturbance using a tapered beam test. It was determined that ischemic rats needed more time to cross the beam. TJs are the main component of BBB and are responsible for paracellular transport. Cavolin-1 is a caveolar protein involved in transcellular transport of specific plasma proteins such as albumin. The expression TJs and caveolin-1 in brain tissue was measured. The results indicated that expression of TJ proteins was not changed following BCCAO, while MMP-2 was up-regulated, suggesting the contribution of MMPs in BBB enhancement following BCCAO. It is concluded that BCCAO induces an increase in permeability of the BBB and gait velocity impairements that is associated with increased MMP-2 expression and no change in TJ proteins expression.

## Introduction

BBB damage has been associated with the pathogenesis of cerebrovascular white matter lesions that is responsible for cognitive impairment in the elderly (Akiguchi et al., 1998) and dysregulation of the blood brain barrier (BBB) has been proposed as a mechanism in the etiology of cerebral small vessel disease (Wardlaw et al., 2003, Wardlaw et al., 2013). White matter lesions can be induced by permanent ligation of the bilateral common carotid arteries in the rat (Farkas et al., 2004).

Endothelial TJ proteins are a main component of BBB that are responsible for paracellular permeability. Disruption of TJ proteins has been reported during ischemia/hypoxia in endothelial cell cultures and in situ models of BBB (Mark and Davis, 2002; Witt et al., 2003). MMPs affect permeability of BBB by alteration of TJ proteins as well as basal lamina proteins in focal ischemia (Asahi et al., 2001; Fukuda et al., 2004). A selective increase in permeability of blood proteins such as albumin under hypoxic condition (Plateel et al., 1997) also indicates the importance of the transendothelial route in BBB permeability. The etiology of BBB dysfunction in chronic cerebral hypoxia is not fully understood. Multiple mechanisms leading to the BBB disruption following brain ischemia have been suggested, including transendothelial passage of selective blood proteins, disruption of basal lamina by MMPs and degradation or phosphorylation of TJs.

Motor disturbances are a common problem in the elderly and some patients with cerebral small vessel disease (CSVD) have a gait disturbance (de Laat et al., 2010). Disruption of white matter tracts connecting important motor regions by white matter lesions and lacunar infarcts are considered as the mechanism of gait disturbance (Chui,

2007). WM lesions in certain brain regions such as periventricular frontal lobe were related to lower gait velocity, shorter stride length and broader stride width in patients with small vessel disease without dementia or Parkinsonism (de Laat et al., 2011). Loss of white matter integrity was related to gait disturbances. Also, a study on cognitively intact individuals has shown that an increase in periventricular (PV) white matter hyperintensity (WMH) was associated with decreased gait performance (increased time and number of steps to walk 30 feet) over time (Silbert et al., 2008).

The objectives of this study were to: 1) assess the extent and duration of changes in BBB permeability; 2) evaluate the role of transcellular and paracellular endothelial pathways in increased permeability of BBB by assessment of caveolin-1, TJs, basal lamina proteins and MMP expression; 3) determine gait and motor impairment following permanent BCCAO in rats.

**Materials and Methods**

*Animals and Surgical Procedure* - All experiments conformed to the guidelines set forth by the Canadian Council for the Use and Care of Animals in Research (CCAC) with approval from the Ottawa Health Research Institute Animal Care Facility. Male Long Evans rats weighing 200-225g (Charles River) received sham or 2VO (two vessel occlusion) surgery and survived for 24h, 72h, 7d, 14d and 28 d. A group of rats did not receive surgery was designated as un-operated control. The rats were anesthetized with 2.5% isoflurane in 30% $O_2$/70% $N_2O$ through a face mask. Following a midline cervical incision, the bilateral common carotid arteries were isolated from adjacent vagus nerves and ligated with silk sutures. The sham-operated animals were treated in a manner

similar to the operated ones, except that the common carotid arteries were not occluded. The skin incision was sutured with 3-0 Nylon Monofilament suture (Ethicon) and each rat received injectable Tylenol 200 mg/kg subcutaneous and 0.1 mL of 0.5 % Bupivicaine Sterile Gel over the incision site. Rats were kept in their quarters with food and water available ad libitum and euthanized on days 1, 3, 7, 14 and 28 following surgery for assessment of BBB permeability following BCCAO.

For evaluation of the expression of TJ proteins following BCCAO two groups of male Long Evans rats (200-225g) received sham or 2VO surgery and were euthanized 72 hours later. Following transcardial perfusion with saline the forebrain was excised and frozen in liquid nitrogen for western blot analysis (n = 3). A number of rats from each group was perfused with 4% paraformaldehyde (PFA) for immunohistochemical studies and stored at 4ºC.

*Evans Blue quantification* - To assess BBB permeability rats were injected with a 2% solution of Evans Blue (EB, 4 ml/kg, femoral vein, Sigma-Aldrich) 1 hour before transcardial perfusion with saline. Using a rat brain matrix a coronal slice was made at the level of optic chiasma and the entire anterior portion of brain was frozen in liquid nitrogen and stored in -80 °C for dye extraction. Brain samples were weighted and placed in 50% trichloroacetic acid solution. After homogenization with a sonicator, samples were centrifuged at 16000 g for 20 minutes at 4ºC. Following the extracted dye dilution with ethanol (1:3) its fluorescence was determined (excitation at 620 nm and emission at 680 nm) by microplate spectrophotometer (Synergy $H_1$, BioTek). Calculations were based on external standards in the same solvent plus albumin (25-3000 ng/ml). The amount of EB dye in the brain tissue was quantified from a linear standard

curve derived from known amounts of the dye and was expressed as μg per gram of tissue.

*Western blot* - Using a rat brain matrix a coronal slice was made at the level of optic chiasma and the entire anterior portion of brain was frozen in liquid nitrogen and stored in -80 °C. Protein samples were extracted by RIPA buffer (Zigma) with protease inhibitor cocktail (Roche). Samples were further centrifuged at 13000 RPM at 4ºC for 10 minutes and the supernatants were collected. Protein concentration was measured using Bio-Rad protein assay solution. Equal amounts of protein (30μl) were then loaded on 4-20% Tris-HCL precast gels (Bio-Rad) for electrophoresis at 100V for 75-90 minutes. After electrophoresis, proteins from gels were transferred to a Polyvinylidene Fluoride (PVDF) membrane, blocked in TBST containing 5% milk and 0.5% Tween-20 for 1 hour and incubated overnight at 4ºC with primary antibodies. The membranes were washed the day after with TBST and incubated with the respective secondary antibodies for 1 hour at room temperature. Blots were developed using Chemiluminescence Reagent Kit (Millipore) and protein bands were visualized on X-ray film. Films were scanned and the proteins were quantified using ImageJ (NIH) software. The primary antibodies used include MMP-2 (1:200; Santa Cruz), MMP-9 (1:250; abcam), claudin-5 (1:50; Santa Cruz), occludin (1μg/ml; Zymed), ZO-1(1μg/ml; Zymed), VE-cadherin (1:200; Santa Cruz), GFAP (1: 2000; Sigma), caveolin-1 (1:200; Santa Cruz).

*Immunofluorescence* - For assessment of BBB permeability following BCCAO, 2% EB was injected in sham and 2VO treated rats by the femoral vein at 72h following surgery, 1h before transcardial perfusion. Brains were removed and rapidly frozen in isopentane at -70ºC. Frozen brains were cut into 20 μm thick sections on a cryostat and

mounted for fluorescent microscopy (Carl Zeiss Inc., Germany). EB Leakage was examined by fluorescent microscope in the sections.

For evaluation of the expression TJ proteins following BCCAO the fixed brains were cryoprotected in 20% sucrose in PBS and left at 4ºC for 48 hours, frozen and stored at -80ºC. Frozen brains were cut into 12 μm thick coronal sections using a cryostat (CM1850, Leica Microsystems). Sections were rinsed in PBS and nonspecific binding sites were blocked by preincubating tissue for 30 minutes at room temperature in PBS containing 10% Triton-X-100 and 5% donkey serum. Brain sections were then incubated at 4ºC overnight with primary antibodies including collagen IV (1:200, abcam), GFAP (1: 200; Sigma), MMP-2 (1:200; Santa Cruze), in PBS, 10% Triton-X-100, and 1% donkey serum. The slides were then rinsed with PBS and incubated with secondary antibodies including donkey anti-mouse or anti rabbit CY3 (red), and donkey anti-rabbit fluorescein isothiocynate (FITC, green) for 3 hours at room temperature. Sections were rinsed 3 times (incubated with DAPI during first rinse for 5 minutes) and mounted in antifade. Slides were photographed with a Zeiss META510 laser scanning confocal microscope. Sections were incubated in the absence of primary antibody and were not immunofluorescent.

*Tapered beam test* - Three groups of male Long Evans rats (200-225g) were trained (5 trials per day for 3 days) to traverse a ledged tapered beam before receiving 2VO or sham surgery (n = 5). One group did not received surgery (un-operated control, n = 3). The beam was 1.65 m in length, tapering from 6 cm to 1.5 cm in width with a ledge beneath the beam extending. If one foot slipped off the beam and landed on the ledge, it was counted as a foot fault. To test the rats, the time to traverse the beam and the number

of foot faults were recorded for 5 consecutive trials. The pre-surgery test was performed a day before surgery. The trial tests were performed on 1, 2, 3 and 4 weeks after surgery.

*Statistical analyses* - Statistical analyses were performed using SPSS 21 and graphs were made by Graph Pad Prism 3 software. Data obtained from BBB permeability experiments were analyzed with two-way ANOVA and data obtained from tapered beam test were analyzed with two-way ANOVA repeated measures. ANOVA tests were followed by a Bonferroni post hoc test and presented as means ± standard error. Probability (P) values of less than 0.05 were considered significant. Stars in graphs refer to significances that were determined in post hoc tests following ANOVA throughout the thesis. Data obtained from the expression of TJ proteins study were analyzed with a t-test.

**Results**

There was a significant difference in dye extravasation between the groups of rats that received 2VO or sham surgery after operation, group effect: $F(1, 50) = 38.58$ ($P < 0.0001$), time effect: $F(4, 50) = 4.48$ ($P < 0.01$) with no interaction. Post hoc results showed that 2VO rats have a significant increase in dye extravasation that began as early as 24hr and lasted up to 2 weeks post surgery. There was no difference between sham and 2VO groups at 28 d after surgery. There was also no difference between unoperated control and sham groups (Figure 2.1A). EB leakage appeared as a red fluorescence in brain sections obtained 3 days after surgery, which was more prominent in 2VO treated group than sham group ($n = 3$, Figure 2.1B).

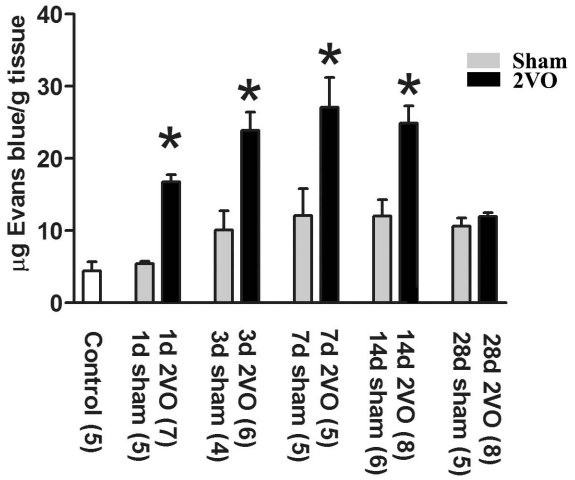


**Figure 2.1A**

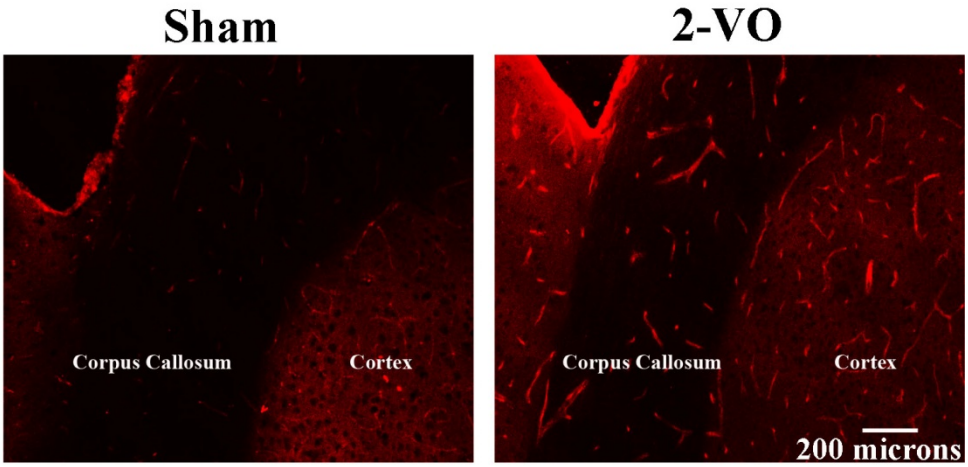


**Figure 2.1B**

**Figure 2.1. Evans Blue dye extravasation following BCCAO. (A)** Bilateral common carotid artery occlusion causes more Evans Blue dye extravasation in the brain for up to 14 days following surgery (control: un-operated rats). **(B)** EB leakage appears as a red fluorescence in brain sections 3 days following surgery, which is more prominent in 2VO rat brains than sham operated animals. Each representative figure is derived from three rat brains of each group (n = 3).

There was no significant difference in expression of tight junction proteins, occludin and ZO-1 at 72 h following BCCAO (Figure 2.2A and B). Also, there was no change in expression of caveolin-1 between the groups (Figure 2.3).

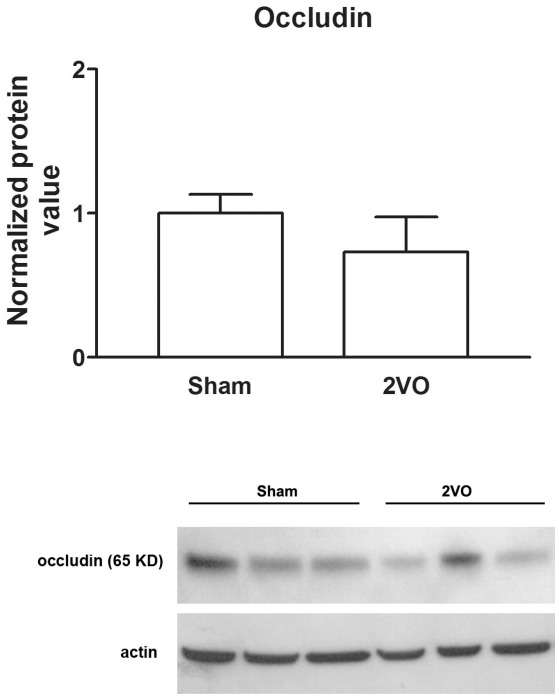


**Figure 2.2A**

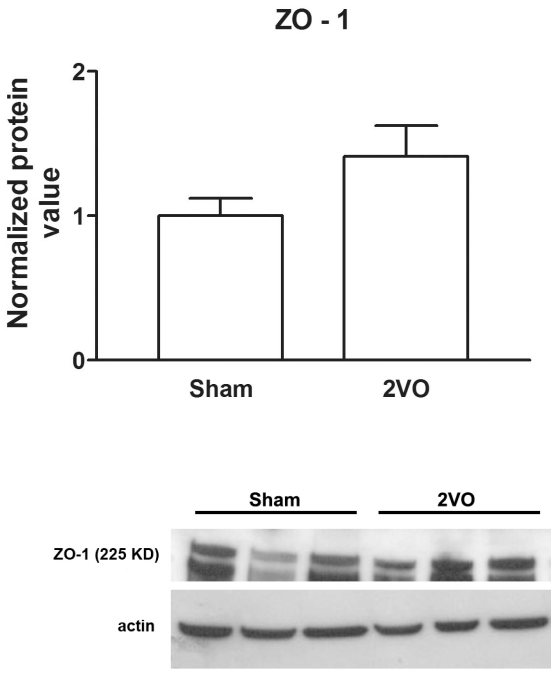


**Figure 2.2B**

**Figure 2.2. Expression of TJ proteins following BCCAO. (A)** There is no change in expression of occludin at 72h following BCCAO **(B)** The expression of ZO-1 does not change at 72h following BCCAO (n = 3).

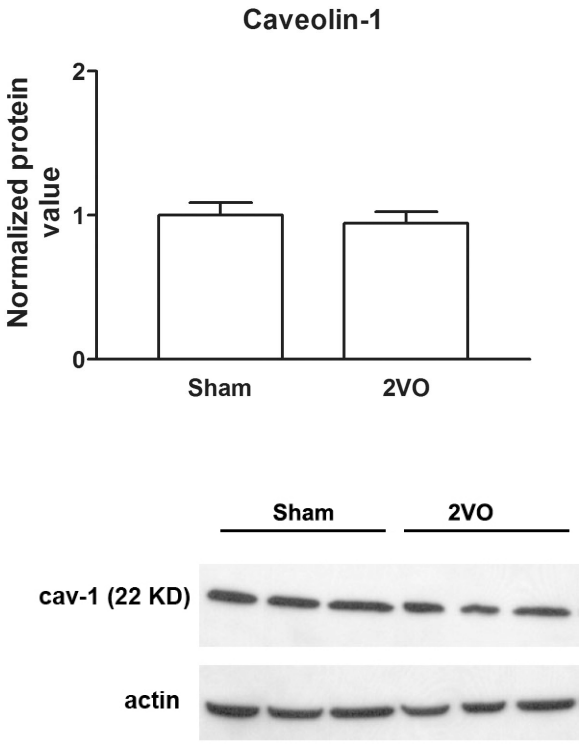
Caveolin-1
Normalized protein value
2
1
0
Sham
2VO
Sham
2VO
cav-1 (22 KD)
actin

**Figure 2.3**

**Figure 2.3. Expression of caveolin-1 following BCCAO.** There is no change in expression of caveolin-1 at 72h following BCCAO (n = 3).

The level of the pro- (72 KD) and activated (63 KD) forms of MMP-2 protein was significantly higher in 2VO group than sham group (Figure 2.4A). However, MMP-9 protein expression did not change significantly following BCCAO (Figure 2.4B). The protein level of GFAP was higher in 2VO group than sham group (Figure 2.5).

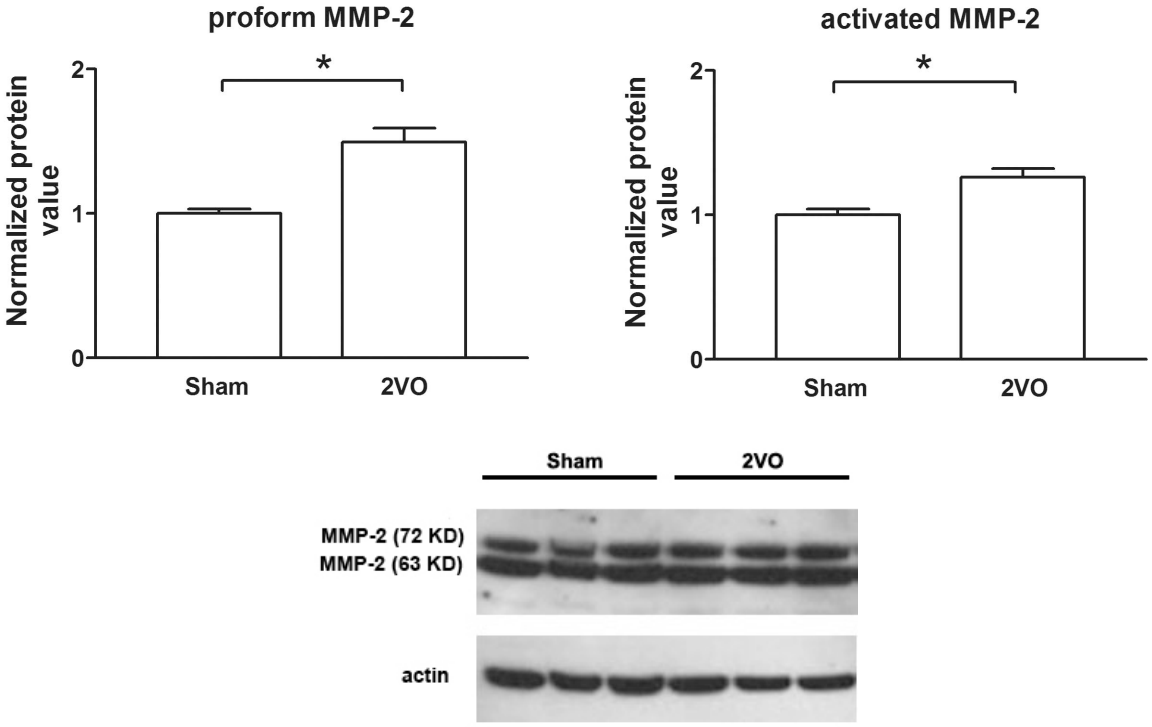


**Figure 2.4A**

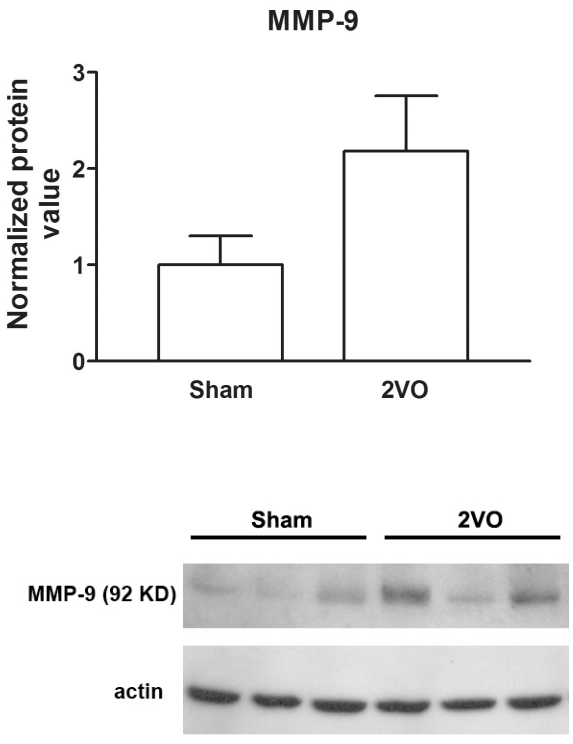


**Figure 2.4B**

**Figure 2.4. Metalloproteinases (MMPs) expression following BCCAO. (A)** Expression of the pro- and activated forms of MMP-2 are increased at 72h following BCCAO. There is a significant difference between sham and 2VO group (n = 3). **(B)** There is no significant change in MMP-9 expression following BCCAO (n = 3).

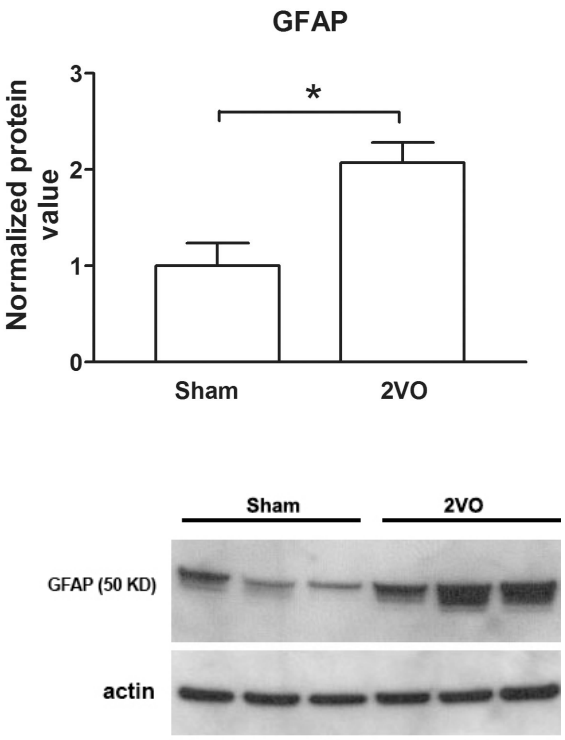
GFAP
Normalized protein value
3
2
1
0
*
Sham
2VO
Sham
2VO
GFAP (50 KD)
actin

**Figure 2.5**

**Figure 2.5. Glial fibrillary acidic protein (GFAP) expression following BCCAO.** Expression of GFAP is significantly higher in 2VO group than sham group (n = 3).

Increased expression of MMP-2 and GFAP was observed in the corpus callosum adjacent to lateral ventricles and cortex (n = 3, Figure 2.6A), which confirmed the results of quantification of these proteins by western blotting. However, there was no difference between the groups in expression of collagen IV, a basal laminar protein (n = 3, Figure 2.6B).

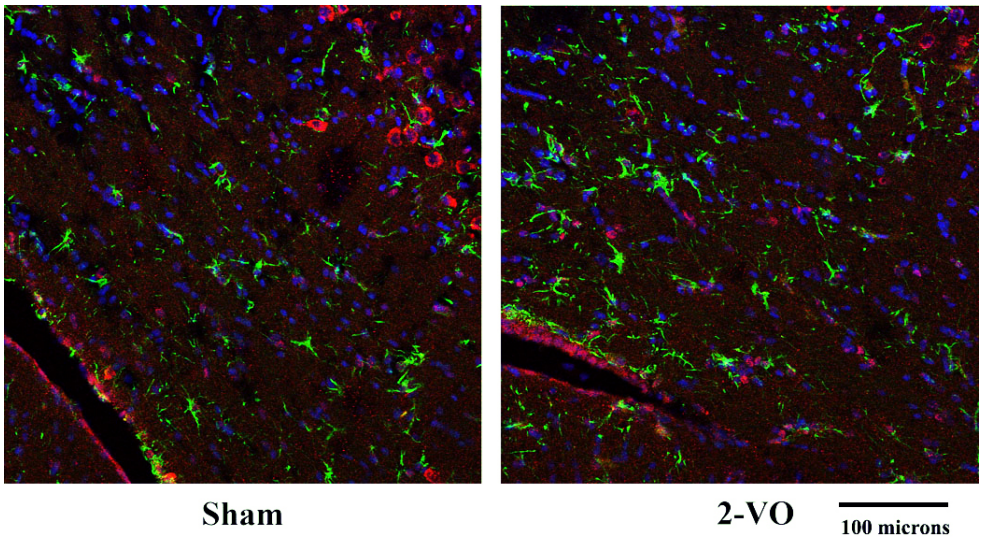


**Figure 2.6A**

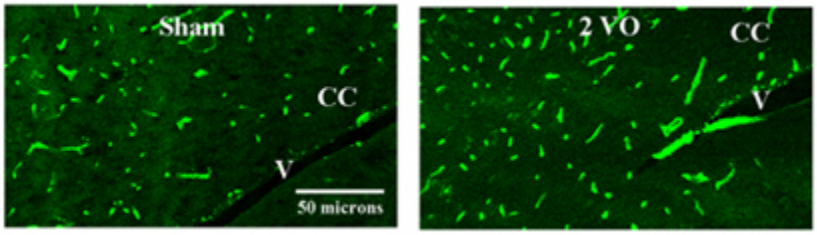


**Figure 2.6B**

**Figure 2.6. Immunological finding. (A)** Fluorescent staining of MMP-2 (red) and GFAP (green) in corpus callosum and cortex indicates increased immunoreactivity of MMP-2 and GFAP in 2VO group at 3 days following BCCAO (blue: DAPI, n = 3, scale bar = 100 μm). **(B)** Fluorescent staining of collagen IV (green) in corpus callosum does not detect any significant difference between the groups at 3 days following BCCAO. Each representative figure is derived from three rat brains of each group (n = 3, CC=corpus callosum, V=lateral ventricle, scale bar = 50 μm).

In the tapered beam test, there was no difference among the groups at pre-surgery test in time to cross the beam or number of foot faults. The 2VO rats needed more time to cross the beam than un-operated control and sham groups at all time points after surgery, which indicates a slower gait velocity following BCCAO, group effect: $F(2,10) = 64.53$ ($P < 0.0001$), time effect: $F(1, 10) = 12.24$ ($P < 0.01$), time*group effect: $F(2, 10) = 31.15$ ($p < 0.0001$) (Figure 2.7A). No difference was detected in number of foot faults among the groups at 1, 2, 3 and 4 weeks after surgery (Figure 2.7B).

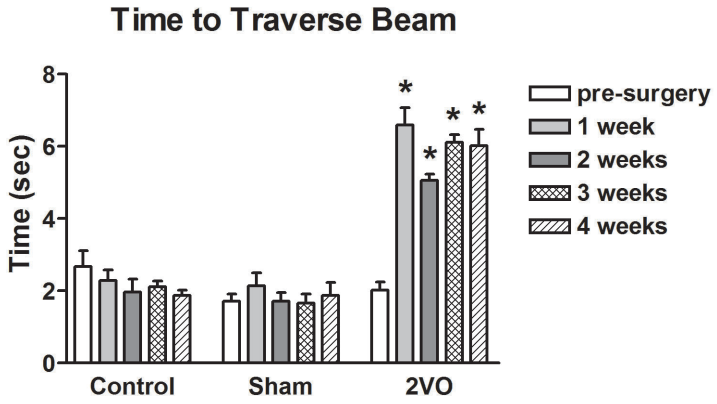


**Figure 2.7A**

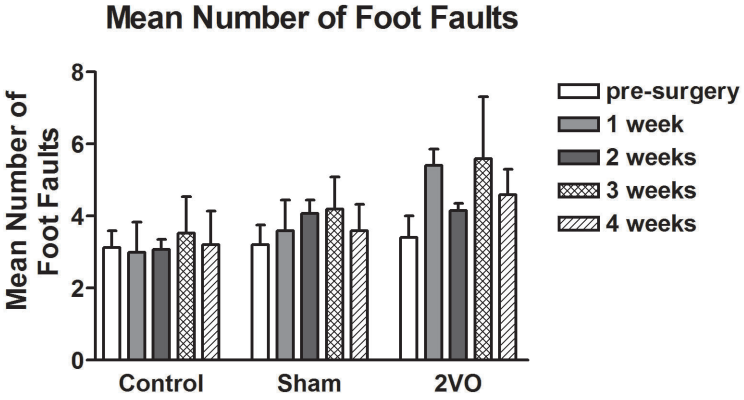


**Figure 2.7B**

**Figure 2.7. Tapered beam test. (A)** There are significant differences between sham and 2VO groups in time to cross the beam after surgery at all time points, with no difference among the groups during pre-surgery test (un-operated control, n = 3; sham , n = 5; 2VO, n = 5). **(B)** There are no significant differences between sham and 2VO groups in mean number of foot faults after surgery at all time points.

**Discussion**

The BBB is relatively vulnerable to ischemia as it becomes permeable to large molecules under severe ischemic conditions. However, there is little evidence in the literature to date of BBB disruption in this rat model of chronic cerebral hypoperfusion (Farkas et al., 2007). Some studies have indicated altered vascular permeability to horse radish peroxidase in the paramedian portion of corpus callosum (Ueno et al., 2002) or extravasation of Evans Blue bound to albumin at 3 days following 2VO surgery (Ueno et al., 2009). The results of this study indicate that BBB permeability increases significantly following permanent BCCAO in rats for up to two weeks. Evans Blue extravasation has been quantified in cortical and thalamic regions at 1, 2, 3, and 6 weeks following 2VO surgery in another study, which indicated BBB breakdown from 2 to 6 weeks of occlusion (Shin et al., 2008). However, no changes were detected at time points earlier than 2 weeks. Although the difference in results between the present study and the Shin's study cannot be explained with certainty, the controls in the Shin's study do not seem appropriate and a different method of Evans Blue measurement (fluorometric vs colorimetric) could be considered as the reasons for discrepancy in results. In another model of CSVD, the stroke-prone spontaneously hypertensive rats fed on a high salt diet, Lee et al. (2007) used MRI to image the brain at regular intervals. They observed focal leakage of an intravascular contrast agent, indicating local breakdown of the BBB, for up to 14 days prior to spontaneous intracerebral hemorrhage.

No change was detected in expression of the tight junction proteins occludin or ZO-1. Although degradation of TJPs has been observed after reperfusion in focal ischemia (Yang et al, 2007), Sood et al (2009) have reported intact TJ proteins in the

corpus callosum, where Evans Blue dye extravasation occurred following BCCAO in rats. In addition, a study on human aging brains with WML indicated an increased BBB permeability, determined by albumin leakage, without significant changes in the endothelial expression of TJPs (Simpson et al., 2010). Increased expression of MMP-2 in demyelinated regions of brain has also been observed in autopsy studies of patients who were diagnosed with vascular dementia (Rosenberg et al., 2001). The unchanged TJ protein expression observed in our study suggests that the observed extravasation of Evans Blue, which is bound to albumin, may occur by a transendothelial rather than a paracellular route. A possible mechanism of transcellular transport of plasma proteins such as albumin is through endothelial caveolae. However, cav-1 expression did not change following BCCAO. Another possible reason for EB extravasation is phosphorylation of TJs such as occludin, claudin-5 and ZO-1 which can affect their function without degradation of proteins (Haorah et al, 2007). Phosphorylation of TJs was not assessed in the present study.

Increased expression of MMP-2 and GFAP following BCCAO confirmed observations that have been reported by others. Recent studies have demonstrated the role of MMPs in both disruption of the BBB and myelin breakdown in conditions of chronic hypoperfusion (Yang and Rosenberg, 2011). The expression of MMP-2, but not MMP-9, and reactive gliosis are characteristic of the rodent model of CCH and these conditions have been associated with opening of the BBB (Ihara et al, 2001; Ueno et al, 2002). In rats treated with a MMP-2 inhibitor white matter lesions were less severe and number of activated astroglia and microglia were lower compared with the vehicle-treated rats. Mice lacking the MMP-2 gene also showed reduced permeability of the

BBB to Evans Blue (Nakaji et al, 2006). In addition, an increase in MMP activity has been associated with degradation of basement membrane proteins (Haorah et al., 2007; Yang et al., 2007). However, no change observed in collagen IV expression in the current study. It has been shown that hypoxia can increase the nonspecific transport of blood-born proteins such as albumin to the brain in an *in vitro* model of BBB (Plateel et al., 1997) and Sood et al. (2009) have reported increased levels of MMP-2 in area of increased Evans Blue extravasation in corpus callosum following BCCAO in rats.

Previous reports of motor impairment in this model of chronic cerebral hypoperfusion are inconclusive. Gait performance following BCCAO was evaluated by means of the elevated platform test (Sarti et al., 2002), and the number of rats falling from bridge and the length of the bridge covered by each animal, was recorded. There was a decrease in the length covered on the bridge at 30, 60, and 90 days in both 2VO and sham-operated rats. However, there was no significant difference between the two groups. In addition, 2VO rats experienced a higher percentage of falls from the bridge compared with sham-operated rats, but this difference did not reach significance. Locomotor function was evaluated in this model of chronic cerebral hypoperfusion (CCH) using footprint test where hind limp stride and interlimb coordination were measured (Ueno et al, 2009). This test was performed by staining of the fore- and hindfeet of the rats with red and blue dye (nontoxic), respectively and measurements of the prints of the hind feet of walking rats preserved on X-ray film as previously described by de Medinaceli et al., (1982). The results indicated that there was no significant difference in the stride length or interlimb coordination between sham and 2VO groups. Therefore, result of the present study should be interpreted with caution as stride length

and stride width were not measured using footprint test. Nevertheless, it has been shown that nondemented elderly with WMLs in the sublobar and limbic areas or lacunar infarcts in the forebrain have a lower gait velocity (de Laat et al., 2010). Although the tapered beam test was originally designed for detection of foot faults in affected rats, the result of this study suggests that gait velocity may offer a better metric.

Motor impairment has been studied in other experimental models of CSVD. Using a novel knock-in mouse with Arg170Cys substitution in murine Notch3 as a model of CSVD, it has been shown that some of these mice had motor defects such as staggering gait and limb paresis as observed by dragging of a limb when stimulated to walk on a tabletop. These motor defects started at 13 months of age. In contrast, none of the other Notch3 transgenic mice displayed neurological symptoms (Wallays et al., 2011). Also, using a stroke-prone SHR model, spontaneously hypertensive rats fed a high fat and cholesterol diet with 1% NaCl water starting at 8 weeks of age and motor impairment was assessed using a Rotorod test at 8, 9 and 10 weeks. The results indicated that the mean times until falling off from the Rotorod were significantly decreased at 10 weeks (Omote et al., 2012).

In summary the results of these studies indicate that BBB permeability increases significantly following permanent BCCAO in rats for up to two weeks. There is no change in expression of tight junction proteins or cavolin-1 following BCCAO. However, increased levels of MMP-2 are associated with BBB permeability enhancement. Also, this is the first report of using the tapered beam test in this rat model of chronic cerebral hypoperfusion, and our data indicate a significant difference in gait velocity between 2VO treated and sham treated rats. We suggest that this is a useful test

to examine some aspects of gait disturbances and can be used for evaluation of potential pharmacological intervention.

# Chapter 3

# Cytokine expression following BCCAO in the rat

**Collaborator Contribution**

**Hamidreza Edrissi: S**urgeries were performed with assistance of Farwah Rubab under supervision of Dr. Antoine Hakim and Dr. Charlie Thomson.

**Farwah Rubab:** Plasma and Protein extraction was performed by Farwah Rubab (research technician).

**Shawn Hayley:** Dr. Shawn Hayley's lab (Carleton University) performed the measurement of cytokines and chemokines. This project was performed with collaboration of Dr. Shawn Hayley from Carleton University.

**Antoine M Hakim:** Dr. Antoine Hakim supervised the work and provided financial support.

**Charlie S. Thompson:** Dr. Charlie Thompson supervised the project.

**Abstract**

The role of inflammatory mediators in the pathogenesis of CSVD is not completely understood. Clinical and experimental studies have indicated that increased levels of pro-inflammatory cytokines occur following acute cerebral ischemia. Cytokines have also an established role in modulation of the BBB. In this study the expression of some 15 cytokines and chemokines was measured in plasma and brain parenchyma of rats subjected to BBCAO for different periods of times using a Milliplex Rat Cytokine/Chemokine kit. The results indicated increased levels of some proinflammatory cytokines and chemokines in brain tissue at different time points after ischemic injury. However, there was no difference in cytokine levels in plasma between the sham and ischemic groups. These results indicated that cytokines within the brain tissue following BCCAO may be involved in pathological consequences of this rat model of chronic cerebral hypoperfusion.

## Introduction

Levels of pro-inflammatory cytokines increase following acute brain injury induced by clinical and experimental cerebral ischemia (Berti et al., 2002; Zaremba and Losy, 2004). However, little is known about the relationship between inflammation and small vessel disease of the brain. There is evidence of inflammatory activation and endothelial dysfunction in individuals with lacunar infarction and white matter lesion (WML) (Hassan et al., 2003). Hoshi et al., (2005) demonstrated that levels of circulating hsCRP and IL-6 were associated with silent brain infarction, suggesting an involvement of inflammation in cerebral small vessel disease.

Nakase et al., (2008) have shown that a high serum level of TNF-α is associated with severe neurological deficits at the onset of lacunar infarction. IL-6 and TNF-α can exacerbate stroke outcome, because they can affect the generation of metalloproteinases (MMPs) in the brain (Castillo and Rodríguez, 2004). MMPs have been reported to increase the permeability of blood brain barrier (BBB) during an inflammatory response.

Many cytokines such as the interleukins IL-0, IL-1, IL-3, IL-4, as well as TNF-α and IFN-γ are able to influence epithelial and endothelial tight junction function and the actin cytoskeleton both *in vivo* and *in vitro* (Ahdieh et al. 2001; Oshima et al. 2001). Cytokines promote opening of the BBB due to degradation and decreased synthesis of TJ proteins (Silwedel and Förster 2006; Yang et al., 2007) or the phosphorylation of TJs affecting their function (Haorah et al., 2007), resulting in compromised junctional integrity. It has been shown that TNF-α enhances MMPs that induce TJs degradation and reorganization of the endothelial cell actin cytoskeleton (Wiggins-Dohlvik et al., 2014;

Yamada et al., 2013). The aim of this study was to analyze the temporal profile of cytokine expression in plasma and brain tissue following permanent BCCAO.

**Materials and Methods**

*Surgical Procedure* - Five groups of male Long Evans (Charles River) rats weighing 175 to 200 g were subjected to either 2VO or sham surgery and were perfused transcardially at days 1, 3, 7, 14, 30 following surgery. Also, a group of un-operated control rats (n = 8) was included later in this study. The rats were anesthetized with 5% isoflurane in 100% $O_2$ and 2-3 ml blood collected from left atrium and centrifuged at 4000 rpm for 20 min to extract 1-2 ml of plasma. Plasma was transferred to a microcentrifuge tube and frozen with liquid nitrogen. After blood collection, the rats were perfused with 100 mL of saline. Using a rat brain matrix a coronal slice was made at the level of optic chiasma and the entire anterior portion of brain was frozen in liquid nitrogen. Both plasma and tissue samples were stored in -80°.

*Protein Extraction* - While keeping the brain tissue samples on dry ice, a slice weighing between 2.4 to 2.7 grams was obtained. This slice of brain was transferred to a microcentrifuge tube and 300 μL of protein lysis buffer was added. Using a Sonic Dismembrator (Fisher Scientific, Model 100) tissue samples were lysed and then centrifuged at 13,200 rpm, 4ºC for 10 minutes. Supernatant was transferred into a new microcentrifuge tube and protein concentration was determined using the protein assay reagent (Bio-Rad). Protein samples were placed in -80° for storage.

*Cytokine kit and prep work* - The expression of 15 cytokines and chemokines including (IL-1β, IL-2, IL-4, IL-6, IL-10, IL-12, IL-18, TNF-α, MCP-1, MIP-1α, INF-γ,

Eotaxin-1, RANTES, G-CSF and GM-CSF) was assessed in the plasma and brain tissue at different time points following surgery using a Milliplex Rat Cytokine/Chemokine kit (Millipore, Inc.) by Dr Shawn Hayley's lab. The kit required 10 μg to 40 μg of protein to be loaded in a total volume of 25 μL on each well. Hence, aliquots of 25 μg of protein were prepared. Plasma samples did not need dilution, but they were aliquoted to avoid freeze-thaw cycles.

*Statistical analyses* - Statistical analyses were performed using SPSS 21 and graphs were made by Graph Pad Prism 3 software. Data were analyzed with two-way ANOVA followed by a Bonferroni post hoc test and presented as means ± standard error. Probability (P) values of less than 0.05 were considered significant.

**Results**

The results indicate a significant difference in several cytokine and chemokine levels in brain tissue between sham and 2VO treated rats at different time points following the onset of chronic cerebral hypoperfusion. They include TNF-α, group effect: $F(1, 68) = 7.079$ ($P < 0.01$), time effect: $F(4, 68) = 12.55$ ($P < 0.0001$) with no interaction; IL-1β, group effect: $F(1, 69) = 21.43$ ($P < .0001$), time effect: $F(4, 69) = 5.63$ ($P < 0.0001$) with no interaction; IL-2, group effect: $F(1, 68) = 27.44$ ($P < 0.0001$), time effect: $F(4, 68) = 24.63$ ($P < 0.0001$) with no interaction; IL-18, group effect: $F(1, 69) = 14.66$ ($P < 0.0001$), time effect: $F(4, 69) = 10.21$ ($P < 0.0001$), time*group effect: $F(4, 69) = 3.26$ ($P < 0.05$); MCP-1, group effect: $F(1, 69) = 18.76$ ($P < 0.0001$), time effect: $F(4, 68) = 27.19$ ($P < 0.0001$), time*group effect: $F(4, 68) = 3.43$ ($P < 0.05$); MIP-1α, group effect: $F(1, 70) = 11.47$ ($P < 0.001$) with no time effect and interaction.

The levels of other cytokines and chemokoines levels that are listed above were not significantly different between sham and 2VO groups in any time point in brain tissue. There was no significant change in the level of any cytokine or chemokine in plasma. Cytokine levels differed markedly between the plasma and brain tissue. In many cases cytokine levels in tissue or plasma were similar in sham and 2-VO operated rats at some of the time points such as 7 and 14 days. Some of the proinflammatory cytokines and were upregulated in brain tissue from 2VO vs. sham operated rats at 24 and 72 h following 2VO surgery (Figure 3.1). Those proinflammatory cytokine levels were also higher in brain tissue of 2VO rats than sham operated rats at 30 days following surgery (Figure 3.1).

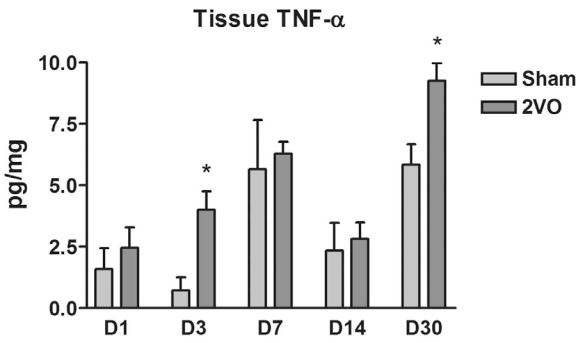


**Figure 3.1A**

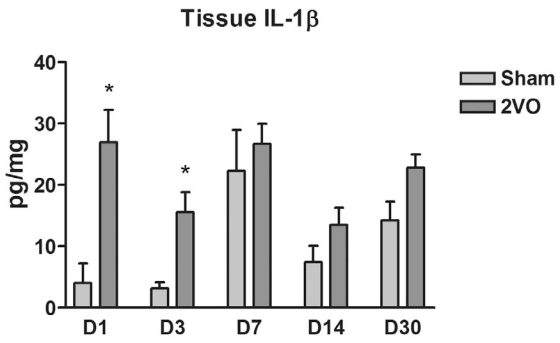


**Figure 3.1B**

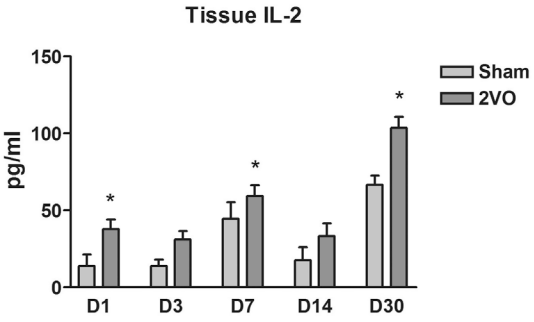


**Figure 3.1C**

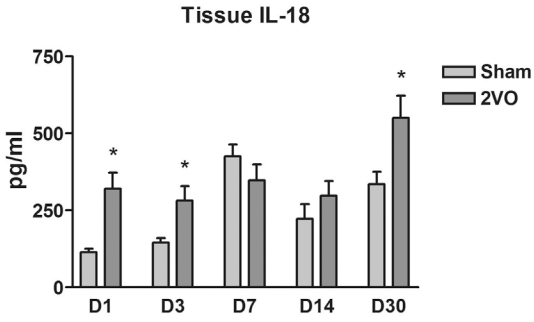


**Figure 3.1D**

**Figure 3.1. Upregulation of proinflammatory cytokines in brain parenchyma following BCCAO. (A)** Tissue level of TNF-α is higher in 2VO than sham treated rats at 3 and 30 days following surgery (n = 8). **(B)** Tissue level of IL-1β is higher in 2VO than sham treated rats at 1 and 3 days following surgery (n = 8). **(C)** Tissue level of IL-2 is higher in 2VO than sham treated rats at 1, 14 and 30 days following surgery (n = 8). **(D)** Tissue level of IL-18 is higher in 2VO than sham treated rats at 1, 3, 30 days following surgery (n = 8).

In addition, the level of monocyte chemoattractant protein-1 (MCP-1), a chemokine, was higher in brain tissue of 2VO group than sham group at 1, 3 and 30 days following surgery (Figures 3.2A). The protein level of another chemokine, macrophage inflammatory protein-1α (MIP-1α) that was not detectable in sham group was only significantly higher in 2VO than sham group at 24h following surgery (Figure 3.2B).

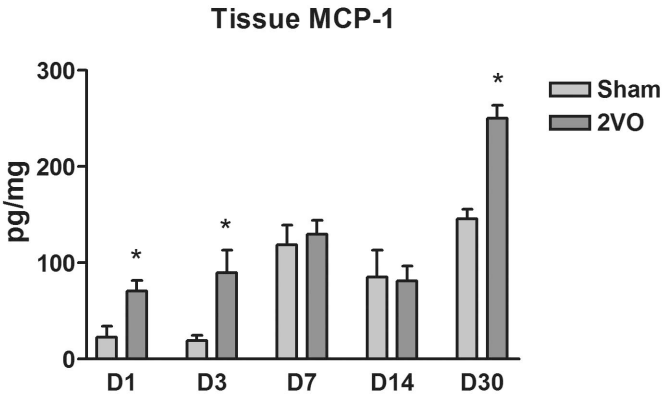


**Figure 3.2A**

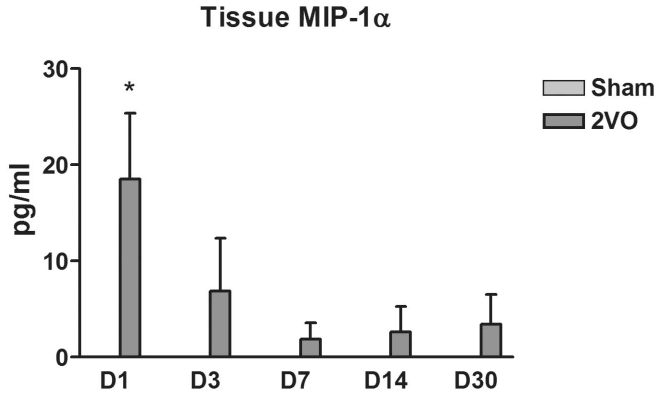


**Figure 3.2B**

**Figure 3.2. Upregulation of chemokines in brain parenchyma following BCCAO.** **(A)** Tissue level of MCP-1 is higher in 2VO than sham treated rats at 1, 3 and 30 days following surgery (n = 8). **(B)** Tissue level of MIP-1α is significantly higher in 2VO than sham treated rats at 1 day following surgery (n = 8).

The plasma levels of the unregulated cytokines and chemokines in brain tissue were not significantly different in 2VO treated rats (Figure 3.3 and 3.4).

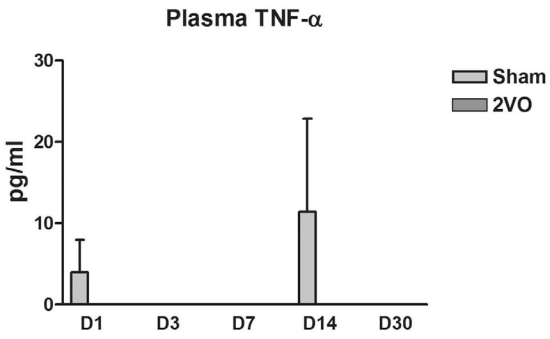


**Figure 3.3A**

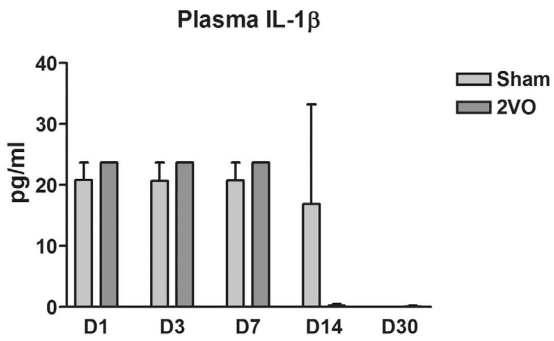


**Figure 3.3B**

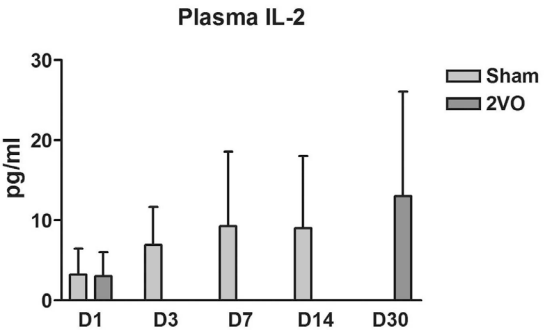


**Figure 3.3C**

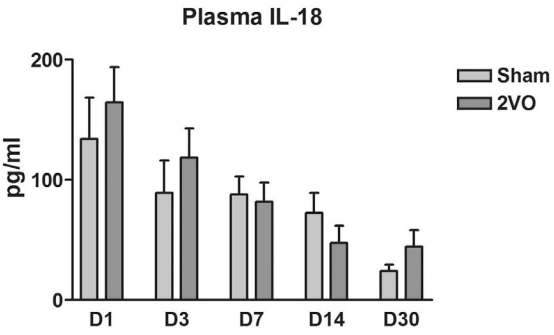


**Figure 3.3D**

**Figure 3.3. No change in proinflammatory cytokines in the plasma following BCCAO.** The plasma levels of TNF-α **(A),** IL-1β **(B)** IL-2 **(C)** and IL-18 **(D)** are not significantly different between sham and 2VO groups (n = 8).

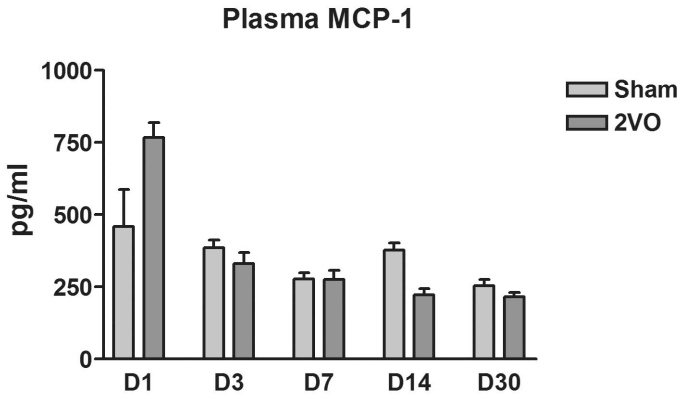


**Figure 3.4A**

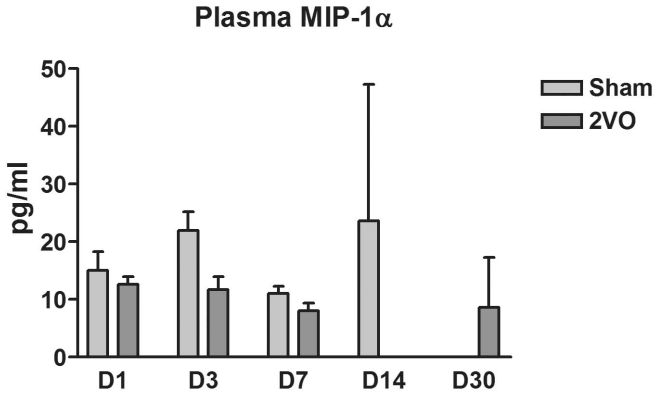


**Figure 3.4B**

**Figure 3.4. No change in chemokines in the plasma following BCCAO.** The plasma levels of MCP-1 **(A)** and MIP-1α **(B)** are not significantly different between sham and 2VO groups (n = 8).

Table-1 presents a summary of proinflammatory of cytokines and chemokines that were upregulated in brain tissue following BCCAO. Note that at some time points the levels of cytokines and chemokines were not significantly different.

**Table 1**

| | Brain tissue | plasma |
|---|---|---|
| TNF-α | ⇧ | _ |
| IL-1β | ⇧ | _ |
| IL-2 | ⇧ | _ |
| IL-18 | ⇧ | _ |
| MCP-1 | ⇧ | _ |
| MIP-1α | ⇧ | _ |

**Table 1. Upregulation of Cytokines and chemokines following BCCAO.** A number of proinflammatory cytokines (TNF-α, IL-1β, IL-2 and IL-18) and chemokines (MCP-1 and MIP-1α) are up-regulated in brain tissue at some time points following BCCAO.

**Discussion**

Several cytokines and chemokines contribute to inflammatory cell recruitment, blood-brain barrier dysfunction, and tissue injury in animal models of ischemic stroke (Huang et al., 2006). Many studies have shown that IL-1β, TNF-α, and their mRNA are up-regulated in the CNS after injury. Overexpression of these cytokines during the early stage of injury can be harmful. On the other hand these cytokines can promote repair processes of the injured tissues during the recovery stage after injury (Wang and Shuaib, 2002).

Plaschke et al., (2001) indicated that twenty minutes following BCCAO the cortical concentrations of TNF-α and IL-1β were markedly increased. However, three weeks after permanent vessel occlusion, no changes were determined in TNF-α and IL-1β cerebral concentrations and permanent BCCAO was associated with almost complete recovery in rat brain cytokine concentrations. Also, BCCAO for 20 min followed by 30 min of reperfusion (a model of transient global ischemia and reperfusion model or I/R insult) increased the plasma levels of IL-1β and TNF-α in rats (Brüning et al., 2012). In another study, induction of transient global cerebral ischemia in rats was associated with increased plasma levels of TNF-α at 2 hours and no significant difference between sham and ischemic groups at 3 and 7 days, while IL-1β levels were highest at 2 hours then markedly decreased at 7 days (Seo, et al., 2013). However, Yoshizaki et al. (2008) could not detect significant changes in TNF-α level between groups following unilateral common carotid artery occlusion. Also, in another study, BCCAO followed by hypoxic–ischemic (HI) damage on rat pups, TNF-α was not detectable in any groups. However, the level of IL-1β in the brain peaked at 12 h following cerebral HI and remained high for

24h (Lin et al., 2006). On the other hand, Duan et al., (2009) showed that in chronic cerebral hypoperfusion by permanent stenosis of bilateral common carotid artery in mice the protein levels of IL-1β, TNF-α, and IL-6 in the corpus callosum were elevated at 7, 14 and 30 days respectively after surgery, and remained significantly different from sham group. We also detected higher expression of TNF-α at 3 and 30 days (Figure 3.1A), and IL-1β in brain tissue at 1 and 3 days following BCCAO (Figure 3.1B). Both TNF-α and IL-1β have been shown to increase the permeability of the blood-brain barrier (Brabers and Nottet, 2006). Therefore, overexpresion of these cytokines following 2VO surgery may be associated with an increase in blood brain barrier permeability during early time points. Increased expression of TNF-α at 30 days following BCCAO may be associated with angiogenesis, one the mechanisms that induces the normalization of blood flow in this rat model of chronic cerebral hypoperfusion. Washida et al. (2010) also indicated that following bilateral common carotid artery stenosis in mice, cerebral mRNA expression of TNF-α was increased at 30 days after surgery.

Higher levels of IL-18 were observed in 2VO treated rats at 1, 3, and 30 days following BCCAO (Figure 3.1D). Although IL-18 is correlated with IL-1 structurally and functionally, results from animal studies suggest that IL-18 is not involved in stroke pathophysiology (Wheeler et al., 2003). However, blood levels of this cytokine increase in acute stroke patients (Yuen et al., 2007).

The expression of monocyte chemoattractant protein-1 (MCP-1) in stroke-prone spontaneously hypertensive rats following transient global ischemia (occlusion of the bilateral carotid arteries for 10 min) indicated that the concentration of MCP-1 protein significantly increased in the hippocampus at 2 days after reperfusion (Sakurai-

Yamashita et al ., 2006). The MCP-1 level was increased in the cerebrospinal fluid of stroke patients (Losy and Zaremba, 2001). In another study, mRNA expression for MCP-1 and MIP-1α (macrophage inflammatory protein-1α) was induced in the rat brain after focal cerebral ischemia (Minami and Satoh, 2003). Following bilateral common carotid artery stenosis in mice, cerebral mRNA expression of MCP-1 was increased at 30 days after surgery (Washida et al., 2010). In addition to recruiting of monocyte to the site of ischemia, MCP-1 also participate in BBB opening through alteration and redistribution of tight junction proteins in endothelial cells (Stamatovic et al., 2005; Dimitrijevic et al., 2006).

We detected increased expression of MCP-1 at 1, 3 and 30 days following BCCAO in brain tissue (Figure 3.2A). Also tissue level of MIP-1α was elevated in 2VO treated rats (Figure 3.2B). Regarding the proinflammatory role of these chemokines (their chemoattractant activity), a specific role for MCP-1 in increasing the BBB permeability, and induction of proinflammatory cytokine synthesis by MIP-1α, their early upregulation may associate with upregulation of other proinflammatory cytokines and BBB dysfunction.

Cytokine and chemokine levels in brain tissue were not different in sham and 2VO groups at some time points such as 7 and 14 days, which could not be explained. However, vulnerability of individual rats to ischemic insult especially young rats (Farkas et al., 2007), human errors in performing the test and cytokine release due to surgical procedure and wound healing could be considered as source of variability. Also, regarding the measured values, available Elisa cytokine kits are not sensitive enough to validate the results of multiplex cytokine study.

In summary, increased expression of several proinflammatory cytokines (TNF-α, IL-1β, IL-2, IL-18) and chemokines (MCP-1, MIP-1α) in brain tissue following BCCAO may suggest a role for them in BBB dysfunction during the early stages of ischemia. However, this study does not provide a causal connection between the elevated levels of these cytokines and chemokines in brain tissue and increased permeability of BBB or motor impairement that occur following BCCAO.

# Chapter 4

## Microparticles generated during chronic cerebral ischemia increase the permeability of microvascular endothelial barriers *in vitro*

**Collaborator Contribution**

**Hamidreza Edrissi:** Surgeries were performed with assistance of Dr. Charlie Thompson in blood and tissue collection and MP extraction. Transcellular endothelial resistance measurements were performed with assistance of Dr. Sarah Schock. Immunohistochemistry was performed with the assistance of Dr. Charlie Thompson. The Chapter was written by author and revised by Dr. Charlie Thompson.

**Sarah C. Schock:** All cell cultures, LDH assay and *in vitro* Evans Blue measurement were performed by Dr. Sarah Schock.

**Antoine M Hakim:** Dr. Antoine Hakim supervised the work and provided financial support.

**Charlie S. Thompson:** Dr. Charlie Thompson contributed in the surgeries and immunohistochemistry and supervised the project.

**Abstract**

Numbers of circulating microparticles (MPs) are elevated in a variety of cardiovascular disorders, and recent studies indicate that they are involved in inflammatory intercellular signaling. In the present study the signaling properties of MPs were assessed in an *in vitro* model of the blood brain barrier. MPs isolated from the plasma of rats exposed to chronic cerebral ischemia caused a significant reduction in the transendothelial electrical resistance (TEER) when applied to *in vitro* endothelial barriers, while MPs isolated from an equal volume of plasma from unoperated or sham operated rats did not. The reduction in TEER was attenuated by the caspase-3 inhibitor AC-DEVD-CHO, the TNF-α inhibitor SPD304, the TACE inhibitor TAPI-0 and the ROCK inhibitor Y27632. The growth factor VEGF stimulated transcellular transport in endothelial barriers while exposure to MPs did not. It is conclude that the increase in permeability of artificial barriers induced by MPs is primarily due to enhanced apoptosis induced by activation of the TNF-α pathway and activated caspase-3 and Rho kinases delivered to endothelial cells by MPs.

## Introduction

Circulating microparticles (MPs) are small (0.1-1.0 microns) vesicles generated by activated or apoptotic cells. Circulating MPs originate from platelets, leukocytes, endothelial cells, and erythrocytes and relative concentrations are determined by the pathophysiological situation. In healthy individuals, circulating MPs are mostly derived from platelets and to a lesser extent leukocyte and endothelial cells (Tushuizen et al., 2011). MPs have well established roles in coagulation, angiogenesis and inflammation and levels of MPs of endothelial, leukocyte and platelet origin are elevated in a variety of cardiovascular disorders. Circulating MPs have proven to be biomarkers of vascular injury and inflammation in cardiovascular pathologies such as acute myocardial infarction, hypertension, and atherothrombosis (Lovren and Verma, 2013). An increase in circulating MPs has also been associated with neurological disorders including ischemic cerebrovascular accidents, transient ischemic attacks, multiple sclerosis, cerebral malaria (Cherian et al., 2003; Simak et al., 2006; Doeuvre et al., 2009), Alzheimer's disease (Xue et al., 2012), and small vessel cerebrovascular disease (SVCD) such as lacunar infarcts and multi-infarct dementias (Lee et al., 1993).

The endothelium is one of the main targets of circulating MPs. MPs contribute to regulation of endothelial cell function under physiological conditions (Owens and Mackman, 2011). However, MPs released from cells under pathological conditions have a different composition and different functions. They may induce a pro-coagulant, pro-inflammatory phenotype that leads to endothelial dysfunction (Diamant et al., 2004), a key element in progression of atherosclerosis and stroke occurrence (Jung et al., 2009),

and an important factor in the etiology of symptomatic cerebral small vessel disease (Lavallée et al., 2013).

One of the features of endothelial dysfunction is an alteration of the endothelial cell barrier permeability. Therefore, it was proposed that circulating MPs derived from plasma of rats subjected to BCCAO can increase the permeability of rat brain microvascular endothelial cell as an *in vitro* model of the BBB (artificial barriers). The specific objectives are to determine the time course of permeability changes in endothelial barriers induced by exposure to MPs *in vitro* and to identify signal transduction pathways that are activated to mediate increases in permeability.

**Materials and Methods**

*Surgical Procedure* - At 24 h after surgery male Long Evans rats (200-225g) were anesthetized and the thoracic cavity opened to expose the heart. Up to 10 ml of blood was withdrawn by cardiac puncture and placed in a BD Vacutainer Blood Collection Tube containing sodium heparin. The collection tubes were centrifuged at 1,200 g for 15 minutes to produce platelet poor plasma (PPP) and stored at -80ºC (Shock et al., 2014).

*Endothelial cell culture* - Cryopreserved primary rat brain microvascular endothelial cells (RBMVECs) were purchased from Cell Applications Inc. RBMVEC were cultured in growth medium (Cell Applications Inc) fully supplemented with essential and non-essential amino acids, 100 U/mL penicillin and gentamicin, 10% fetal bovine serum and growth factors, at 37ºC in a 5% $CO_2$, 95% air humidified incubator. Cells were maintained by serial passages in 10 cm dishes coated with cell attachment factor (Cell Applications). The cells in this study were used at passage 5, as RBMVEC

can be cultured and propagated to passage 5 and beyond without losing their morphological and phenotypic properties (Shock et al., 2014).

*Artificial endothelial barriers* - RBMVECs (200000 cells per ml) were seeded on inserts of a 24 cell culture plate, polycarbonate, 0.4 μm (Millicell), coated with cell attachment factor (Cell Applications). PPP was thawed and spun at 13,000 g for 3 minutes to remove apoptotic bodies and other cellular debris. The supernatant was spun at 18,000 g for 20 minutes to produce a pellet enriched in MPs. The pellet was then resuspended in endothelial cell growth medium, diluted 50% and added to cell culture inserts. For these experiments, PPP from at least 5 rats for each experimental group was pooled to obtain a representative mixture of MPs. Endothelial cell permeability was assessed every 2 to 3 days by measuring transendothelial electrical resistance (TEER) as an indicator of paracellular permeability using Voltohmmetre (World Precision Inc.) until a plateau was reached. The TEER of cell-free inserts coated with cell attachment factor was subtracted from the TEER of filters with cells. The inserts containing confluent RBMVECs were treated with MPs for 24 h (n = 3), or pretreated with inhibitors 60 min prior to addition of MPs (n = 3). Also, control inserts were treated with inhibitor alone (n = 3). The applied inhibitors included an inhibitor of TNF-α, SPD-304 (Cayman Chemical; 50 uM), a TACE inhibitor, TAPI-0 (Santa Cruz, 500 nM), a caspse-3 inhibitor, AC-DEVD-CHO (Enzo Life Sciences; 20 uM), a ROCK inhibitor, Y-27632 (Millipore; 10 uM), and TRAIL neutralizing antibody (Abcam; 10 ng/ml). Also, some inserts were only treated with TNF-α (10 or 50 ng/ml, n = 2) in order to compare the MP treatment effect with TNF-α treatment on endothelial cells. TEER was measured at 1, 10, 30 min, and 1, 2, 3, 4, 6, 8 and 24 h after treatments.

Permeability was also measured using Evans Blue bound to rat albumin. 2% Evans Blue, 5% rat albumin were added to culture media as a 100X stock solution. Cells were treated with either VEGF (50 ng/ml; ProSpec, n = 3) or MPs. A 1:100 dilution of the Evans Blue/albumin stock was added immediately after this to both control and treated inserts. Following addition of Evans Blue at 1, 5, 10, 30 min, and 1, 2, 4, 6, 8 and 24 h, 50 µl of the media from the bottom cell culture chamber was removed and put onto a 96 well plate for assaying and 50 µl of normal media was put back in the bottom chamber to keep the volume at a constant level. After 24 hours the media from all time points was collected and the amount of Evans Blue in the bottom chamber was determined by measuring fluoresce with an excitation of 620 nm and an emission of 680 nm.

*Cell death assay* - Cell death was quantitatively assessed by measurement of lactate deyhdrogenase (LDH) activity released in the media following exposure to MPs. The LDH assay was performed using the CytoTox96 Non-Radioactive Cytotoxicity Assay Kit (Promega) according to the manufacturer's instructions. Cytotoxicity was determined by measuring wavelength absorbance at 490 nm. Cell death was expressed as a percentage of experimental LDH release/maximal LDH release.

TUNEL assay - TUNEL assays were performed using in Situ Cell Death Detection Kit (Roche) according to the manufacturer's protocol. RBMECs were grown to confluence on 96 well plates. Confluent RBMVECs were treated with MPs for 24 h, washed, fixed, permeabilized and exposed to TUNEL detection reagents. Nuclei were stained with DAPI. Pictures were taken by Ziess Meta 510 laser scanning confocal microscope. For statistical analysis three equal fields of view of 20 µm ×20 µm were

randomly selected from control and MPs treated wells (n = 3), and the number of TUNEL positive nuclei were counted. The result was presented as a percentage of TUNEL positive nuclei to total nuclei and statistical analysis performed using t-test.

*Immunofluorescence* - RBMVECs were grown to confluence on the 8 well Ibidi μ-Slide with silicone inserts. Following treatments as described above cells were fixed in 4% paraformaldehyde containing 7% (v/v) saturated picric acid for 20 minutes at room temperature and then washed with 10 mM phosphate buffered saline. Cells were permeabilized with 0.25% Triton X-100 and blocked for 20 min with 5% serum donkey and 2% Triton X-100 in PBS on shaker table. The cells were then incubated with primary antibodies in blocking buffer overnight. Primary antibodies included VE-cadherin (Santa Cruz) and ROCK II (Santa Cruz) at 2μg/ml. After rinsing in PBS, slides were incubated in Texas Red or FITC conjugated secondary antibodies for 3 h at room temperature. Cells were also stained with Rhodamine-phalloidin (1:1000; Invitrogen) to examine the structure of filamentous (F)-actin and DAPI to stain cells nuclei. Images were captured with a Ziess Meta 510 laser scanning confocal microscope. Representative images of three separate wells for each treatment are shown (n = 3). The immunofluorescence results were not quantified but used to visually confirm the results of measurement of TEER in artificial barriers and cell death in LDH assays.

*Statistical analyses* - Statistical analyses were performed using SPSS 21 and graphs were made by Graph Pad Prism 3 software. Data were analyzed with one-way ANOVA or two-way ANOVA repeated measures (to quantify the artificial barriers results) followed by a Bonferroni post hoc test and presented as means ± standard error. Probability (P) values of less than 0.05 were considered significant. Stars on the artificial

barrier graphs refer to significance at 24h following treatment, which was determined with a post hoc test following ANOVA.

**Results**

Total numbers of circulating MPs and endothelial derived MPs are elevated at various time points following surgery in rats subjected to 2VO (appendix: Figure1A, Schock et al., 2014). In order to determine if circulating MPs purified from un-operated, sham and 2VO rats have different effects on RBMVEC barrier permeability, artificial barriers were treated for 24 hours with MPs isolated from a specific volume of plasma. The results indicate that there is a significant difference in the induced reduction of TEER between MPs isolated from 2VO rats and MPs isolated from sham or un-operated groups at 24h following treatment, treatment effect: $F(3,7) = 4.95$ ($P < 0.05$), time effect: $F(10, 70) = 29.78$ ($P < 0.0001$), time*treatment effect: $F(30, 70) = 5.54$ ($P < 0.0001$) (Figure 4.1A). There were no differences among control (endothelial cells with no MPs treatment), un-operated and sham groups. When MPs isolated from the plasma of rats that received 2VO surgery and survived for different period of time following surgery were applied to confluent RBMVECs they induced cell death (appendix: Figure 1B, Schock et al., 2014). By comparing the toxicity of MPs isolated from identical volumes of plasma at different time points following surgery (1 h, 3 h, 24 h, 48 h, 72 h and 6 weeks), it was found that plasma from rats 24 h after surgery was most toxic when applied on cultured RBMVECs (appendix: Figures 1B and 2A, Schock et al., 2014). The toxicity of MPs on cultured cell is time and concentration dependent (appendix: Figures 2A and 2B, Schock et al., 2014) and MPs from an equal volume of plasma from rats

subjected to 2VO surgery are more toxic than MPs from sham operated rats when applied to RBMVECs (appendix: Figure 2B, Schock et al., 2014). Therefore, rats were euthanized 24 h following surgery to obtain circulating MPs from plasma for further experiments. Since the effect of MPs on cell death is concentration dependent it was determined that a 50% dilution of isolated MPs induces about 25% cell death when applied to RBMVECs.

TNF-α is an important mediator of inflammation and acts as a trimer to promote receptor trimerization to activate proinflammatory and/or apoptotic signaling pathways (McCoy and Tansey, 2008). MPs generated during cerebral ischemia have been shown to act as vectors of TNF-α signaling (Schock et al., 2014) and TNF-α is known to affect brain endothelial cell barrier permeability (Wiggins-Dohlvik et al., 2014). Therefore, to examine whether TNF-α mediates the effect of MPs on TEER reduction, confluent RBMVECs were pretreated with two different concentrations of TNF-α (10 and 50 ng /ml). A high concentration of TNF-α (50 ng /ml) induced a significant reduction in TEER at 2h and later time points, while there was no difference in TEER between a low concentration of TNF-α (10 ng/ml) and the control group, $F(2,3) = 44.86$ ($P < 0.01$) time effect: $F(10, 30) = 14.88$ ($P < 0.0001$), time*treatment effect: $F(20, 30) = 11.44$ ($P < 0.0001$) (Figure 4.1B).

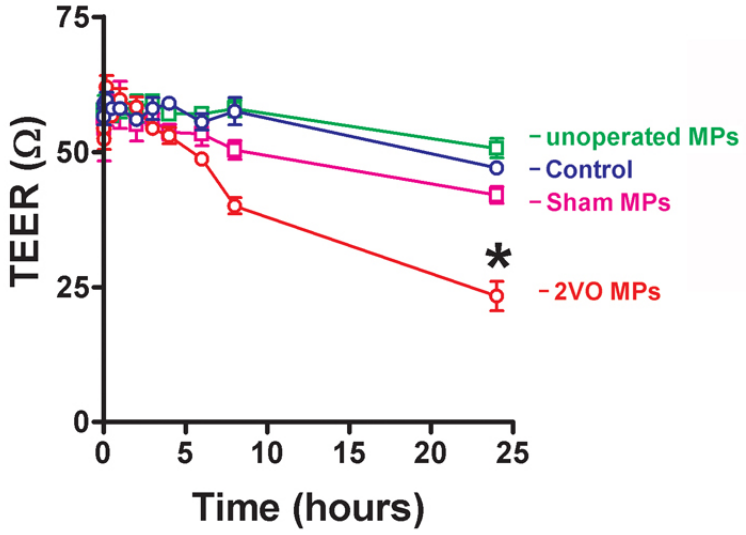


**Figure 4.1A**

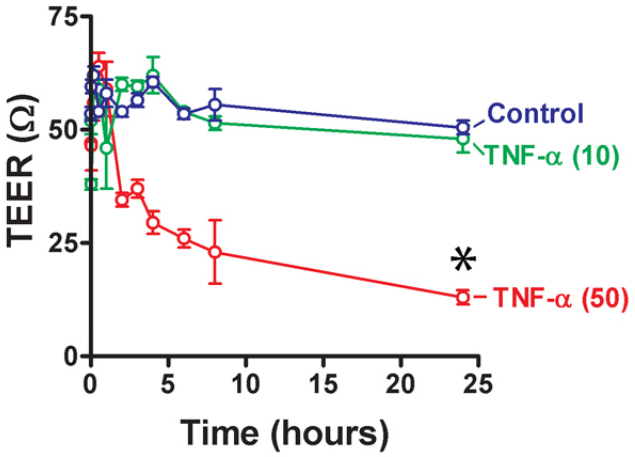


**Figure 4.1B**

**Figure 4.1. The effect of MPs and TNF-α on endothelial cell permeability. (A)** Circulating MPs derived from 2VO rats induce a reduction in confluent RBMVECs permeability, while MPs from un-operated and sham operated rats do not induce any significant difference (n = 3). **(B)** Treatment of confluent RBMVECs with a high concentration of TNF-α (50ng/ml) induces a significant reduction in endothelial permeability, while the low a concentration does not induce any effect (n = 2). Control groups are endothelial cells without MP treatment.

Changes in the actin cytoskeleton and expression of junctional proteins that are responsible for endothelial barrier formation were assessed. Circulating MPs induced an increase in stress fiber formation in endothelial cells for the first hour after exposure and caused F-actin disassembly at 8 and 24 h following MP treatment (Figure 4.2A). MP treatment also led to disruption of VE-cadherin staining (a main adherence junction protein) at 8 and 24 h. The same result was obtained when endothelial cells were treated with TNF-α (50 ng/ml) (Figure 4.2B).

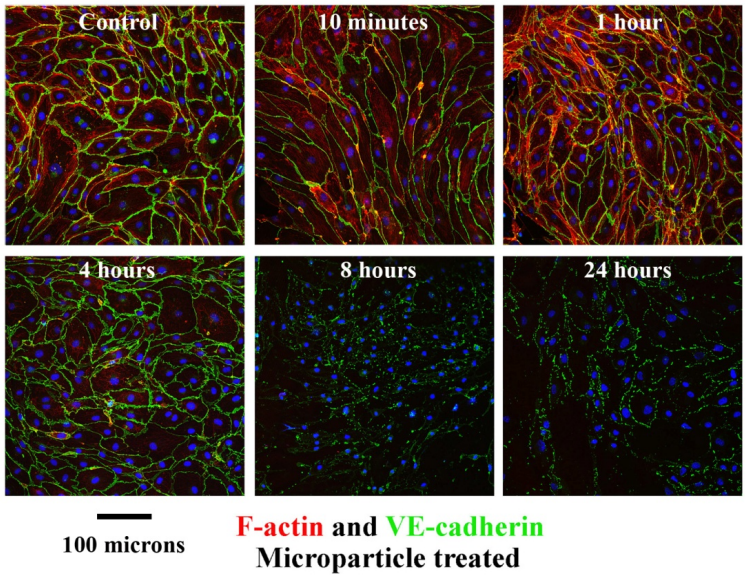


**Figure 4.2A**

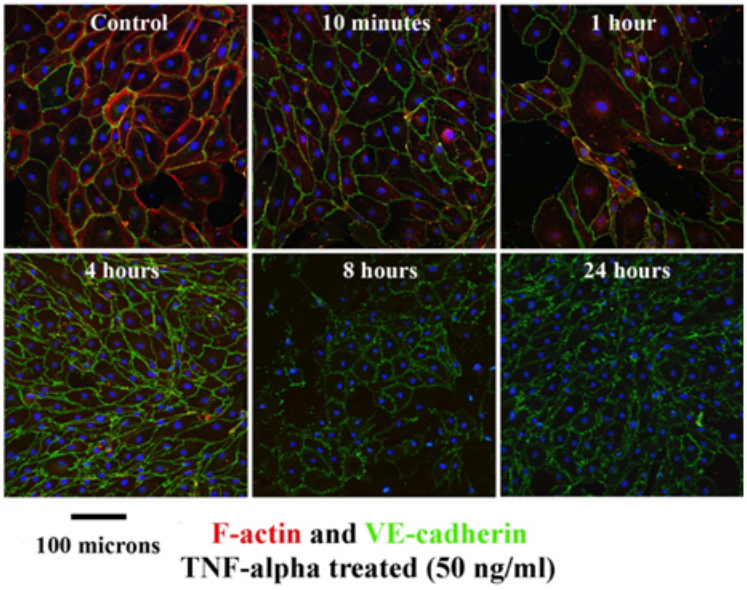


**Figure 4.2B**

**Figure 4.2. The effect of MPs and TNF-α on the actin cytoskeleton and adherens junctions. (A)** MP treatment of confluent RBMVECs induces increased F-actin formation during the first hour and disassembly of these fibers at 8 and 24 h. VE-cadherin is disrupted at 8 and 24 h following MP treatment (n = 3, scale bar = 100 μm). **(B)** Treatment of confluent RBMVECs with TNF-α induces disassembly of F-actin and disruption of VE-cadherin at 8 and 24 h (n = 3, scale bar = 100 μm).

To determine whether MP-induced increased permeability in RBMVECs was mediated by apoptotic cell death, the effect of MPs on DNA fragmentation was determined with TUNEL staining. The results indicated a significant increase in the percentage of TUNEL positive cells compared with control (Figure 4.3). The high percentage (%) of apoptotic nuclei detected by TUNEL in comparison to 25% cell death determined by LDH assay indicates that DNA fragmentation precedes the cell rupture and LDH release. Schock et al., (2014) have shown that only the pellets containing MPs (centrifugation of plasma at 18000g) induced significant amount of cell death. Pellets containing apoptotic bodies (13000g) or exosomes (100000g) were not toxic when applied to cultured NRK (normal rat kidney) cells (appendix: Figure 2C, Schock et al., 2014).

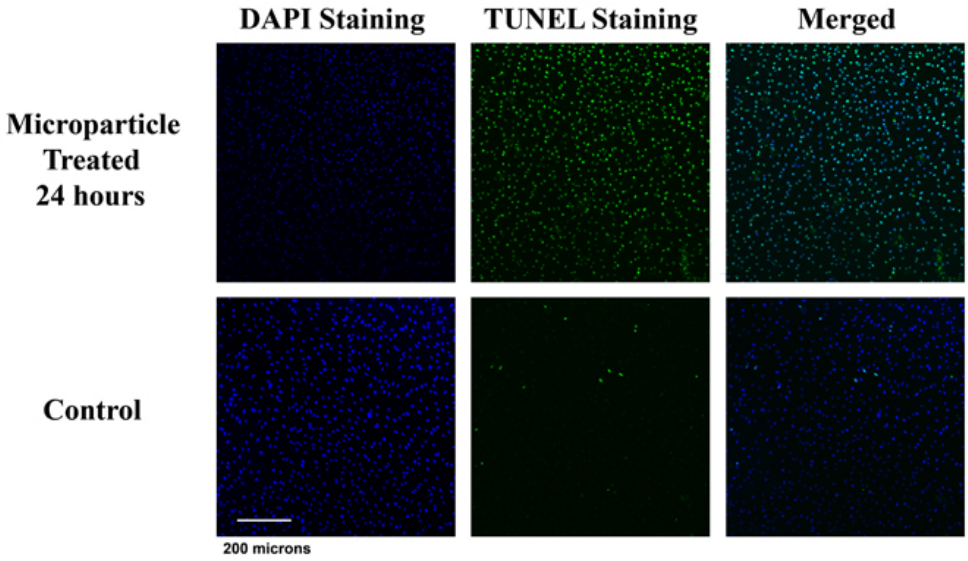


**Figure 4.3A**

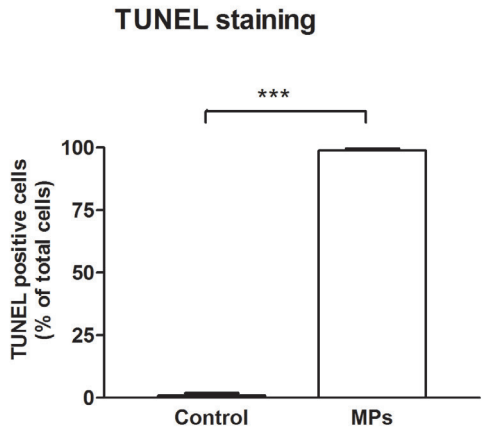


**Figure 4.3B**

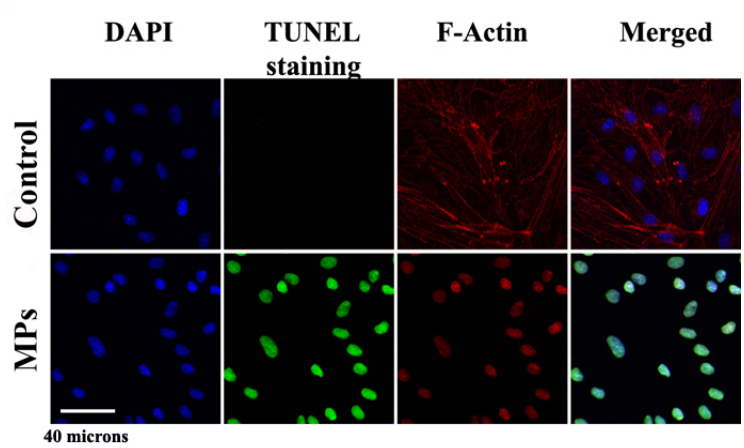


**Figure 4.3C**

**Figure 4.3. MPs induced apoptosis in cultured RBMVECs. (A)** ECs are exposed to fluorometric TUNEL staining (green) 24 h after MP treatment. Nuclei are stained with DAPI (blue, n = 3, scale bar = 200 μm). **(B)** The percentage of TUNEL positive cells in Figure 4.3A are analyzed (***P < 0.001, n = 3). **(C)** TUNEL staining confirms DNA fragmentation in MP-treated cells. Disassembly of F-actin only occur in MP treated cells (Red: F-actin; Green: VE-cadherin; Blue: nuclei. Scale bar = 40 μm). Control groups are endothelial cells without MP treatment.

In order to confirm that TNF-α mediates the effect of MPs on TEER reduction, confluent RBMVECs were pretreated with SPD-304 (Schock et al., 2014), a small molecule inhibitor of TNF-α, prior to addition of the circulating MPs that were isolated from plasma of 2VO rats. SPD-304 binds to the biologically active TNF-α trimer and promotes displacement of a single subunit to prevent binding to TNF receptor 1 (TNFR1) and inactivate the cytokine (He et al, 2005). The results indicated that SPD-304 significantly reduced the effect of MPs on endothelial permeability and there were no differences among control, MPs plus inhibitor and inhibitor alone groups, treatment effect: $F(3, 7) = 9.55$ ($P < 0.01$), time effect: $F(10, 70) = 74.37$ ($P < 0.0001$), time*treatment effect: $F(30, 70) = 4.45$ ($P < 0.0001$) (Figure 4.4A). Also, pretreatment of endothelial cells with SPD-304 before MP treatment reduced disruption in VE-cadherin staining (Figure 4.4B).

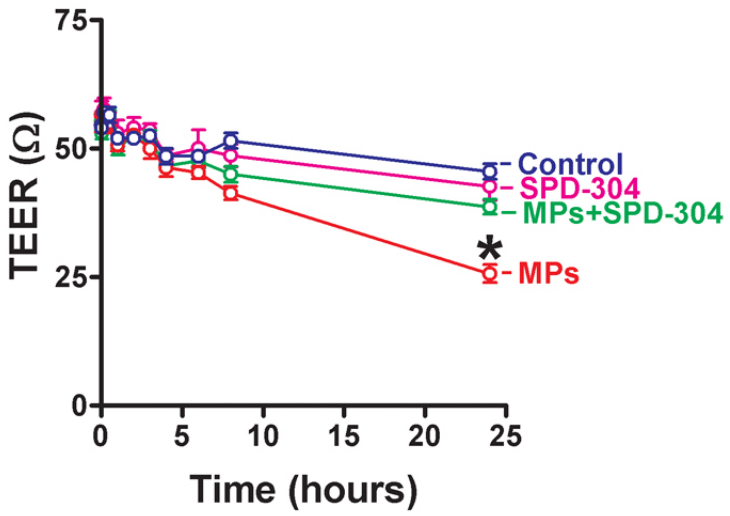


**Figure 4.4A**

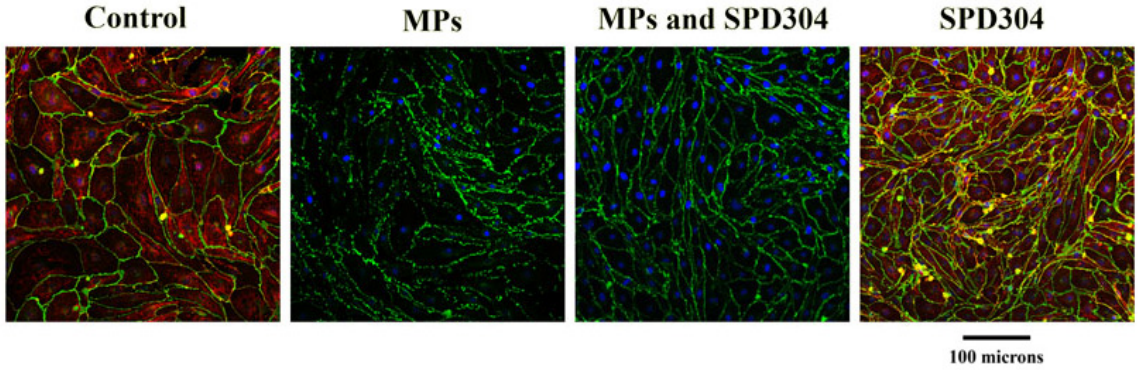


**Figure 4.4B**

**Figure 4.4. Inhibition of TNF-α. (A)** Pretreatment of confluent RBMVECs with a TNF-α inhibitor prevents an increase in endothelial permeability following treatment of endothelial cells with MPs (n = 3). **(B)** Treatment of the confluent RBMVECs with circulating MPs for 24 h induces disassembly of F-actin (red) and disruption of VE-cadherin (green). Pretreatment of endothelial cells with a TNF-α inhibitor, SPD-304 reduces VE-cadherin disruption (n = 3, scale bar = 100 μm).

TNFR1 can be activated by both the membrane-bound and soluble trimeric forms of TNF. TACE (TNF-α converting enzyme/ADAM17) is a sheddase located in the plasma membrane of cells. One function of TACE is to cleave transmembrane pro-TNF-α to release a soluble TNF-α ligand (McCoy and Tansey, 2008). In order to determine whether soluble TNF-α is released from MPs by TACE, circulating MPs were treated with TAPI-0, a TACE inhibitor (Schock et al., 2014). MPs were then centrifuged and resuspended in culture medium prior to treating the confluent RBMVECs. The results indicated that treatment with a TACE inhibitor could significantly reduce the effect of MPs on endothelial cell permeability at 24h, and there was no significant difference among groups treated with TAPI-0 alone, exposed to MPs treated with TAPI-0 and controls, treatment effect: $F(3, 7) = 0.51$ ($P > 0.05$), time effect: $F(10, 70) = 37.06$ ($P < 0.0001$), time*treatment effect: $F(30, 70) = 8.80$ ($P < 0.0001$) (Figure 4.5A). Pretreatment of circulating MPs with TAPI-0 before treatment of RBMVECs with MPs prevented F-actin disassembly and VE-cadherin disruption in endothelial cells at 24 h following treatment (Figure 4.5B). Also, it has been reported that treatment of MPs with TAPI-0 results in a significant increase in cell survival when applied to RBMVECs (appendix: Figure 3A, Schock et al., 2014).

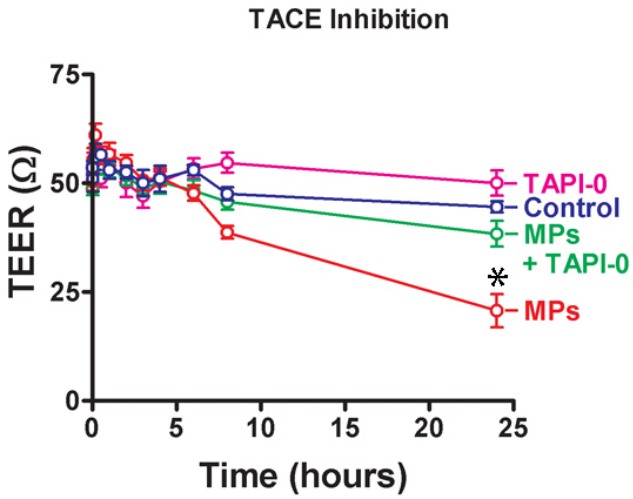


**Figure 4.5A**

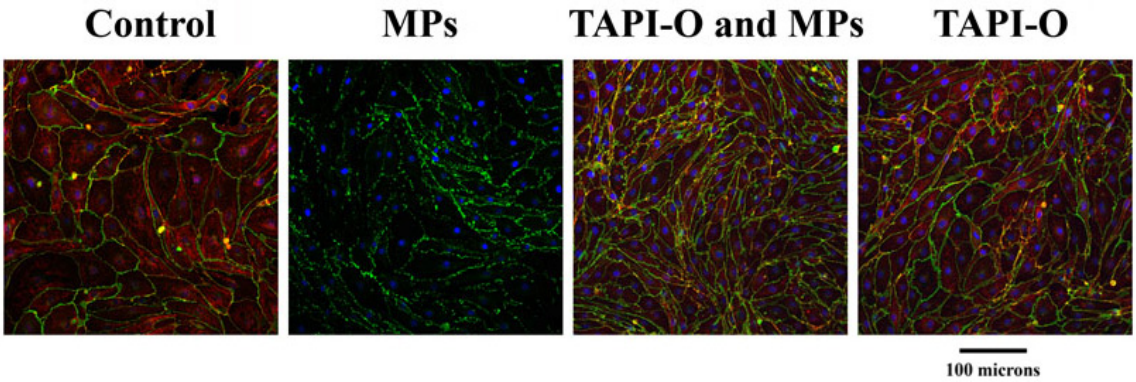


**Figure 4.5B**

**Figure 4.5. Inhibition of soluble TNF-α release.** (**A)** Pretreatment of MPs with a TACE inhibitor prevents the MPs effects on endothelial permeability (n = 3). **(B)** Pretreatment of circulating MPs with a TACE inhibitor prior to addition of the MPs to the confluent RBMVECs, reduces F-actin disassembly (red) and VE-cadherin disruption (green) in endothelial cells at 24 h following MP treatment (n = 3, scale bar = 100 μm).

MPs have been reported to contain caspase-3 and to induce caspase3-dependent apoptosis in several types of cells (Rautou et al., 2011). In order to determine whether caspase-3 is involved in MP-induced increase in endothelial barrier permeability, confluent RBMVECs were treated with AC-DEVD-CHO, a caspase-3 inhibitor prior to MP treatment. This significantly reduced the increase in barrier permeability following exposure to MPs. However, there was still a significant difference between control barriers and barriers treated with MPs and AC-DEVD-CHO or barriers treated with AC-DEVD-CHO alone, treatment effect: $F(3, 7) = 61.735$ ($P < 0.001$), time effect: $F(10, 70) = 67.24$ ($P < 0.0001$), time*treatment effect: $F(30, 70) = 17.83$ ($P < 0.0001$) (Figure 4.6A). Also, pretreatment of confluent RBMVECs with AC-DEVD-CHO before MP treatment reduced VE-cadherin disruption in endothelial cells (Figure 4.6B).

In order to determine if caspase-3 presence in MPs is responsible for TEER reduction or if it is activated in endothelial cells following MP treatment, MPs were pretreated with a caspase-3 inhibitor, spun down, and used for treatment on confluent RBMVECs. The results indicated that pretreatment of MPs with a caspase-3 inhibitor reduces the MPs effect on endothelial permeability, treatment effect: $F(3, 7) = 8.89$ ($P < 0.01$), time effect: $F(10, 70) = 11.25$ ($P < 0.0001$), time*treatment effect: $F(30, 70) = 3.48$ ($P < 0.0001$) (Figure 4.6C). Therefore, the MP-induced reduction in endothelial permeability partially depends on the presence of caspase-3 in MPs.

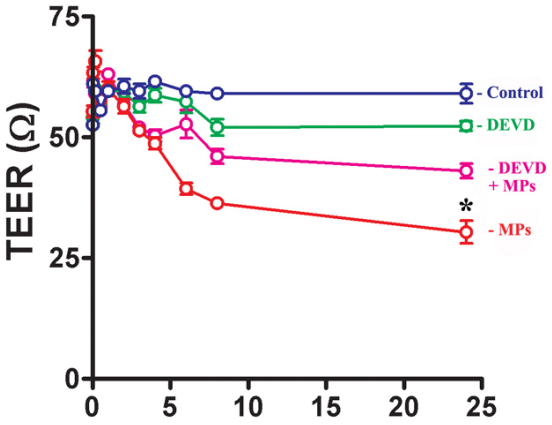


**Figure 4.6A**

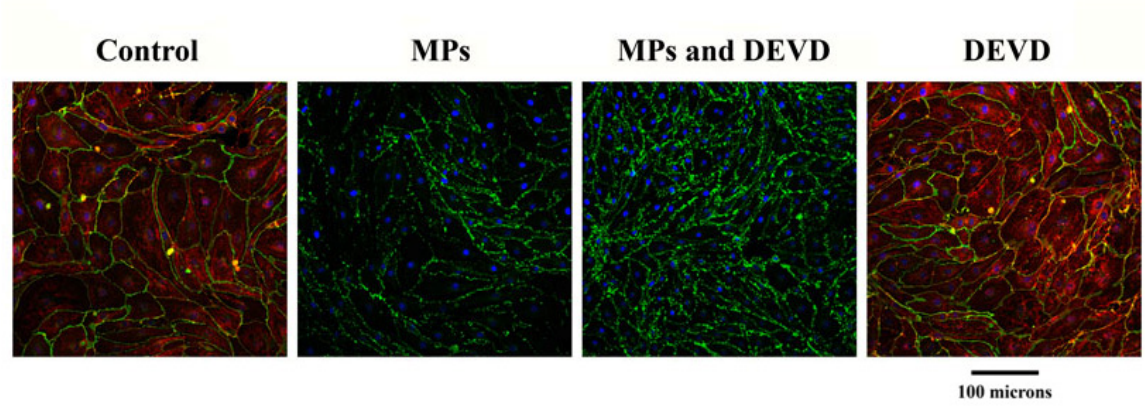


**Figure 4.6B**

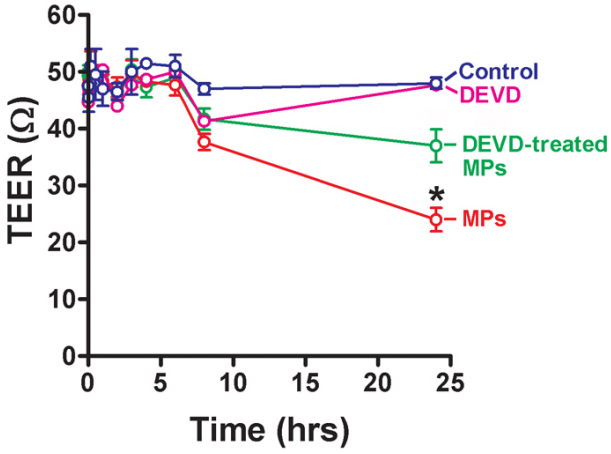


**Figure 4.6C**

**Figure 4.6. Inhibition of caspase-3. (A)** Pretreatment of RBMVECs with a caspase-3 inhibitor reduces the MP effect on endothelial permeability (n = 3). **(B)** Pretreatment of confluent RBMVECs with a caspase-3 inhibitor prior to addition of MPs reduces VE-cadherin disruption (green) in endothelial cells at 24 h following MP treatment (n = 3, scale bar = 100 μm). **(C)** Pretreatment of MPs with a caspase-3 inhibitor significantly reduces the MP effect on endothelial permeability (n = 3).

MPs generated during cerebral ischemia activate endothelial receptors for the cytokine TRAIL, another member of TNF-α family, and blocking TRAIL signaling reduces the degree of apoptosis induced by exposure to MPs in normal rat kidney cells (appendix: Figure 3B, Schock et al., 2014). TRAIL is a cytokine that belongs to the tumor necrosis factor (TNF) ligand family, and induces apoptosis in a wide variety of transformed and tumor cell lines. To determine whether this signaling pathway is involved in the MP-induced increase in endothelial barrier permeability, the confluent RBMVECs were pretreated with an anti-TRAIL antibody (Schock et al., 2014) before MP treatment. The results indicated that anti-TRAIL antibody did not prevent the effect of MPs on endothelial permeability and there was no difference between MPs treated group with MPs plus anti-TRAIL antibody treated group (Figure 4.7A). However, pretreatment of endothelial cells with anti-TRAIL antibody before MP treatment slightly improved a disruption in VE-cadherin staining in IF (Figure 4.7B). On the other hand, treatment of cultured RBMVECs with recombinent Trail protein itself could increase permeability of endothelial cells and anti-TRAIL antibody reduced this effect at 24h following exposure, treatment effect: $F(3, 7) = 6.90$ ($P < 0.05$), time effect: $F(10, 70) = 30.47$ ($P < 0.0001$), time*treatment effect: $F(30, 70) = 3.59$ ($P < 0.0001$) (Figure 4.7C).

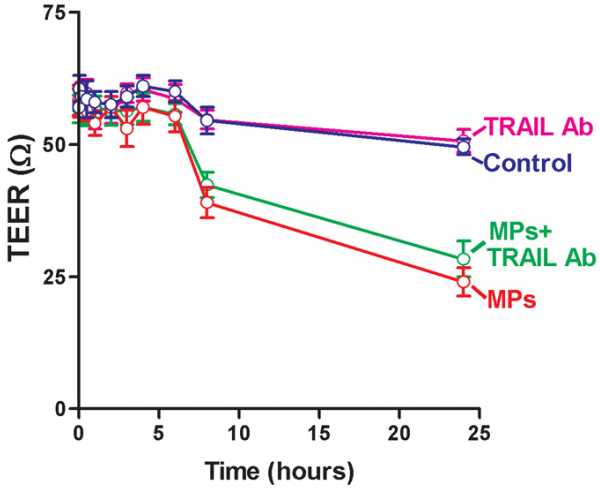


**Figure 4.7A**

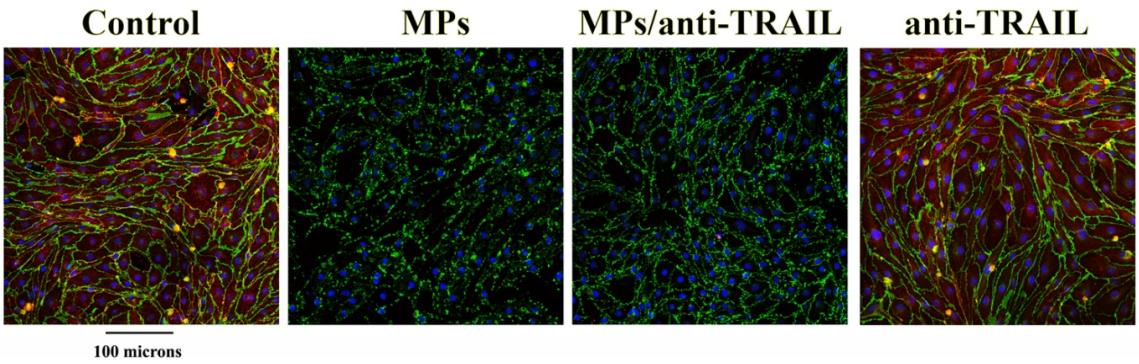


**Figure 4.7B**

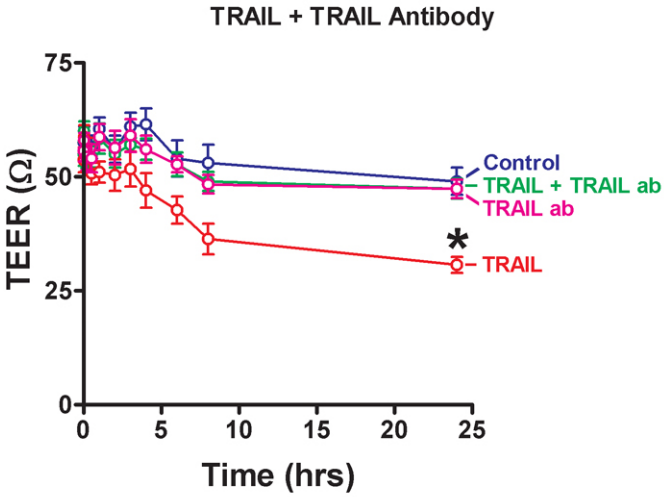


**Figure 4.7C**

**Figure 4.7. TRAIL and TRAIL inhibition. (A)** Pretreatment of the confluent RBMVECs with an anti-TRAIL antibody does not prevent an increase in endothelial permeability following MP treatment (n = 3). **(B)** Pretreatment of the confluent RBMVECs with an anti-TRAIL antibody slightly reduces VE-cadherin disruption (green) in endothelial cells at 24 h following MP treatment (n = 3, scale bar = 100 μm). **(C)** The cytokine TRAIL causes a significant increase in permeability (n = 3).

The RhoA /Rho kinase (ROCK) signaling has been reported to be involved in the maintenance of endothelial barrier permeability (van Nieuw Amerongen et al., 2007), the early phase of apoptosis (Street and Bryan, 2011) and endothelial MP release (Gao et al., 2012). To determine whether this signaling pathway is involved in the MP-induced increase in endothelial barrier permeability, confluent RBMVECs were pretreated with a ROCK inhibitor, Y-27632 (Ma et al., 2012) prior to MP treatment. Y-27632 treatment significantly reduced effect of MPs on endothelial barrier permeability, treatment effect: $F(3, 7) = 10.94$ ($P < 0.01$), time effect: $F(10, 70) = 105.38$ ($P < 0.0001$), time*treatment effect: $F(30, 70) = 11.09$ ($P < 0.0001$). However, the ROCK inhibitor alone could increase endothelial permeability by itself. Although there was a significant difference between the MPs plus inhibitor treated group and controls or MPs treated group at 24h, no difference was observed between MPs plus inhibitor treated group and inhibitor only treated group (Figure 4.8A). Also, pretreatment of the confluent RBMVECs with Y-27632 reduced VE-cadherin disruption in endothelial cells at 24 h following MP treatment (Figure 4.8B).

In order to determine if ROCK presence in MPs is responsible for TEER reduction or if it is activated in endothelial cells following MP treatment, MPs were pretreated with a ROCK inhibitor, spun down, and used for treatment on confluent RBMVECs. The results indicated that pretreatment of MPs with a ROCK inhibitor reduces the MPs effect on endothelial permeability, treatment effect: $F(3, 7) = 7.74$ ($P < 0.05$), time effect: $F(10, 70) = 78.09$ ($P < 0.0001$), time*treatment effect: $F(30, 70) = 5.80$ ($P < 0.0001$) (Figure 4.8C). Therefore, the MP-induced reduction in endothelial permeability partially depends on the presence of ROCK in MPs.

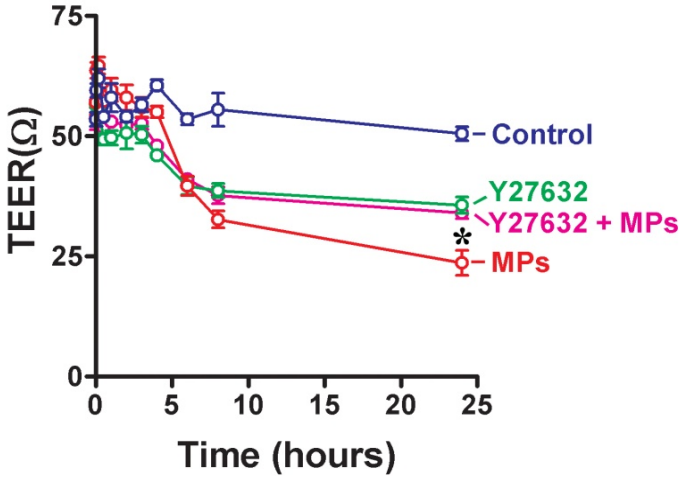


**Figure 4.8A**

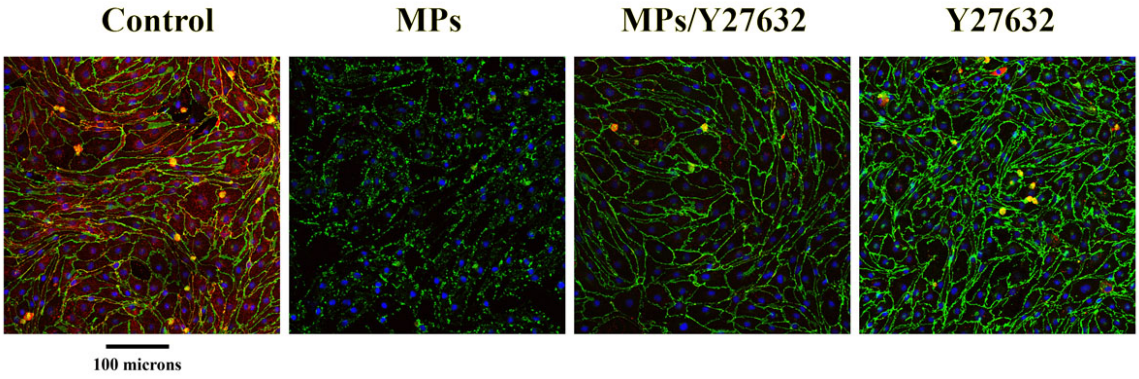


**Figure 4.8B**

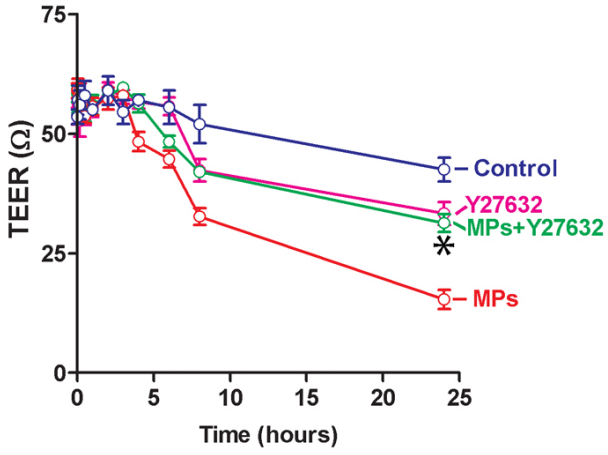


**Figure 4.8C**

**Figure 4.8. Inhibition of Rho kinases. (A)** Pretreatment of confluent RBMVECs with a ROCK inhibitor significantly reduces an increase in endothelial permeability following MP treatment (n = 3). **(B)** Pretreatment of confluent RBMVECs with a ROCK inhibitor reduces VE-cadherin disruption (green) in endothelial cells at 24 h following MP treatment (n = 3, scale bar = 100 μm). **(C)** Pretreatment of MPs with a ROCK inhibitor significantly reduces the MP effect on endothelial permeability (n = 3).

On the other hand, circulating MPs induced an increase in the expression of ROCK-II in RBMVECs at 8 and 24 h following treatment (Figure 4.9A), and the same effect was observed following treatment with TNF-α (50 ng/ml) (Figure 4.9B). Pretreatment of RBMECs with a caspase-3 inhibitor before MP treatment reduced the increase in expression of ROCK-II (Figure 4.9C).

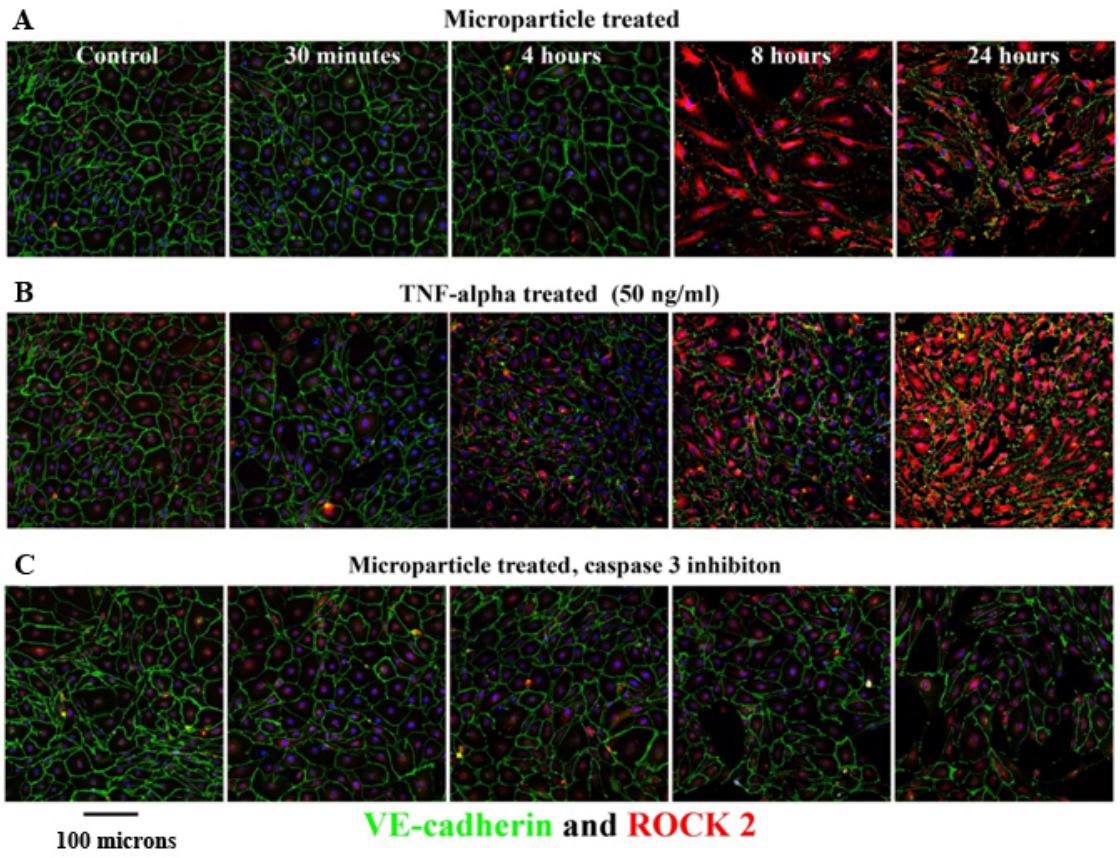
A
Microparticle treated
Control
30 minutes
4 hours
8 hours
24 hours
B
TNF-alpha treated (50 ng/ml)
C
Microparticle treated, caspase 3 inhibiton
100 microns
VE-cadherin and ROCK 2

**Figure 4.9**

**Figure 4.9. ROCK II expression in endothelial cells following MPs and TNF-α exposure. (A)** MP treatment of confluent RBMVECs induces a disruption in VE-cadherin and increases the expression of ROCK-II (n = 3). **(B)** Treatment of RBMVECs with TNF-α (50ng/ml) induces the same effects as MP treatment (n = 3). **(C)** Pretreatment of RBMVECs with a caspase-3 inhibitor reduces these effects following MP treatment (Blue: DAPI, n = 3, scale bar = 100 μm).

Pretreatment of the confluent RBMVECs with Y-27632 before exposure to MPs significantly increased cell survival indicating that ROCK is involved in induction of apoptosis, $F(3,15) = 68.34$ ($P < 0.0001$). However, ROCK inhibitor by itself causes a significant increase in apoptosis (Figure 4.10).

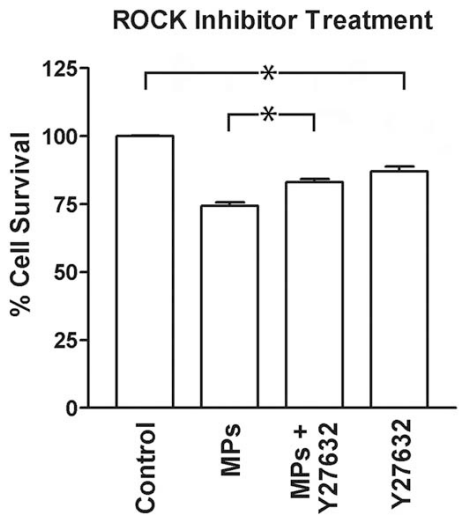
ROCK Inhibitor Treatment
% Cell Survival
125
100
75
50
25
0
*
*
Control
MPs
MPs + Y27632
Y27632

**Figure 4.10**

**Figure 4.10. The effect of ROCK inhibition on MP-induced endothelial cell death.** Y-27632 significantly improves cell survival following exposure to MPs but Y-27632 by itself causes a significant increase in apoptosis (n = 4).

The growth factor VEGF is known to stimulate both the caveolae-mediated transcellular pathway and the paracellular pathway but the initial increase in permeability is due entirely to an increase in caveolae-mediated transcellular transport (Feng et al., 1999; Behzadian et al., 2003). In order to determine if MPs can increase the permeability of endothelial barriers through a transcellular transport, the effect of treatment of RBMVECs with MP was compared with that of VEGF. When VEGF is applied to artificial barriers there is a significant increase in the transport of Evans Blue labeled rat albumin across the barrier at 2 hours and all subsequent time points. MPs do not cause a significant increase over control until 8 and 24 hours, treatment effect: $F(2, 6) = 14.311$ ($P < 0.01$), time effect: $F(10, 70) = 377.58$, ($P < 0.0001$), time*treatment effect: $F(30, 70) = 27.21$ ($P < 0.0001$). (Figure 4.11) The MP effect is significantly greater than VEGF effect at 24 hours.

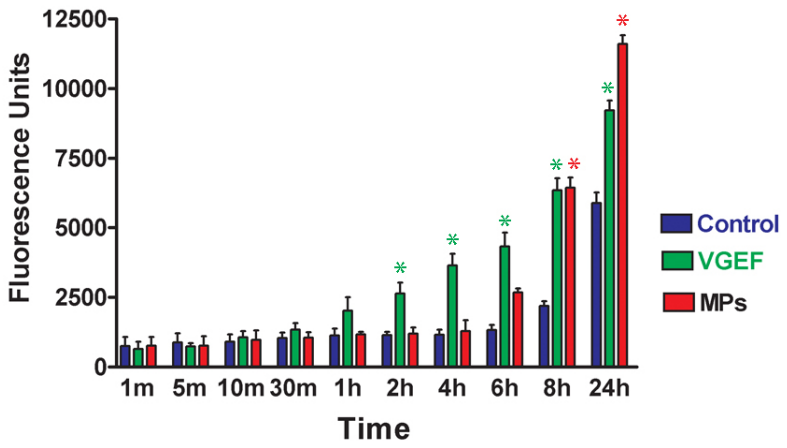
12500
10000
7500
5000
2500
0
Fluorescence Units
1m
5m
10m
30m
1h
2h
4h
6h
8h
24h
Time
Control
VGEF
MPs

**Figure 4.11**

**Figure 4.11. MPs and endothelial transcellular transport.** VEGF treatment significantly increases transport of Evans Blue-labeled albumin across endothelial barriers from 2 hours on while MPs do not significantly increase transport over control until 8 hours (n = 3).

**Discussion**

Chronic cerebral hypoperfusion in the rat induced an increase in the number of circulating MPs in the plasma. When MPs were isolated from plasma and applied to RBMVEC barriers the endothelial barrier permeability was increased. A role for MPs in induction of brain endothelial dysfunction and alterations in BBB permeability has been described in the pathogenesis of cerebral malaria (Combes et al., 2006). Also, dysregulation of BBB is one of earliest cerebrovascular abnormalities seen in multiple sclerosis and is associated with cytokine-induced shedding of endothelial microparticles into plasma during cerebral endothelial cell activation (Minagar and Alexander, 2003).

Circulating MPs stimulate a proinflammatory process in endothelial cells. These MPs originate from platelets, leukocytes and endothelial cells and stimulation of endothelial cells with MPs from different origins results in the release of cytokines and a rise in expression of adhesion molecules such as intracellular adhesion molecule-1 (ICAM-1), vascular cell adhesion molecule-1 (VCAM-1), and E-selectin that are indicators of proinflammatory responses (Lovern and Verma, 2013). On the other hand, pro-inflammatory stimuli such as TNF-α promote MP release from endothelial cells (Brown et al., 2011; Peterson et al., 2008). Microparticles contain a concentrated set of cytokines such as TNF-α (Mause and Weber, 2010). TNF-α stimulates severe changes in microvascular endothelial cells, including cytoskeletal reorganization, redistribution of junctional protein, production of proinflammatory cytokines and apoptosis (Gnant et al., 2000; Sawant et al., 2013; Wiggins-Dohlvik et al., 2014). In the present study it is clear that MPs generated in the setting of cerebral ischemia are acting as major vectors of TNF-α signaling. Application of a TNF-α inhibitor (SPD-304) reversed the induced

structural and functional change in RBMVECs by circulating MPs. TNF-α is a monomeric type-2 transmembrane protein. This cytokine is inserted into membrane as a homotrimer transmembrane protein and is cleaved by the TNF-α converting enzyme metalloprotease TACE (ADAM17) to release soluble TNF-α (circulating timer), which may then activate TNF receptors. TNFR1 is preferentially activated by soluble TNF and TNFR2 by transmembrane TNF (McCoy and Tansey, 2008). It has been shown that MPs with human atherosclerotic plaques origin hold active TACE/ADAM 17, which cleaves TNF and its receptors TNF-R1 and TNF-R2 (Canault et al., 2007). Pretreatment of circulating MPs with a TACE inhibitor (TAPI-0) before adding them to cultured RBMVECs indicated that TNF-α has to be cleaved off from the MPs membrane and function as a soluble mediator in order to transfer information to endothelial cells. TACE inhibition could protect F-actin by inhibiting pathways not inhibited by the other compounds that have been used in this study. The reason could be that TACE has other functions in addition to activation of TNF-α, such as release of other membrane anchored cytokines (Müllberg et al., 1995). TAPI-0 can also inhibit other metalloproteases such as MMP-2 that can cleave F-actin (Wu and Huang, 2003).

Tumor necrosis factor-related apoptosis-inducing ligand (TRAIL) is a member of TNF family that is expressed in most normal tissues and induces apoptosis primarily in tumor cells (Hu et al., 1999). The role of TRAIL in MPs formation from endothelial cell has been indicated following thrombin stimulation of human endothelial cell line (Simoncini, et al., 2009). Thrombin induced the expression of both transmembrane and soluble forms of TRAIL, and knockdown of TRAIL expression reduced the ability of cell supernatants to generate MPs. In addition, MP release was induced by exogenous soluble

Trail. Shock et al. (2014) have also shown that pretreatment of NRKs with a neutralizing antibody to TRAIL before MP treatment induced a significant increase in cell survival. However, pretreatment of RBMVECs with anti-TRAIL antibody did not protect the endothelial barrier function in this study, although there appeared to be less adherens junction disruption. Therefore, TRAIL signaling does not have an important role in MP-induced hyperpermeability following MP treatment of cultured RBMVECs.

It has been reported that MPs derived from human umbilical vein endothelial cells and human platelets contain caspase-3 (Abid Hussein et al, 2005; Böing et al, 2008). Circulating MPs can induce apoptosis in a concentration-dependent manner in esophagus and pancreas carcinoma cells by the transfer of caspases into target cells (Schneider et al., 2012). On the other hand, high concentration of TNF-α (>10ng/ml) induces increased paracellular permeability and apoptosis in human brain endothelial cell line (hCMEC/D3) due to caspase-3/7 activation (Lopez-Ramirez et al., 2012). The fact that a caspase-3 inhibitor also significantly inhibited the MPs effect on RBMVEC function (endothelial permeability) and reduced disruption of VE-cadherin, as determined by IF in this study, indicates that caspase-3 signaling is involved in MPs-induced increase in permeability of cultured RBMVECs.

Rho associated protein kinases (ROCK or Rho kinase) are key regulators of actin cytoskeletal dynamics and promote the formation of stress fibers and focal adhesions. ROCK stabilizes actin microfilaments and promotes cellular contraction. RhoA/ROCK can be activated by TNF-α, which in turn contributes to endothelial barrier dysfunction in brain microvascular endothelial cells through F-actin rearrangement (Peng et al., 2011). ROCK proteins are also cleaved following caspase 2 and 3 activity in early apoptosis,

which induces phosphorylation of myosin light chain (MLC) and contraction of cortical actin filaments. This early phase of apoptosis where adherent cells begin to retract away from their neighbors is dependent on ROCK/MLC signaling, which leads to membrane blebbing (Street and Bryan, 2011). Since MP formation starts with the outward blebbing of the plasma membrane, cytoskeletal re-organization is an essential step in MP formation (Burger et al., 2013). Rho-kinase activity is involved in endothelial cell vesiculation and endothelial microparticle (EMPs) release. It has been shown that INF-α induces apoptosis in human pulmonary microvascular endothelial cells, which is accompanied by EMPs release following ROCK induced F-actin rearrangement (Gao et al., 2012). Rho-kinase ROCK-II is also required for the generation of EMPs from thrombin stimulated microvascular endothelial cell line 1 (HMEC-1), and pretreatment of HMEC-1 with a caspase-2 selective inhibitor Z-VDVAD-FMK before exposure to thrombin prevents ROCK-II cleavage and inhibits the thrombin-induced EMP release (Sapet et al., 2006). The present study indicates increased expression of ROCK-II following MP treatment of cultured RBMVECs, which could be reduced by pretreatment of RBMVECs with a caspase-3 inhibitor before MP treatment indicating the role of TNF-α and caspase-3 in enhanced ROCK-II expression. Although ROCK II is cleaved by caspase-2 (Ark et al, 2010), it has been demonstrated that activation of caspase-3 results in cleavage and activation of caspase-2 (Cullen and Martin, 2009). Therefore, it seems that activation of TNF-α signaling through activation of TNF-R1 leads to activation of caspase-2 and caspase-3 which in turn results in increased expression of ROCK II in endothelial cells. Also, protection of the endothelial barrier provided by pretreatment of endothelial cells with a ROCK inhibitor indicates a role for ROCK activation in increased

endothelial permeability following MP treatment. It has shown that basal Rho kinase activity contributes to the regulation of endothelial barrier integrity (van Nieuw Amerongen et al., 2007). Therefore, the observed reduction in endothelial permeability could be expected following pretreatment of RBMVECs by the ROCK inhibitor alone. Pretreatment of MPs with the ROCK inhibitor prior to adding to cultured endothelial cells also reduced the effect of MPs on TEER suggesting that MPs may deliver activated ROCK proteins to target cells.

In conclusion, the increase in permeability of artificial microvascular endothelial barriers following exposure to MPs generated during BCCAO appears to be due primarily to apoptosis. There is no early increase in caveolae-mediated transcellular transport and large gaps develop between adjacent cells as they lose cell volume. It is suggested that apoptosis is induced by activation of TNF-α receptors, which activates caspase-3 and Rho kinases in endothelial cells, and also through delivery of activated caspase-3 and Rho kinases to endothelial cells by MPs.

# Chapter 5:

# Phosphodiesterase inhibition protects the BBB from chronic cerebral ischemia

**Collaborator Contribution**

**Hamidreza Edrissi: S**urgeries were performed with assistance of Dr. Charlie Thompson in blood and tissue collection and MP extraction. Transcellular endothelial resistance measurements were performed with assistance of Dr. Sarah Schock. Immunohistochemistry was performed with the assistance of Dr. Charlie Thompson. Tapered beam test and cilostazol administration to the rats performed by author.

**Sarah C. Schock:** All cell cultures and LDH assays were performed by Dr. Sarah Schock.

**Antione M Hakim:** Dr. Antoine Hakim supervised the work and provided financial support.

**Charlie S. Thompson:** Dr. Charlie Thompson contributed in the surgeries and immunohistochemistry and supervised the project.

**Abstract**

Cilostazol, a type III phosphodiesterase inhibitor, has antiapoptotic effects and prevents white matter vacuolation and rarefaction induced by BCCAO in rats. It also protects barrier integrity of different endothelial cell lines and reduces the level of platelet MPs (PMPs) in plasma of patient with noninsulin dependent diabetes mellitus. In this study the protective effect of cilostazol administration on increased BBB permeability following BCCAO was investigated by measuring Evans Blue extravasation in brain tissue. The effects of treatment on plasma toxicity, cerebral white matter rarefaction and glial activation and gait disturbances were also evaluated. In addition, the effect of cilostazol on *in vitro* endothelial barriers was studied. It was determined that cilostazol could improve the increased BBB permeability, gait and visual impairement and microglial activation in optic tract following BCCAO. Cilostazol induced trends towards reductions in WMLs in optic tract and plasma toxicity in 2VO rats at 2 weeks following surgery. It also reduced apoptosis and TEER reduction induced by MP treatment of RBMVECs. It is concluded that circulating MPs may play a role in BBB dysfunction, as well as, motor and visual impirement in this rat model of chronic cerebral hypoperfusion. Cilostazol, a selective phophodiestrase inhibitor, is suggested to reverse these consequences of BCCAO through a reduction of plasma toxicity or number of circulating MPs.

## Introduction

Results of the present study indicate that MPs mediate many of the effects of cerebral ischemia on endothelial cells. The plasma of rats exposed to chronic cerebral hypoperfusion (CCH) becomes more toxic to cultured endothelial cells, presumably because there are more MPs present (Schock et al., 2014). A number of compounds have been reported to improve outcome following the induction of cerebral ischemia *in vivo* (Wang et al., 2010; Lee et al., 2006; Cho et al., 2006; Zhang et al., 2015) and it is logical to ask if these compounds reduce toxicity of circulating MPs, presumably by reducing the MP load.

Cilostazol is a type III phosphodiesterase inhibitor and has been reported to be neuroprotective against apoptotic white matter damage and cognitive impairment in rats that received BCCAO (Lee et al., 2006; Watanabe et al., 2006; Lee et al., 2007; Kwak et al., 2012). Cilostazol has also been shown to activate maxi-K channels that protect neurons from excitotoxicity. Cilostazol also suppresses production of the intracellular reactive oxygen species (ROS) and cytokines such as TNF-α and IL-1β (Shin et al., 2004).

Cilostazol is a quinolinone derivative that was developed as a selective inhibitor of cyclic nucleotide phosphodiesterase III (PDE III) ($IC_{50}$ = 200 nM) (Kimura et al., 1985; Rondina and Weyrich, 2012). It is an antithrombotic and vasodilating drug (Dawson et al., 1998). Cilostazol increases intracellular cyclic AMP levels in platelets and blood vessels by suppression of cyclic AMP degradation, which leads to inhibition of platelet aggregation and dilation of vessels (Kimura et al., 1985). Its chemical name is 6-[4-(1-cyclohexyl-1H-tetrazol-5-yl) butoxy]-3, 4-dihydro-2(1H)-quinolinone and its

molecular weight is 369.47 (Lee et al., 2007). The molecular formula of cilostazol is C20H27N5O2. Cilostazol is absorbed after oral administration. Cilostazol is metabolized in humans by hepatic cytochrome P-450 enzymes, CYP3A4, CYP2D6 and CYP2C19, and four major metabolites are found, two of which are active (Abbas et al. 2000; Hiratsuka et al. 2007). However, the CYP isoforms that metabolized cilostazol in rats are still unknown (Kamada et al., 2011). These metabolites are mainly excreted in the urine. Elimination half-lives of cilostazol and its active metabolites are about 11 to 13 hours (Bhatt et al., 2015). Cilostazol is 95 % protein bound, mostly to albumin (Suri et al., 1998). Cilostazol is eliminated mainly by metabolism and subsequent excretion of metabolites in urine. The main route of elimination is via the urine (74%) and excretion in feces (20%).

Cilostazol has been used in different experimental models of cerebral ischemia in rodents with different concentrations and different routes of administration such as intravenous, intraperitoneal and oral, from10 to 60 mg/kg (Lee et al., 2007). In rats, around 90% of the cilostazol dose is absorbed after oral dosing at 10 mg/kg (Akiyama et al., 1985). *In vitro*, cilostazol has been applied from 0.1 to 100 $\mu$M (Hong et al., 2003).

Although cilostazol has been shown to support barrier integrity in rat brain capillary endothelial cells (Horai et al., 2013), and ameliorates ethanol induced endothelial dysfunction in human brain microvascular endothelial cells (Takagi et al., 2014), there is no evidence that cilostazol could protect BBB in a chronic cerebral ischemic state *in vivo*. There is also no effective neuroprotective therapy available for ischemic white matter lesions (WML). It has been suggested that inflammation plays an important role in etiology of WML induced by chronic cerebral hypoperfusion (CCH)

(Duan et al., 2009) and application of anti-inflammatory or anti-apoptotic agents can protect against 2VO-induced WML and cognitive impairment (Wang et al., 2010; Lee et al., 2006).

The purpose of these studies was to determine if cilostazol protects cultured RBMVECs against MP toxicity. The specific objectives were to determine if cilostazol administration to rats subjected to BCCAO for 24h reduces plasma toxicity and to verify the impact of cilostazol pretreatment of cultured RBMVECs on MP-induced endothelial cell dysfunction. Other objectives were to evaluate the impact of cilostazol administration on BBB integrity and to assess the effect of cilostazol treatment on gait performance using the tapered beam test and on the severity of lesions in vulnerable white matter regions (optic tract and corpus callosum) following BCCAO. Plasma toxicity was measured at 2 weeks following BCCAO in order to determine the association between the numbers of circulating MPs and the pathological consequences of cerebral ischemia.

**Materials and Methods**

*Cilostazol and MPs* – In order to determine if cilostazol administration to 2VO rats protects cultured RBMVECs against MPs isolated from plasma four groups of male Long Evans rats (200-225g) received 2VO or sham surgery (Chapter 2). One group of rats that received 2VO surgery were injected with cilostazol (Cayman, 25mg/kg dissolved in 20% DMSO in saline) through IP injection when the rats were anesthetized before surgery (n = 7). Other groups received 2VO surgery and vehicle (n = 5), sham surgery (n = 4), or sham surgery and cilostazol injection (n = 4). Transcardial perfusion was

performed at 24h following surgery and circulating MPs was isolated from rats' plasma as described earlier (Chapter 4).

*Cilostazol and BBB permeability* - In order to evaluate the impact of cilostazol administration on BBB integrity following BCCAO groups of male Long Evans rats (200-225g) that underwent sham or 2VO surgery received cilostazol (60 mg/kg) mixed with 1 g cookie dough (Corbett et al., 2012) or vehicle before anesthesia and daily following surgery for 72 h orally. Then, they received Evans Blue injection through femoral vein one hour before transcardial perfusion at 72 h. The amount of dye present in brain homogenates was determined by its fluorescence (Chapter 2).

*Cilostazol and gait* - In order to assess the effect of cilostazol treatment on gait performance following BCCAO male Long Evans rats (200-225g) that received 2VO or sham surgery were administered cilostazol (60 mg/kg oral) before surgery and for 14 days daily following surgery. The rational to use oral *vs.* IP route is ease of use and the fact that multiple IP injections increase the risk of infection and induce anxiety, which is not desirable for tapered beam test. Cilostazol was mixed with 1 g cookie dough (Corbett et al., 2012). The tapered beam test was performed prior to surgery and at days 7 and 14 after surgery to assess gait disturbance.

*Cilostazol and visual impairement* - To evaluate the impact of BCCAO and cilostazol administration on visual system all rats were trained once and tested (one trial) in the water maze with an elevated platform (Tian et al., 2014) that could be visually located at 7 days following surgery. The rats' pupils were also examined under a bright light before euthanizing them.

*Kulver barrera and Luxol fast blue staining* - After transcardial perfusion and fixation with 4% paraformaldehyde (PFA), brains were removed and placed in a rat brain matrix. One slice was made at the level of the optic chiasm and a second 2 mm slice behind the optic chiasm level. Brain sections were kept in 4% PFA for 48 hours and then washed with 1% phosphate buffered saline (PBS). The anterior forebrain was sent to the pathology department for paraffin embedding. Culver Barrera and Luxol fast blue staining were used to determine white mater rarefaction. Images were acquired using Axiophot microscope (Zeiss), and image analysis performed using Northern Eclipse software under 10 × objectives. The images were captured as gray scale (16 bit) and the whole area of optic tract or medial part of corpus callosum was selected. Then the areas that showed white matter rarefaction and vacuolation and did not take up the Kulver barrera or Luxol fast blue stain were measured by threshold to the background and recorded as % object area of rarefied fibers of the total selected area.

*Immunofluorescence* - The 2 mm thick coronal sections were immersed in 20% sucrose for 48 h and then were frozen and kept in -80°C. Double staining was performed on 12 μm thick coronal sections using a rabbit polyclonal antibody against ionized calcium-binding adaptor molecule (Iba-1, 1:500; Wako Pure Chemicals; a marker of active microglia), and a mouse monoclonal antibody against GFAP (glial fibrillary acidic protein, an astrocyte marker, 1:500). Images were acquired using a Ziess Meta 510 confocal microscope and image analysis performed using Northern Eclipse software under 20 × objectives. Images captured as gray scale (16 bit) with a fixed exposure and intensity measured as % object area of immunoreactive cells of the total selected area (Juma et al., 2011).

Endothelial cell culture, TEER measurement, immunofluorescence for *in vitro* experiments and cell death (LDH) assay were performed as described in Chapter 4. The LDH assay was used as a cell death test instead of the TUNEL assay, because in the TUNEL assay cell death could not be quantified as easily as in the LDH assay and also there is less variability in results obtained using LDH assay.

*Statistical analyses* - Statistical analyses were performed using SPSS 21 and graphs were made by Graph Pad Prism 3 software. Data were analyzed with one-way ANOVA or two-way ANOVA repeated measures followed by a Bonferroni post hoc test and presented as means ± standard error. Probability (P) values of less than 0.05 were considered significant.

**Results**

Results of the LDH assay indicated that MPs isolated from the plasma of the 2VO group that was treated with cilostazol were significantly less toxic than those isolated from plasma of the 2VO vehicle group, when they were used to treat confluent RBMVECs, $F(3, 15) = 25.01$ ($P < 0.0001$) (Figure 5.1A). Pretreatment of confluent RBMECs with cilostazol (10 μM) before MP treatment significantly reduced the cell death as well, $F(3, 15) = 15.12$ ($P < 0.001$) (Figure 5.1A).

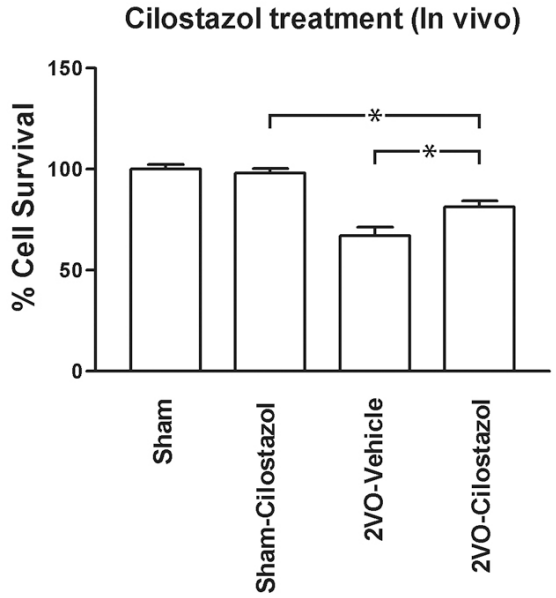


**Figure 5.1A**

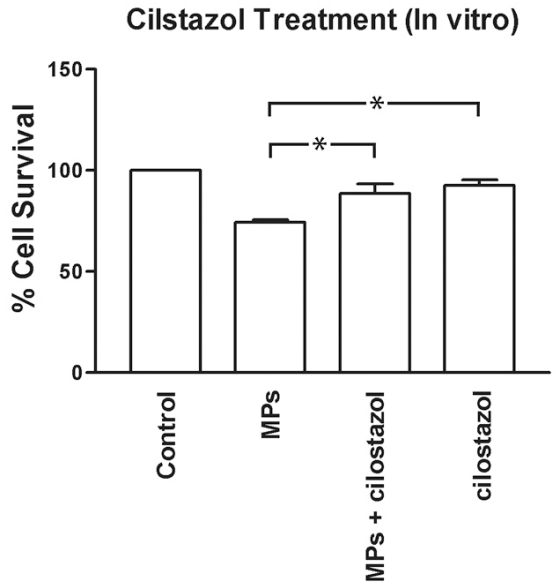


**Figure 5.1B**

**Figure 5.1. Cilostazol protects cultured RBMECs against MP-induced cell death.** (A) Cilostazol treatment significantly reduces plasma toxicity compared to the 2VO-vehicle group. This drug does not induce any effect in the sham group that received cilostazol (n = 4). **(B)** Pre-treatment of RBMVECs with cilostazol (10 μM) reduces the induced cell death by MPs (n = 4). Cytotoxicity is determined by measuring wavelength absorbance at 490 nm. Cell death is expressed as a percentage of experimental LDH release/maximal LDH release.

Treatment of rats subjected to 2VO with cilostazol significantly reduced the effect of circulating MPs isolated from their plasma on endothelial barrier permeability at 24h , treatment effect: $F(3, 7) = 1.27$ ($P > 0.05$), time effect: $F(10, 70) = 18.37$ ($P < 0.0001$), time*treatment effect: $F(30, 70) = 4.90$ ($P < 0.0001$) (Figure 5.2A). Treatment of the confluent RBMECs with MPs isolated from plasma of the 2VO group that received cilostazol reduced the disruption in VE-cadherin (Figure 5.2B).

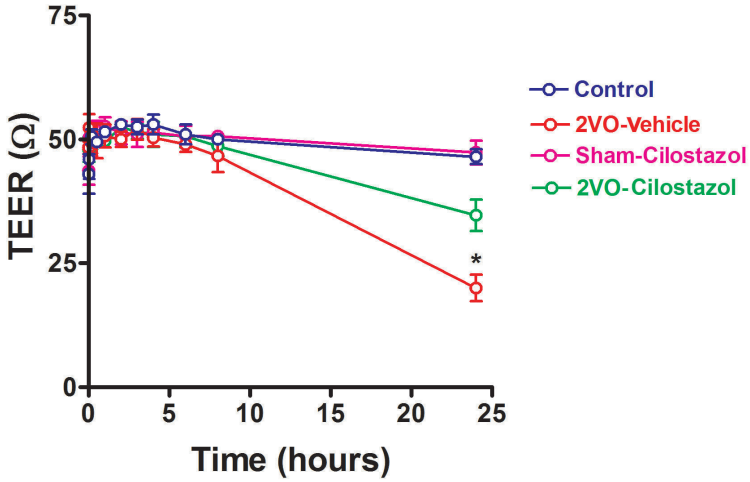


**Figure 5.2A**

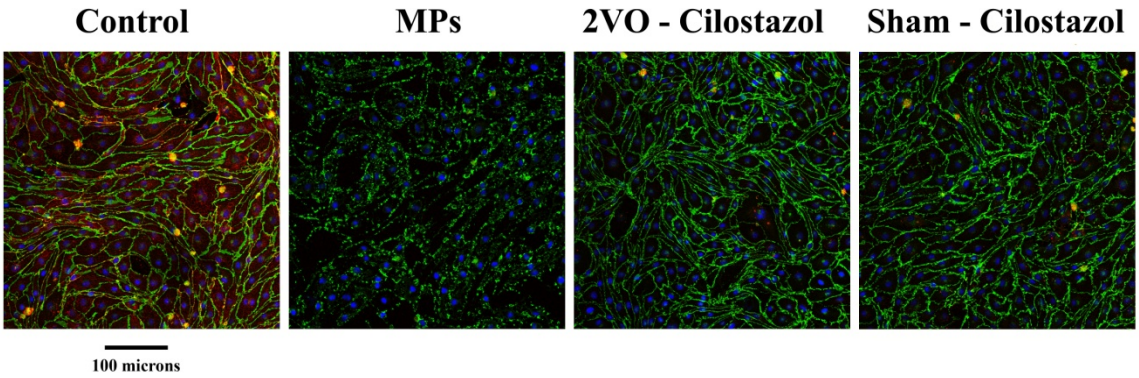


**Figure 5.2B**

**Figure 5.2. Cilostazol treatment of rats subjected to BCCAO. (A)** Circulating MPs isolated from plasma of cilostazol treated 2VO rats cause a smaller increase in endothelial permeability than MPs isolated from plasma of vehicle treated 2VO rats (n = 3). **(B)** Treatment of confluent RBMECs with MPs isolated from plasma of 2VO rats that received cilostazol, reduces the disruption in VE-cadherin (green) at 24 h following treatment (n = 3, scale bar = 100 μm).

In addition, the confluent RBMECs were pretreated with cilostazol (1 μM) before MP treatment, to examine if cilostazol can strengthens barrier integrity in RBMECs. The results indicated that cilostazol significantly reduced the effect of MPs on endothelial barrier permeability at 24 h, treatment effect: $F(3, 7) = 1.26$ ($P > 0.05$), time effect: $F(10, 70) = 27.86$ ($P < 0.0001$), time*treatment effect: $F(30, 70) = 7.139$ ($P < 0.0001$) (Figure 5.3A). Cilostazol also reduced a disruption in VE-cadherin staining (Figure 5.3B).

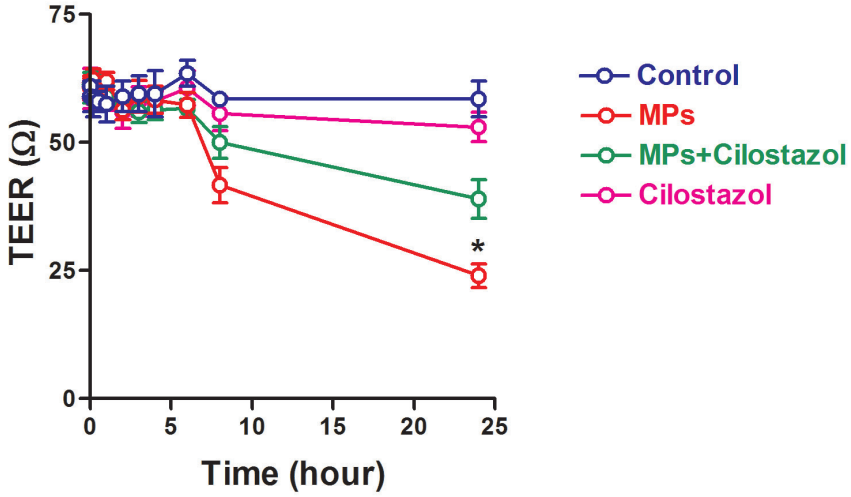


**Figure 5.3A**

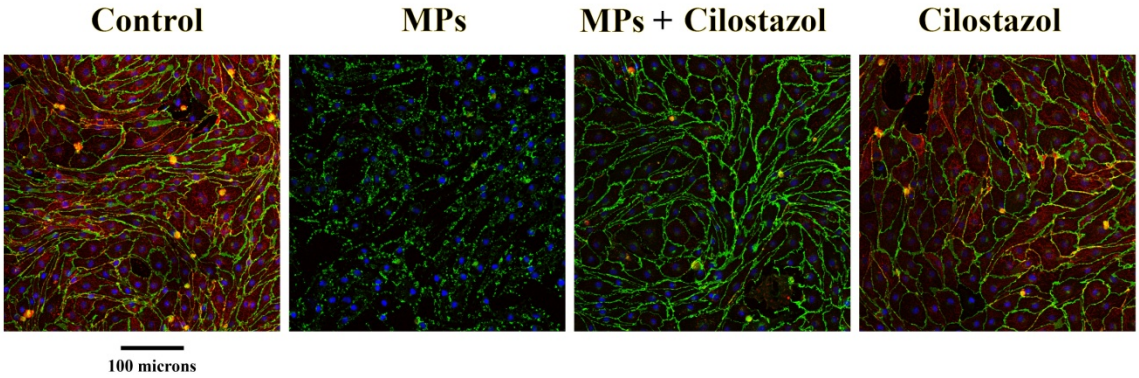


**Figure 5.3B**

**Figure 5.3. Cilostazol reduces MP-induced barrier dysfunction in cultured RBMECs. (A)** Pretreatment of confluent RBMVECs with cilostazol significantly reduces an increase in endothelial permeability at 24 h following MP treatment (n = 3). **(B)** Pre-treatment of confluent RBMECs with cilostazol (1 μM) prior to addition of MPs reduces disruption in VE-cadherin (green, n = 3, scale bar = 100 μm).

Rats that received cilostazol treatment, showed a significantly lower increase in BBB permeability following BCCAO (Figure 5.4) than the vehicle treated group, $F(4, 26) = 23.05$ ($P < 0.0001$).

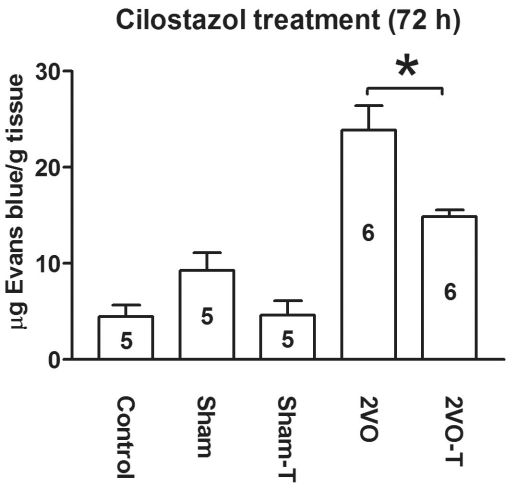
Cilostazol treatment (72 h)
μg Evans blue/g tissue
30
20
10
0
*
5
5
5
6
6
Control
Sham
Sham-T
2VO
2VO-T

**Figure 5.4**

**Figure 5.4. Cilostazol treatment protects BBB integrity following BCCAO.** Adminstration of cilostazol (60 mg/kg, oral) significantly reduces Evans Blue extravasation at 72h following BCCAO (control: un-operated rats, 2VO-T: cilostazol-treated 2VO group, sham-T: cilostazol-treated sham group).

There was a significant difference between 2VO and other groups in time to cross the beam at 7 and 14 days following surgery, group effect: $F(4, 25) = 12.26$ ($P < 0.0001$), time effect: $F(1, 25) = 1.05$ ($P > 0.05$), time*group effect: $F(4, 25) = 8.87$ ($P < 0.0001$) (Figure 5.5A). However, there was no difference in number of foot faults among the groups at any time point following surgery (Figure 5.5B). The 2VO group that received cilostazol (2VO-T) was significantly faster than the 2VO group, while it was not different from un-operated control, sham and sham group that received cilostazol (sham-T).

The rationale to choose 7 days following surgery as the earliest time point was that 2VO operated rats usually lose weight during the first few days and return to normal by one week following surgery. We chose 14 days as the last time point because we wanted to study the effect of BBB dysfunction on gait disturbances and our earlier data showed increased permeability of BBB for 2 weeks following 2VO surgery.

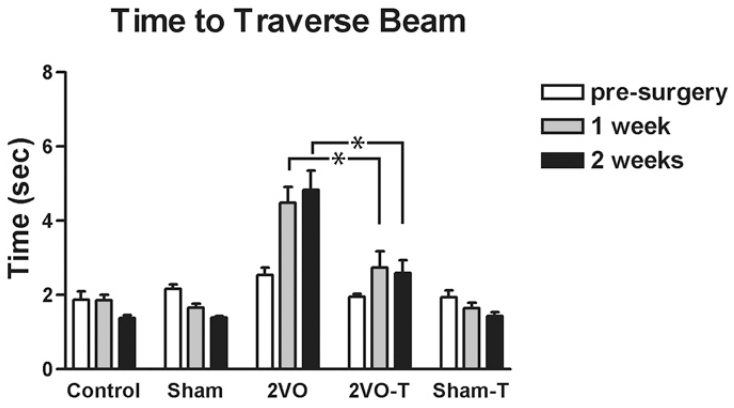


**Figure 5.5A**

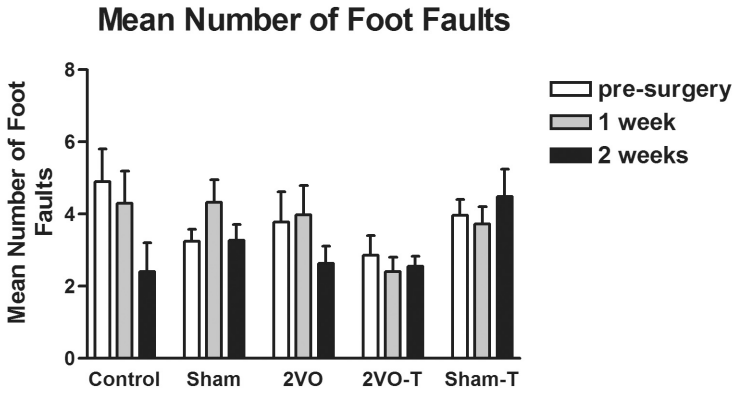


**Figure 5.5B**

**Figure 5.5. Cilostazol improves gait disturbance following BCCAO. (A)** There is a significant difference between 2VO and 2VO-T groups in time to cross the beam after surgery. Also, the 2VO treated group are significantly slower than unoperated control, sham and sham-T groups. **(B)** There is no difference among the groups in the number of foot fault (control or un-operated control: n = 2, sham: n = 5, 2VO: n = 8, 2VO-T or cilostazol-treated 2VO group: n = 10, sham-T or cilostazol-treated sham group: n = 5).

White matter areas that have been proven to be vulnerable to cerebral hypoperfusion in this rat model of CCH were stained with Kluver Barrera and Luxol fast blue. The results indicted white matter rarefaction and vacuolation in the optic tract of 2VO rats are reduced upon treatment with cilostazol, as indicated by both Kluver-Barrera staining, $F(2, 21) = 5.358$ ($P < 0.05$, Figure 5.6) and Luxol fast blue staining, $F(2, 21) = 4.052$ ($P < 0.05$, Figure 5.7), although it did not reach statistical significance. There was less intense change in corpus callosum with no significant difference among the groups.

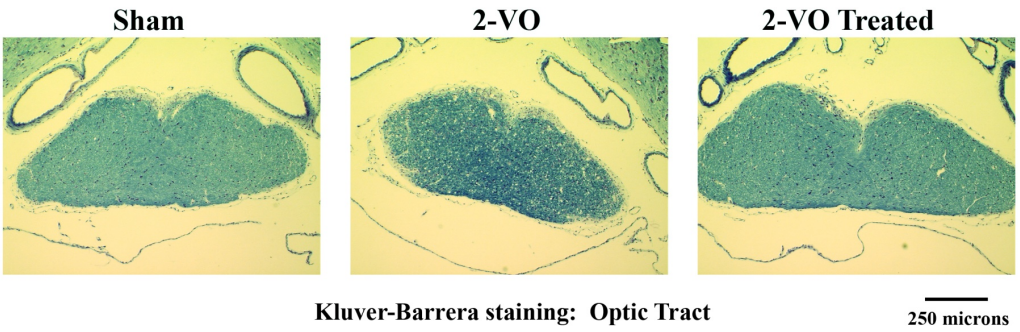
Sham
2-VO
2-VO Treated
Kluver-Barrera staining: Optic Tract
250 microns

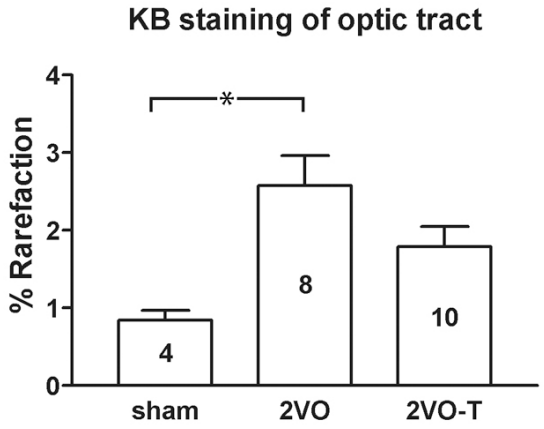
KB staining of optic tract
% Rarefaction
0
1
2
3
4
*
4
8
10
sham
2VO
2VO-T

**Figure 5.6**

**Figure 5.6. KB staining of optic tract.** White matter rarefaction and vacuolation in optic tract are improved by cilostazol treatment but do not reach statistical significance (scale bar = 250 μm).

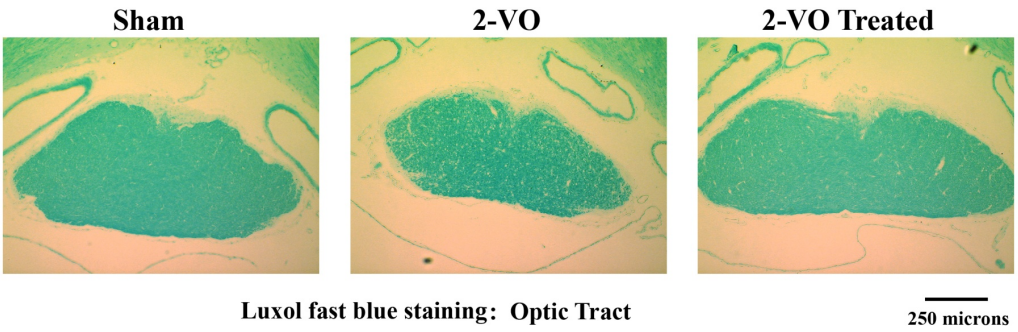
Sham
2-VO
2-VO Treated
Luxol fast blue staining: Optic Tract
250 microns

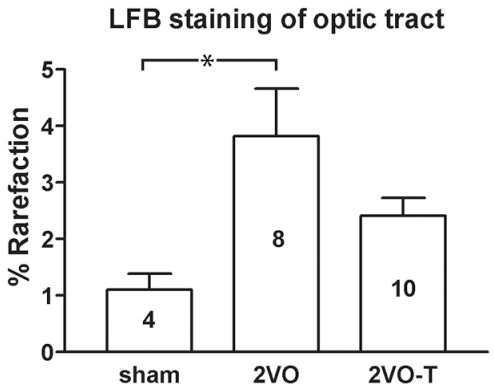
LFB staining of optic tract
% Rarefaction
0
1
2
3
4
5
*
4
8
10
sham
2VO
2VO-T

**Figure 5.7**

**Figure 5.7. LFB staining of optic tract.** White matter rarefaction and vacuolation in optic tract are improved by cilostazol treatment but do not reach statistical significance (scale bar = 250 μm).

Since the optic tract was affected, the rats were examined to see if they have any visual disturbance at one week after surgery. The rats were examined using an elevated platform in water maze a week after surgery to determine if they can locate the platform and climb on it in 2 minutes. All the rats in sham group could find the platform compared to 50% in vehicle group and 90% in cilostazol treated group (Figure 5.8A). It was also determined that the rats in sham or sham treated group had a constricted pupil when exposed to bright light at 2 weeks following surgery (n = 5). However, 37.5% of the rats in 2VO group (n = 8) and 60% in cilostazol treated group (n = 10) had a constricted pupil (Figure 5.8B).

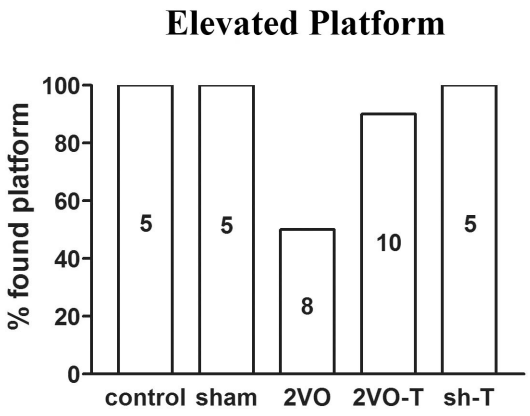


**Figure 5.8A**

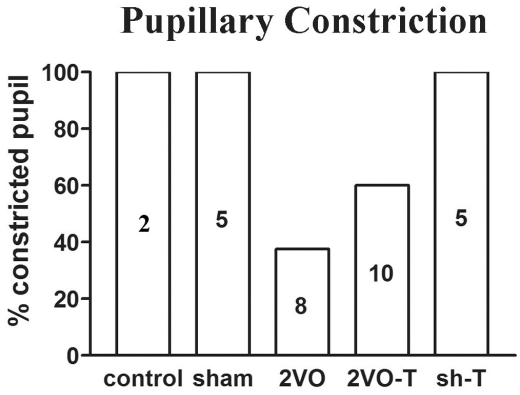


**Figure 5.8B**

**Figure 5.8. Visual disturbances following BCCAO. (A)** All rats in the sham group (n = 5) and the sham-treated group with cilostazol (sham-T, n = 5) can find the platform compared to 50% in 2VO group and 90% in 2VO group treated with cilostazol (2VO-T). **(B)** 37.5% of the rats in 2VO group (n = 8) and 60% in cilostazol treated group (n = 10) have a constricted pupil. Note that there are no error bars because the experimental animals displayed either constricted or dilated pupil.

In order to determine if visual disturbance affected performance of the rats on the tapered beam test, 2VO and 2VO-T rats were divided into groups based on the pupillary dilatation. The results indicated that there was a significant difference between 2VO rats with constricted pupils (n = 3) and the ones with dilated pupils (n = 5) at 7 and 14 d following surgery. Although, 2VO rats with constricted pupils were significantly slower than 2VO-T rats with constricted pupils (n = 6), they were not different from 2VO-T rats with dilated pupils (n = 4). Furthermore, 2VO-T rats with dilated pupils were not different from 2VO rats with dilated pupils (n = 5) at 7 d, but they were significantly faster at 14 d following surgery. It is worth noting that all 2VO rats with constricted and dilated pupils were significantly slower than sham rats, group effect: $F(6, 23) = 31.52$ ($P < 0.0001$), time effect: $F(2, 46) = 28.03$ ($P < 0.0001$), time*group effect: $F(12, 46) = 28.90$ ($P < 0.0001$) (Figure 5.9).

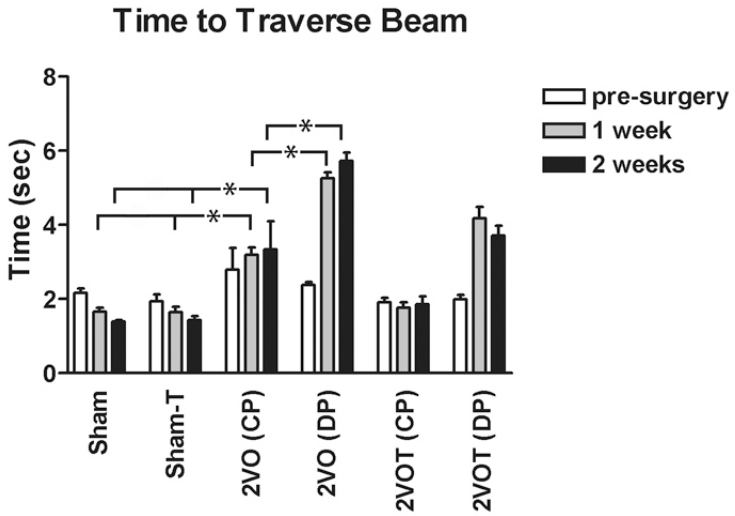
Time to Traverse Beam
Time (sec)
8
6
4
2
0
pre-surgery
1 week
2 weeks
*
*
*
*
Sham
Sham-T
2VO (CP)
2VO (DP)
2VOT (CP)
2VOT (DP)

**Figure 5.9**

**Figure 5.9. Visual disturbances affect performance of the rats on the tapered beam test following BCCAO.** There is a significant difference between 2VO rats with constricted pupil with 2VO rats with dilated pupil in time to cross the beam after surgery (CP = constricted pupil, DP = dilated pupil; n: sham = 5, sham-T = 5, 2VO (CP) = 3, 2VO (DP) = 5, 2VOT(CP) = 6, 2VOT (DP) = 4).

Microglial activation was detected in the vehicle group by increased number of Iba-1-positive cells that significantly reduced in the cilostazol treated group, $F(4, 19) = 4.591$ ($P = 0.019$) (Figures 5.10A and B). Also, GFAP staining increased in the 2VO group and decreased in the cilostazol treated group but these changes did not reach statistical significance (Figures 5.10A and C). Less intense change albeit not significant, in Iba-1-positive microglia was observed in corpus callosum (Figures 5.11A and B) with no significant difference in GFAP staining among the groups (Figures 5.11A and C).

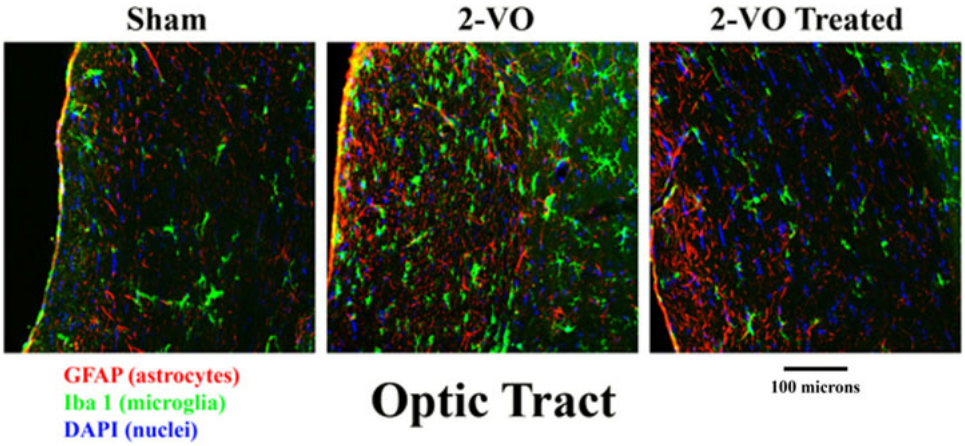


**Figure 5.10A**

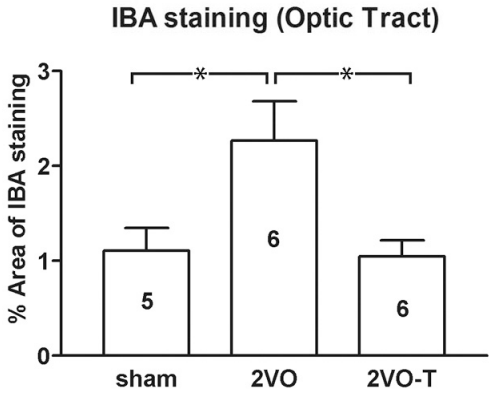


**Figure 5.10B**

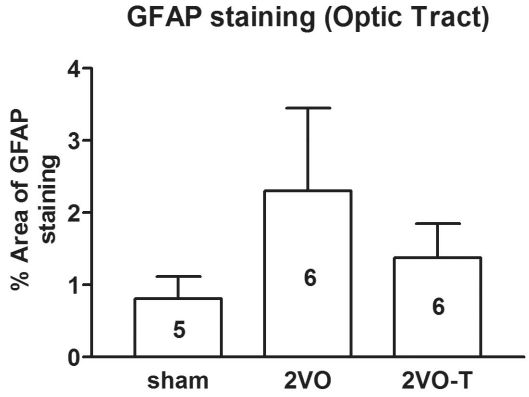


**Figure 5.10C**

**Figure 5.10. Effects of cilostazol treatment on microgliosis and astrogliosis in the optic tract following BCCAO. (A)** Immunostainig of Iba-1 and GFAP in the optic tract of sham, 2VO and 2VO-T rats. **(B)** Microglial activation is observed in 2VO group and reduced in ciloastazol treated group. **(C)** A trend towards astrogelial activation is observed in the 2VO group with a trend towards a reduction in ciloastazol treated group, but no significant difference is observed among the groups (scale bar = 100 μm).

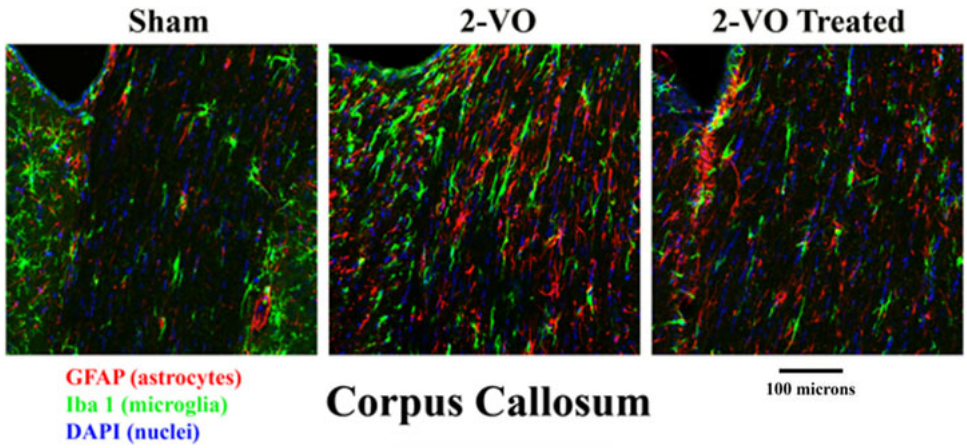


**Figure 5.11A**

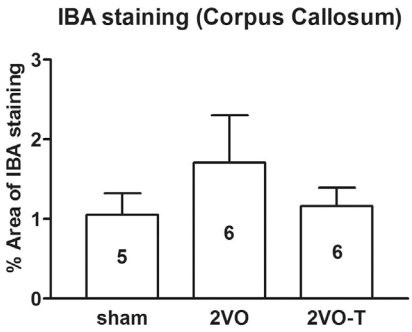


**Figure 5.11B**

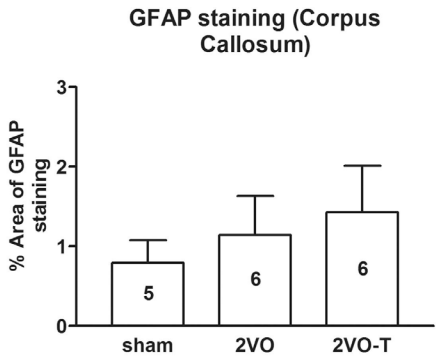


**Figure 5.11C**

**Figures 5.11. Effect of cilostazol treatment on microgliosis and astrogliosis in corpus callosum following BCCAO. (A)** Immunostainig of Iba-1 and GFAP in the corpus callosum of sham, 2VO and 2VO-T rats. **(B)** Less intense albeit non significant microglial activation is observed in 2VO-T group compared to the 2VO group. **(C)** No difference in GFAP staining is detected among the groups (scale bar = 100 μm).

In order to determine the relationship between circulating MPs and the pathological consequences of BCCAO (14d), plasma toxicity was measured (as a marker of circulating MP number) using the LDH assay by isolating and pooling MPs from the plasma of the rats from sham, sham-T, 2VO and 2VO-T groups and treatment of RBMVECs culture with MPs. The results indicated that MPs isolated from 2VO group induced significantly more cell death than MPs isolated from other groups in RBMVECs culture, $F(4, 19) = 4.591$ ($P = 0.019$). This effect was reduced in 2VO-T group (cilostazol treated), while it did not reach statistical significance (Figure 5.12).

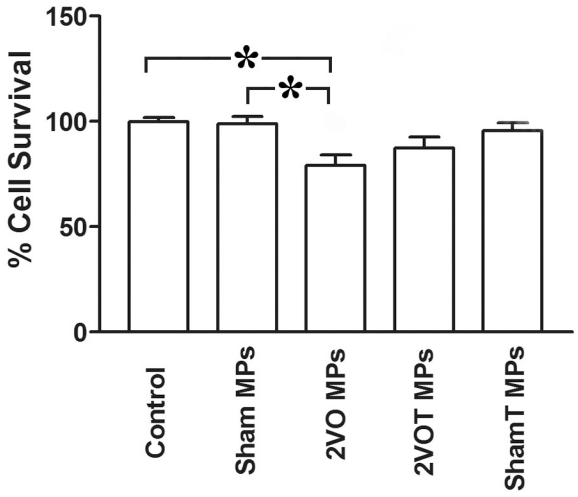
150
100
50
0
% Cell Survival
*
*
Control
Sham MPs
2VO MPs
2VOT MPs
ShamT MPs

**Figure 5.12**

**Figure 5.12. Effect of cilostazol treatment on plasma toxicity following BCCAO.** Plasma toxicity increases in vehicle group and reduces by cilostazol treatment (n = 4). Control is endothelial cells without MP treatment.

**Discussion**

In this study administration of cilostazol could reduce the plasma toxicity in rats subjected to 2VO for 24h and prevent an increase in endothelial barrier permeability following treatment of cultured RBMECs with MPs isolated from plasma, suggesting that cilostazol may reduce the number of circulating MPs following BCCAO in rats. Cilostazol could also reduce the MP-induced cell death and increased endothelial barrier permeability when cultured RBMECs were pretreated with cilostazol. Other studies have also indicated the protective effect of cilostazol on endothelial cells. Cilostazol reduced neuronal damage by suppressing apoptotic cell death (Lee et al., 2008), and strengthened barrier integrity in primary rat brain capillary endothelial cells (RBEC) and immortalized human brain endothelial cell line hCMEC/D3 (Horai et al., 2013). It increased TEER and reduced the flux of sodium fluorescein through the RBEC monolayer. Cilostazol also improved TEER in a triple co-culture BBB model (RBEC, rat pericytes and rat astrocytes) following oxygen glucose deprivation (OGD) and re-oxygenation and increased the localization of cytoskeletal F-actin fibers at the cell border (Horai et al., 2013). Torii et al. (2007) have shown that cilostazol could protect human umbilical vein endothelial cell (HUVEC) permeability under hypoxia/reoxygenation (H/R) through the preservation of the actin cytoskeleton and the redistribution of junctional proteins. Although rhodamine-phalloidin staining showed F-actin disassembly following treatment of RBMECs with MPs in current study, pretreatment of the endothelial cells with cilostazol could not preserve actin cytoskeleton. However, cilostazol could recover discontinuous VE-cadherin staining that were induced by MP treatment and improved cell survival. Diverse effects of cilostazol on actin cytoskeleton or junctional proteins

following MP treatment *vs.* OGD/ and re-oxygenation or H/R could be the result of applying different types of cell insult or using different cell lines. The ability of cilostazol to attenuate hyperpermeability of RBMVECs is probably due to its antiapoptotic effect. It has been shown that cilostazol protects HUVECs against induction of apoptosis by LPS or TNF-α (Kim et al., 2006; Lim et al., 2009).

It was determined that cilostazol could improve the increased BBB permeability following BCCAO. Although cilostazol has been reported to tighten the endothelial barrier of post capillary venules from rat mesentery in situ (Sugiura et al., 2014), and reduce permeability of BBB of the ipsilateral hemisphere following focal cerebral ischemic injury in rats (Lee et al., 2004), to best of our knowledge this is the first report that indicates cilostazol can protect BBB integrity in a rat model of chronic cerebral hypoperfusion.

The other major findings were that rats subjected to BCCAO for 14 days expressed a motor impairment as slower gait velocity associated with increased number of vacuoles and marked rarefaction changes in the white matter including optic tract accompanied by increased plasma toxicity, some of which were improved by treatment with cilostazol. Chronic cerebral hypoperfusion induced microglial activation in optic tract, which was significantly reduced by the cilostazol treatment.

Marked white matter lesions in the optic tract and moderate changes in corpus callosum after 14 days in the vehicle group is consistent with other reports (Wakita et al., 1994; Lee et al., 2006) and suggests the possible role of visual disturbance in the performance of 2VO rats in tapered beam test. It has been shown that about 50% of 2VO rats lose their pupillary reflex (Farkas et al, 2007). Davidson et al. (2000) has reported

that pupillary reflex loss occurred within 5 days after surgery, which makes the retina vulnerable to light exposure. Degeneration of the optic nerve has been observed in eyes that lost pupillary reflex at 3, 15 and 90 days after surgery (Stevens et al., 2002). Although retinal ganglion cells were affected as early as 7 days, a severe loss of photoreceptors occurred by 3 to 4 months following surgery (Stevens et al., 2002; Yamamoto et al., 2006). Therefore, chronic BCCAO produces a delayed neuronal cell death in the retina.

The fact that 50% of 2VO rats could not find the elevated platform in the present study is in agreement with the literature, where about half of 2VO rats display an impaired visual ability (Davidson et al., 2000; Stevens et al., 2002). Nevertheless, regarding the gradual progression of retinal damage following BCCAO, it is unlikely that 2VO rats were completely blind at this stage (14 days). In addition, 90% of 2VO-T rats could find the platform despite the fact that 40% had dilated pupil. Therefore, the main pathology is myelin degeneration that was quantified as white matter rarefaction in optic tract. This degeneration was improved, albeit not significantly, by cilostazol administration. We did not examine retinal and thalamic areas for degenerative changes responsible for pupillary reflex and visual impairment. However, the presence of dilated pupils under bright light suggests a reduction of visual acuity that may affect rat performance in motor performance. Therefore, this experiment suggests that BCCAO compromises the gait performance, which is aggravated by impaired visual ability.

It has been shown that microglial activation in the optic tract following BCCAO exacerbates the white matter lesions (WMLs), since the activated microglia produce proinflammatory cytokines such as TNF-α (Wakita et al., 1994; Taupin et al., 1997),

accompanied by enhanced caspase-3 activity, increased TUNEL-positive cells and loss of oligodendroglia, the myelin-forming cells of the brain (Lee et al., 2006). Apoptosis of oligodendrocytes contributes to WMLs, as demonstrated after focal cerebral ischemia in the rats (Tanaka et al., 2001). Cilostazol could reverse the increased number of microglia and decreased number of oligodendrocytes that were observed following BCCAO (Lee et al., 2006). Cilostazol could also reduce TNF-α and caspase-3 immunoreactivity, and TUNEL positive cells in rat WMLs (Lee et al., 2006) and increased cAMP-responsive element binding protein phosphorylation (p-CREB), which induced activation of anti-apoptotic cascade such as upregulation of Bcl-2 following rat chronic cerebral hypoperfusion (Watanabe et al., 2006). Therefore, suppression of microgliosis in optic tract by cilostazol treatment following BCCAO in the present study indicates that cilostazol may ameliorate the apoptotic cell damage and reduce WMLs induced by BCCAO.

The increase in plasma toxicity of the 2VO treated group confirms our earlier observation which demonstrated increased plasma toxicity at different time points up to 6 weeks following BCCAO (Schock et al., 2014). Cilostazol could also induce a trend towards a reduction in plasma toxicity at 14 days following BCCAO that not did reach a statistical significance, suggesting a possible role for circulating MPs in WML formation. On the other hand, cilostazol could reduce significantly plasma toxicity at 24h following BCCAO. This discrepancy could be explained by a trend in reduction of plasma toxicity at later time points following BCCAO (Schock et al., 2014, Appendix I, Figure 1B). Although cilostazol could MPs can be released following activation or apoptosis from cell types such as platelets, leukocytes, microglia (Chahed et al., 2010) and astrocytes

(Bianco et al., 2009). MPs are involved in coagulation, angiogenesis and inflammation. An increase in circulating MPs has been associated with ischemic cerebrovascular accidents, transient ischemic attacks (Cherian et al., 2003; Simak et al., 2006; Doeuvre et al., 2009), and small vessel cerebrovascular disease such as lacunar infarcts and multi-infarct dementias (Lee et al., 1993). As mentioned earlier MPs may be involved in pathogenesis of cerebral malaria and multiple sclerosis through induction of brain endothelial dysfunction and alterations in BBB permeability (Combes et al., 2006; Minagar and Alexander, 2003). Cilostazol decreases the level of PMPs in patients with noninsulin dependent diabetes mellitus (Nomura et al., 1998). We have not determined the origin of circulating MPs or if cilostazol suppresses MPs derived from a specific cell type. Since cilostazol reduced (not significantly) the plasma toxicity, the increased BBB permeability and WMLs in optic tract, it is suggested that circulating MPs may be involved in induction of these pathological changes following BCCAO.

In summary, cilostazol protects BBB integrity, suppresses microgliosis in optic tract and improves the motor impairment following BCCAO. It also induces a trend in reduction of plasma toxicity at 2 weeks following BCCAO that may reflect the ability of cilostazol in reducing the number of MPs. Therefore, circulating MPs may play a role in BBB dysfunction and motor impairment in this rat model of chronic cerebral hypoperfusion.

# Chapter 6

# General Discussion

The research presented in this thesis focuses on the occurrence, mechanisms, factors involved and consequences of BBB dysfunction in the rat model of chronic cerebral hypoperfusion, BCCAO. In Chapter 2 it was determined that BBB permeability was increased following BCCAO. Then the consequence of ischemic injury on motor performance was assessed. The role of transcellular and paracellular pathways through the BBB was also studied in order to reveal the involved mechanism in BBB dysfunction. In the next chapters a variety of factors that may be involved in BBB dysfunction following BCCAO, such as cytokines and MPs were studied. In Chapter 3 the expression of cytokines and chemokines was evaluated in plasma and brain tissue of rats subjected to BCCAO. In Chapter 4 it was determined that MPs generated following surgery, can induce an increase in permeability of confluent RBMVECs. In an *in vitro* model of the BBB the permeability increase was due to an induction of apoptosis and the role of some signaling pathways involved in this effect was studied. In Chapter 5 data are presented that show cilostazol, a type III phosphodiesterase inhibitor, protected the BBB against ischemic injury *in vivo* and also improved endothelial cell barrier integrity following MP treatment *in vitro*. A neuroprotective role of cilostazol was also indicated *in vivo* by its effect on motor impairment and microgliosis in optic tract. In this section, fundamental findings of this research are briefly presented.

**Impact of BCCAO on BBB permeability, TJs and motor performance**

Considering the possible role of BBB dysfunction in the pathogenesis of CSVD, our first question was do BBB permeability changes occur following BCCAO in the rodent model of CSVD? Although some evidence had suggested that BBB permeability

increased during 2-3 days of the acute phase of ischemia after surgery (Ueno et al., 2002, Ueno et al., 2009), the overall timecourse of increased permeability was not determined. The finding that BBB permeability was increased for two weeks following BCCAO suggests that leakage of plasma components into the vessel wall and surrounding brain tissue may be involved in pathological consequences following ischemia.

This finding led to the next question of what the roles of transcellular and paracellular pathways are in induction of BBB dysfunction. Evans Blue dye extravasation into brain tissue was used to measure BBB permeability. Evans Blue is bound to albumin in the plasma. Since albumin is transferred by endothelial caveola (Nag et al., 2011), the expression of caveolin-1 was measured in the brain tissue. There was no difference between sham and 2VO groups. TJs proteins are the main components of BBB that are responsible for paracellular permeability (Dejana et al., 2009). There were no difference between groups in expression of occludin and claudin-5. However, we could detect increased levels of MMP-2 as previously reported (Ihara et al, 2001; Ueno et al, 2002) suggesting that MMP-2 may be involved in increased BBB permeability following 2VO surgery. Since phosphorylation of TJs can increase BBB permeability (Haorah et al, 2007), one possible direction could be measuring of phosphorylated form of these proteins.

Given that some patients with CSVD have mild motor impairments such as gait disturbances (de Laat et al., 2010), the next step was to determine if rats subjected to BCCAO would reveal any gait disturbance using a tapered beam test. The main purpose of this study was to validate this test as a useful tool for study of gait disturbances following CSVD and for evaluating the pharmacological interventions. The results

indicated that ischemic rats are significantly slower than sham operated rats in crossing the beam. There was no difference in number of foot faults. One problem with this experimental design was that rats could learn to grab the beam edges to avoid touching the ledge that is extending beneath the beam, which is considered by experimenter as a foot fault. However, 2VO rats revealed lower gait velocity which is also observed in patients with CSVD.

**Cytokine expression following BCCAO in rat**

The next question was what factors are involved in increased BBB permeability following BCCAO? Regarding the contribution of cytokines and chemokines to inflammatory cell recruitment, BBB dysfunction and tissue injury in animal models of ischemic stroke (Huang et al., 2006), the purpose of this study was to determine if the level of these proteins that regulate inflammatory process are altered in plasma and brain tissue following BCCAO. There are a few clinical studies that relate cytokine levels to silent brain infarction (Hoshi et al., 2005) and lacunar infarction (Nakase et al., 2008). Therefore, another purpose of this study was to determine the temporal profile of cytokines and to find out if they can be used as biomarkers in this model of CSVD.

Although there are few studies which indicate upregulation of individual cytokines and chemokines at certain time points following surgery in animal models of cerebral ischemia, this is the first report that tried to screen the temporal profile of 15 cytokines and chemokines in the plasma and brain tissue at several time points following srgery in a rat model of CCH. Our data are in agreement with other studies which show upregulation of some the proinflammatory cytokines and chemokines in brain tissue

(Plaschke et al., 2001; Duan et al., 2009; Washida et al. 2010). However, we could not find any significant difference in level of these proteins in plasma between sham and 2VO groups. This discrepancy with other studies could be explained by application of different type of ischemic insult or different rat strains or cytokine measurement at very early time points such as 2 h following insult (Brüning et al., 2012; Seo, et al., 2013). Generally, increased levels of some of the proinflammatory cytokines and chemokines may suggest their contribution in increased BBB permeability in early stage of ischemic injury.

It should be mention that there was a very large variability from animal to animal in the levels of most of the cytokines. In many cases cytokine levels in tissue or plasma were similar in sham operated and 2VO operated rats. The role of vagus nerve stimulation (as a consequence of surgery) in cytokine release can be considered as a source of variation in results, as stimulation of vagus nerve, a novel therapy in resistant epilepsy, has been associated with marked peripheral increases in pro- and anti-inflammatory circulating cytokines (Corcoran et al., 2005). The variability in the 2VO model in inducing severe ischemic injury in some rats, especially in young rats less than 250 g, may result in variability in cytokine expression (Farkas et al., 2007).

**Effects of MPs on endothelial barriers *in vitro***

MPs are associated with ischemic cerebrovascular disorders (Doeuvre et al., 2009) and induce BBB dysfunction in cerebral malaria (Combes et al., 2006) and multiple sclerosis (Minagar and Alexander, 2003), suggesting that MPs may have a role in pathogenesis of CSVD and BBB dysfunction. A previous study from our lab showed

that the total number of circulating MPs is increased following 2VO surgery (Schock et al., 2014). Therefore the next question is do MPs induce a change in permeability of endothelial cells, the main components of BBB, and what are the mechanisms involved? Since MPs transfer information to target cells (Mause and Weber, 2010) what are the signaling pathways involved? In this study MPs isolated from a specific volume of plasma from rats exposed to chronic cerebral ischemia, sham operated and unoperated rats were applied to artificial endothelial cell barriers at one half the concentration found *in vivo*. Only MPs from ischemic rats caused a significant reduction in TEER within 24 hours, implying that MPs are mediating inflammatory signaling during cerebral ischemia.

Since MPs contain cytokines such as TNF-α (Mause and Weber, 2010) and TNF-α induces proinflammatory and apoptotic changes in microvascular endothelial cells (Wiggins-Dohlvik et al., 2014), it is logical to ask whether TNF receptor activation mediates MP effects on endothelial cells. Inhibition of TNF-α with SPD-304 and a TACE inhibitor significantly reduced MP effects. This suggests that pro-TNF-α carried by MPs is cleaved and soluble biologically active TNF-α is released. Binding of trimeric TNF-α to TNF-α receptors on target cells then mediates the effects of MPs on endothelial cells. TNF-α can induce an inflammatory and pro-survival or an apoptotic effect on target cell, depending on TNF-α concentration (McCoy and Tansey, 2008). Comparison of the effects of MPs with low (10 ng/ml) and high (50 ng/ml) concentrations of TNF-α on TEER reduction of cultured RBMVECs indicated that the higher concentration has an effect similar to MPs, which suggests the occurrence of apoptosis in endothelial cells. Regarding the role of caspases in induction of apoptosis and evidence that indicates MPs contain caspase-3 (Schock et al., 2014) it was determined whether caspase-3 is involved

in the MP effect on endothelial cells. Treating cultured endothelial cells with a caspase-3 inhibitor prior to exposure to MPs and treating MPs themselves prior to adding them to cultured endothelial cells both significantly reduced the increase in TEER. Thus, MPs activate apoptotic signaling pathways in cultured cells and deliver activated caspase-3 to the target cells. This confirms previous reports that MPs both contain caspase-3 and induce caspase3-dependent apoptosis in several types of cells (Abid Hussein 2005, Böing 2008). Since lower concentrations of TNF-α and caspase-3 induce increased paracellular flux and redistribution of TJs and AJs in brain endothelial cells without apoptosis induction (Lopez-Ramirez et al., 2012), DNA fragmentation (TUNEL) assays were performed on MP treated cultured RBMVECs to confirm that apoptosis occurred.

Regarding the role of Rho kinase (ROCK) in the maintenance of endothelial barrier permeability (van Nieuw Amerongen et al., 2007), the early phase of apoptosis (Street and Bryan, 2011) and endothelial MP release (Gao et al., 2012), it was determined whether this pathway is also involved in MP effect on endothelial cells. In the present study inhibition of ROCK significantly decreased the impact of MPs on TEER and on apoptosis. However, Y-27632 by itself caused a significant decrease in TEER and induced apoptosis. Treating MPs with Y-27632 prior to adding them to cultured endothelial cells also reduced the effect of MPs on TEER suggesting that MPs may deliver activated ROCK proteins to target cells. The consequences of activating the Rho/ROCK pathway are not completely understood, as ROCK signaling may be pro-survival or pro-apoptotic, depending on cell type and ambient physiological conditions (Street and Bryan, 2011).

The next question was do MPs induce the permeability change only through induction of apoptosis? To show this cultured RBMVECs were treated with MPs in comparison to VEGF. VEGF induces an early increase in permeability of endothelial cells through a transcytosis mechanism mediated by caveolin-coated vesicles (Feng et al., 1999; Behzadian et al., 2003). While VEGF could induce a significant increase in transcellular transport in early stage MPs could only increase permeability later at 8 and 24 h following exposure that indicates MPs cannot induce increased permeability through a transcellular pathway.

Taken together, the data presented in this chapter support the idea that the increase in permeability of microvascular endothelial barriers following exposure to MPs generated during cerebral ischemia appears to be due primarily to apoptosis, the activation of the TNF-α pathways, caspase-3 and signaling via Rho kinases.

**Phosphodiesterase inhibition protects the BBB from chronic cerebral ischemia**

It is clear that plasma toxicity is increased in rats subjected to BCCAO. This term refers to the ability of MPs isolated from plasma to induce endothelial barrier dysfunction and cell death, when they are applied to cultured RBMVECs. Increased plasma toxicity most likely represents an increased number of MPs in plasma. Since the introduction of permanent BCCAO as a rodent model of chronic cerebral hypoperfusion a number of compounds have been assessed for their ability to reduce the structural and functional impacts of ischemia on the brain (Wang et al., 2010; Lee et al., 2006 Cho et al., 2006; Zhang et al., 2015). Therefore, the next question was whether administration of a compound that was found to be protective could reduce the plasma toxicity. For

choosing a compound some criteria were considered, such as the ability of the agent to improve endothelial cell barrier integrity and to have antiapoptotic effects. These criteria were met by cilostazol, a type III phosphodiestrase inhibitor. Cilostazol strengthens barrier integrity in primary rat brain capillary endothelial cells (Horai et al., 2013), is protective against apoptotic white matter damage in rats subjected to BCCAO (Lee et al., 2006; Watanabe et al., 2006; Lee et al., 2007; Kwak et al., 2012), inhibits platelet aggregation and decreases the level of platelet MPs (PMPs) in patients with noninsulin dependent diabetes mellitus (Nomura et al., 1998).

In the present study administration of cilostazol to rats subjected to BCCAO for 24 h was found to reduce plasma toxicity. Endothelial barrier dysfunction and cell death in cultured RBMVECs were significantly reduced following treatment with MPs isolated from the plasma. Cilostazol has been reported to attenuate the hyperpermeability of endothelial cells under hxpoxia/reoxygenation (Torii et al., 2007), suppress production of the cytokines such as TNF-α and IL-1β (Shin et al., 2004) and protect endothelial cells against lipopolysaccharide-induced apoptosis (Lim et al., 2009) via activation of cAMP-dependent protein kinase (Kim et al., 2006). Therefore, it is suggested that cilostazol reduces endothelial barrier hyperpermeability through a reduction of apoptosis, as is observed using inhibitors of TNF-α, caspase-3 and Rho kinase signaling pathways to treat artificial endothelial barriers.

There are no reports in the literature of the effect of cilostazol on the BBB during CCH *in vivo*. Therefore, the effect of cilostazol on BBB permeability was examined in rats subjected to BCCAO. The results indicated that cilostazol could reduce ischemia induced increase in BBB permeability.

The next question was whether cilostazol reduces the impact of ischemic injury on gait disturbance that was demonstrated earlier. The results of tapered beam test indicated that cilostazol treatment improved the slower gait velocity observed following ischemic insult. Since white matter rarefaction mostly occurred in optic tract that was determined by histological study of brain sections, the role of visual impairment in tapered beam performance was assessed. The result of an elevated platform test in the Morris water maze showed that half of the rats in the 2VO group could not find the platform, while 62.5% of the rats had dilated pupils. In the cilostazol treated group 90 % could find the platform, while 40% had dilated pupils. This suggests that the rats with dilated pupils were not completely blind at two weeks following BCCAO. Even 2VO treated rats with constricted pupils were significantly slower than sham treated rats. Therefore, the observed difference in gait velocity is not entirely dependent on visual disturbance.

White matter rarefaction and microgliosis in the optic tract were improved in cilostazol treated rats. This has been reported in other studies (Lee et al., 2006), suggesting that cilostazol reduces apoptosis in white matter lesions (Lee et al., 2006; Watanabe et al., 2006). The finding that cilostazol reduced plasma toxicity in rats subjected to BCCAO, although not significantly, suggests the involvement of circulating MPs in formation of white matter lesions in optic tract through induction of apoptosis. This presumption is supported by Schock et al. (2014) and the present studies that show MPs isolated from plasma of 2VO treated rats can induce cell death and apoptosis in cultured RBMVECs. Because circulating MPs can originate from different types of cells such as blood cells, microglia (Chahed et al., 2010) and astrocytes (Bianco et al., 2009), it

is possible that MPs other than endothelial MPs participate in induction of pathological consequences observed following BCCAO.

In summary, the data presented in this Chapter indicate that cilostazol protects BBB integrity, suppresses microgliosis and improves motor impairment following BCCAO surgery.

**Relevance of the results of current studies to human CSVD**

White matter hyperintensities, lacunes and microbleeds are considered to be characteristic MRI expressions of CSVD (Gouw et al., 2010). It causes lacunar stroke that accounts for a quarter of ischemic strokes (Wardlaw et al., 2003). CSVD is the most common cause of "vascular cognitive impairment" or "vascular dementia" (Bath and Wardlaw, 2015). The etiology of CSVD is incompletely understood. A number of mechanisms have been considered to be involved in pathogenesis of the disease that include ischemia/hypoxia, hypoperfusion due to altered cerebrovascular autoregulation, inflammation, degeneration and amyloid angiopathy and blood brain barrier leakage (Pantoni, 2010). In this study, we focused on the role of BBB dysfunction in pathogenesis of CSVD.

Increasing evidence from neuro imaging, neuropathology and epidemiology suggest that the primary underlying cause of CSVD is BBB derangement (Wardlaw, 2010). BBB dysfunction may initiate some years before the first symptoms, leading to structural changes in small vessel such as vessel wall thickening, disorganization and breakdown and perivascular changes such as edema, enlarged perivasular spaces and

tissue damage (Wardlaw, 2005; Wardlaw, 2010). These changes occur due to increase in permeability of vascular endothelium to substances such as proteins, inflammatory mediators and red blood cells, leading to pathological damage in the walls of small vessels and perivascular edema (Inzitari et al., 2009).

The experimental model used in this study, permanent BCCAO in rat, is one of most widely used models to study VCI (Jiwa et al., 2010) and has been also used as a common experimental model of CSVD (Hainsworth et al., 2012). Lesions are mainly in WM characterized by vacuolation of myelin, axonal damage, and demyelination in corpus callosum, internal capsule, and caudate putamen (Wakita et al., 1995, 2002; Farkas et al., 2004). These lesions are preceded by temporary BBB opening (for 72h) in white matter areas with collagen deposition in vessel walls (Ueno et al., 2002). In current study we found that BBB permeability was elevated for two weeks following surgery. Therefore, this is an appropriate model to assess the role of BBB dysfunction in the pathogenesis of CSVD. Our data also indicates that, following BCCAO, rats have a lower gait velocity in the tapered beam test. Gait disturbance is frequently observed in humans with CVSD (de Laat et al., 2011).

In the present study it was determined that there is no change in the expression of TJ proteins following BCCAO while increased expression of MMP-2 accompanies the increase in Evans Blue dye extravasation in brain tissue. These results are in agreement with studies on the aging human brain. In WMLs there is an increase in BBB permeability, determined by albumin leakage, without significant changes in the endothelial expression of TJPs (Simpson et al., 2010). Increased expression of MMP-2 in

demyelinated regions of brain has also been observed in autopsy studies of patients who were diagnosed with vascular dementia (Rosenberg et al., 2001).

There are few studies of inflammatory activation in individuals with lacunar infarction and white matter lesion (WML) (Hassan et al., 2003) and elevated levels of circulating hsCRP and IL-6 are associated with silent brain infarction (Hoshi et al., 2005). In the Framingham Heart Study higher levels of circulating TNF-R 2 were detected in the presence of cerebral microbleeds, a hemorrhagic marker of CSVD (Shoamanesh et al., 2015) and Nakase et al., (2008) have shown that a high serum level of TNF-α is associated with severe neurological deficits at the onset of lacunar infarction. However, we could not detect any significant change in plasma levels of cytokines and chemokines in the present study between 24h to 30 days following BCCAO. Therefore, it will be worthy to examine plasma levels of cytokines at later time points following 2VO surgery and in aged rats that provide more relevant information about inflammatory activation in human CSVD. Still, our data determined there are elevated levels of some proinflammatory cytokines and chemokines in brain tissue which may suggest the role for them in inducing BBB dysfunction.

There is little evidence regarding the association of circulating MPs with CSVD. It has been shown that platelet microparticles (PMPs) are elevated in patients with acute-phase cerebral infarction due to small vessel occlusion (Lee et al., 1993; Kuriyama et al., 2010). Shock et al. (2014) have shown that the number of total MPs and EMPs is increased in a model of chronic cerebral hypoperfusion and circulating MPs deliver proapoptotic signals to cultured endothelial cells. The current study also confirmed the

presence of apoptosis in MP treated RBMVECs. Although there is little evidence of apoptosis occurrence in human CSVD, in a single case study, apoptotic cells were 2.5X more frequent in periventricular hyperintensities compared to nearby normal white matter in post-mortem brain examination of a patient with Leukoaraiosis, suggesting that oliogodendroglial apoptosis could be a pathophysiological mechanism (Brown et al., 2002). In addition, it has been suggested that neuronal apoptosis may contribute to cortical atrophy and cognitive impairment in patients with CADASIL due to axonal damage in white matter (Gray et al., 2007). Apoptotic cells were identified using in situ end labeling and activated caspase-3 immunostaining in brain tissue form patients with CADASIL, with Binswanger disease (a sporadic form of subcortical vascular dementia) and controls. Apoptosis of vascular cells was elevated in basal ganglia and subcortical white matter in CADASIL cases, while neuronal apoptosis was determined in cortical layers 3 and 5. Apoptotic neurons in the Binswanger cases were infrequent and were not detected in the controls (Gray et al., 2007).

It has been shown that fasudil, a potent Rho-kinase inhibitor, improves early neurological deficits in patients with acute ischemic stroke (Shibuya et al., 2005) but there are no data available for CSVD (Bath and Wardlaw, 2015). Regarding the role of Rho kinases in the early phase of apoptosis (Street and Bryan, 2011) and endothelial MP release (Gao et al., 2012), our data indicate that MPs isolated from the plasma of 2VO rats may deliver activated ROCK proteins to brain endothelial cells and ROCK is involved in cell apoptosis and barrier dysfunction. Thus, inhibition of Rho/Rho kinase signaling may present a novel approach for treatment of CSVD.

It has been shown that cilostazol reduces recurrent ischemic stroke with fewer haemorrhagic complications than aspirin (Bath and Wardlaw, 2015). Anti-platelet therapy increases the risk of bleeding in stroke patients, especially those with CSVD (Mok and Kim, 2015). Hemorrhagic stroke is less frequent in the cilostazol treated group than in the aspirin treated group among patients with lacunar stroke (Uchiyama et al., 2014). The effects of cilostazol in the treatment of acute lenticulostriate stroke have also been reported (Kondo et al., 2013). Cilostazol treatment decreases cerebral arterial pulsatility in patients with mild white matter hyperintensities (Han et al., 2014). In experimental studies, cilostazol improves motor and cognitive function and reduces infarct size (Omote et al., 2012) and alleviates cerebral small-vessel pathology and white-matter lesions (Fujita et al., 2008) in stroke-prone spontaneously hypertensive rats. Moreover, cilostazol has an endothelial protective effect and prevents blood brain barrier disruption in focal cerebral ischemic injury (Nonaka et al., 2009; Lee et al., 2004). The results of current study support the effectiveness of cilostazol in treatment of CSVD although there are some limitations. The experimental model used does not reproduce all aspects of human CSVD. In addition, in our experiments, cilostazol induced a trend towards improvement in some of the paradigms that did not reach statistical significance.

In summary, in this research project the impact of permanent BCCAO in the rat on BBB permeability, motor performance and proinflammatory cytokine expression was determined. The pathophysiological consequences of applying MPs generated in the setting of chronic cerebral ischemia to artificial endothelial barriers *in vitro* were assessed. The effect of therapeutic intervention *in vivo* was also evaluated. The author

hopes that this study sheds some light on the mechanisms of BBB dysfunction in a well defined model of chronic cerebral ischemia.

## References


Abbas R, Chow CP, Browder NJ, Thacker D, Bramer SL, Fu CJ, Forbes W, Odomi M, Flockhart DA. 2000. *In vitro* metabolism and interaction of cilostazol with human hepatic cytochrome P450 isoforms. Hum Exp Toxicol. 19(3):178-84.

Abbott NJ. 2000. Inflammatory mediators and modulation of blood-brain barrier permeability. Cell Mol Neurobiol. 20(2):131-47.

Abid Hussein MN, Nieuwland R, Hau CM, Evers LM, Meesters EW, Sturk A. 2005. Cell-derived microparticles contain caspase 3 *in vitro* and *in vivo*. J Thromb Haemost. 3(5):888-96.

Ahdieh M, Vandenbos T, Youakim A. 2001. Lung epithelial barrier function and wound healing are decreased by IL-4 and IL-13 and enhanced by IFN-gamma. Am J Physiol Cell Physiol. 281:C2029-C2038.

Akiguchi I, Tomimoto H, Suenaga T, Wakita H, Budka H. 1998. Blood-brain barrier dysfunction in Binswanger's disease; an immunohistochemical study. Acta Neuropathol. 95(1):78-84.

Akiyama H, Kudo S, Shimizu T. 1985. The absorption, distribution and excretion of a new antithrombotic and vasodilating agent, cilostazol, in rat, rabbit, dog and man. Arzneimittelforschung. 35(7A):1124-32.

Angelopoulos P, Agouridaki H, Vaiopoulos H, Siskou E, Doutsou K, Costa V, Baloyiannis SI. 2008. Cytokines in Alzheimer's disease and vascular dementia. Int J Neurosci. 118(12):1659-72.

Ark M, Ozdemir A, Polat B. 2010. Ouabain-induced apoptosis and Rho kinase: a novel caspase-2 cleavage site and fragment of Rock-2. Apoptosis. 15(12):1494-506.

Asahi M, Wang X, Mori T, Sumii T, Jung JC, Moskowitz MA, Fini ME, Lo EH. 2001. Effects of matrix metalloproteinase-9 gene knock-out on the proteolysis of blood-brain barrier and white matter components after cerebral ischemia. J Neurosci. 21(19):7724-32.

Behzadian MA, Windsor LJ, Ghaly N, Liou G, Tsai NT, Caldwell RB. 2003. VEGF-induced paracellular permeability in cultured endothelial cells involves urokinase and its receptor. FASEB J. 17(6):752-4.

Benveniste EN. Cytokine actions in the central nervous system. 1998. Cytokine Growth Factor Rev. 9, 259-275.

Berti R, Williams AJ, Moffett JR, Hale SL, Velarde LC, Elliott PJ, Yao C, Dave JR, Tortella FC. 2002. Quantitative real-time RT-PCR analysis of inflammatory gene expression associated with ischemia-reperfusion brain injury. J Cereb Blood Flow Metab. 22(9):1068-79.

Bhatt NM, Chavada VD, Patel DP, Sharma P, Sanyal M, Shrivastav PS. 2015. Determination of cilostazol and its active metabolite 3,4-dehydro cilostazol from small plasma volume by UPLC−MS/MS. Journal of Pharmaceutical Analysis. 5(1): 1-11.

Bianco F, Perrotta C, Novellino L, Francolini M, Riganti L, Menna E, Saglietti L, Schuchman EH, Furlan R, Clementi E, Matteoli M, Verderio C. 2009. Acid sphingomyelinase activity triggers microparticle release from glial cells. EMBO J. 28(8):1043-54.

Böing AN, Hau CM, Sturk A, Nieuwland R. 2008. Platelet microparticles contain active caspase 3. Platelets. 19(2):96-103.

Boiten J, Lodder J, Kessels F. 1993. Two clinically distinct lacunar infarct entities? A hypothesis. Stroke. 24(5):652-6.

Bowler JV. 2005. Vascular cognitive impairment. J Neurol Neurosurg Psychiatry. 76 Suppl 5:v35-44.

Brabers NA, Nottet HS. 2006. Role of the pro-inflammatory cytokines TNF-alpha and IL-1beta in HIV-associated dementia. Eur J Clin Invest. 36(7):447-58.

Brown MD, Feairheller DL, Thakkar S, Veerabhadrappa P, Park JY. 2011. Racial differences in tumor necrosis factor-α-induced endothelial microparticles and interleukin-6 production. Vasc Health Risk Manag. 7:541-50.

Brown WR, Moody DM, Challa VR, Thore CR, Anstrom JA. 2002. Apoptosis in leukoaraiosis lesions. J Neurol Sci. 203-204:169-71.

Brüning CA, Prigol M, Luchese C, Jesse CR, Duarte MM, Roman SS, Nogueira CW. 2012. Protective effect of diphenyl diselenide on ischemia and reperfusion-induced cerebral injury: involvement of oxidative stress and pro-inflammatory cytokines. Neurochem Res. 37(10):2249-58.

Burger D, Schock S, Thompson CS, Montezano AC, Hakim AM, Touyz RM. 2013. Microparticles: biomarkers and beyond. Clin Sci (Lond). 124(7):423-41.

Canault M, Leroyer AS, Peiretti F, Lesèche G, Tedgui A, Bonardo B, Alessi MC, Boulanger CM, Nalbone G. 2007. Microparticles of human atherosclerotic plaques enhance the shedding of the tumor necrosis factor-alpha converting enzyme/ADAM17 substrates, tumor necrosis factor and tumor necrosis factor receptor-1. Am J Pathol. 171(5):1713-23.

Candelario-Jalil E, Yang Y, Rosenberg GA. 2009. Diverse roles of matrix metalloproteinases and tissue inhibitors of metalloproteinases in neuroinflammation and cerebral ischemia. Neuroscience. 158(3):983-94.

Castillo J, Rodríguez I. 2004. Biochemical changes and inflammatory response as markers for brain ischemia: molecular markers of diagnostic utility and prognosis in human clinical practice. Cerebrovasc Dis. 17 Suppl 1:7-18.

Cauwe B, Van den Steen PE, Opdenakker G. 2007. The biochemical, biological, and pathological kaleidoscope of cell surface substrates processed by matrix metalloproteinases. Crit Rev Biochem Mol Biol. 42:113-185.

Chabriat H, Joutel A, Dichgans M, Tournier-Lasserve E, Bousser MG. 2009. Cadasil. Lancet Neurol. 8(7):643-53.

Chahed S, Leroyer AS, Benzerroug M, Gaucher D, Georgescu A, Picaud S, Silvestre JS, Gaudric A, Tedgui A, Massin P, Boulanger CM. 2010. Increased vitreous shedding

of microparticles in proliferative diabetic retinopathy stimulates endothelial proliferation. Diabetes. 59(3):694-701.

Chandler S, Coates R, Gearing A, Lury J, Wells G, Bone E. 1995. Matrix metalloproteinases degrade myelin basic protein. Neurosci Lett. 201:223-6.

Cherian P, Hankey GJ, Eikelboom JW, Thom J, Baker RI, McQuillan A, Staton J, Yi Q. 2003. Endothelial and platelet activation in acute ischemic stroke and its etiological subtypes. Stroke. 34(9):2132-7.

Cho KO, La HO, Cho YJ, Sung KW, Kim SY. 2006. Minocycline attenuates white matter damage in a rat model of chronic cerebral hypoperfusion. J Neurosci Res. 83(2):285-91.

Choy M, Ganesan V, Thomas DL, Thornton JS, Proctor E, King MD, van der Weerd L, Gadian DG, Lythgoe MF. 2006. The chronic vascular and haemodynamic response after permanent bilateral common carotid occlusion in newborn and adult rats. J Cereb Blood Flow Metab. 26(8):1066-75.

Chui HC. 2007. Subcortical ischemic vascular dementia. Neurol Clin. 25(3):717-40.

Combes V, Coltel N, Faille D, Wassmer SC, Grau GE. 2006. Cerebral malaria: role of microparticles and platelets in alterations of the blood-brain barrier. Int J Parasitol. 36(5):541-6.

Corbett A, McGowin A, Sieber S, Flannery T, Sibbitt B. 2012. A method for reliable voluntary oral administration of a fixed dosage (mg/kg) of chronic daily medication to rats. Lab Anim. 46(4): 318-24.

Corcoran C, Connor TJ, O'Keane V, Garland MR. 2005. The effects of vagus nerve stimulation on pro- and anti-inflammatory cytokines in humans: a preliminary report. Neuroimmunomodulation. 12(5):307-9.

Cullen SP, Martin SJ. 2009. Caspase activation pathways: some recent progress. Cell Death Differ. 16(7):935-8.

Davidson CM, Pappas BA, Stevens WD, Fortin T, Bennett SA. 2000. Chronic cerebral hypoperfusion: loss of pupillary reflex, visual impairment and retinal neurodegeneration. Brain Res. 859(1):96-103.

Dawson DL, Cutler BS, Meissner MH, Strandness DE Jr. 1998. Cilostazol has beneficial effects in treatment of intermittent claudication: results from a multicenter, randomized, prospective, double-blind trial. Circulation. 98(7):678-86.

Dejana E, Tournier-Lasserve E, Weinstein BM. 2009. The control of vascular integrity by endothelial cell junctions: molecular basis and pathological implications. Dev Cell. 16(2):209-21.

de Laat KF, van Norden AG, Gons RA, van Oudheusden LJ, van Uden IW, Bloem BR, Zwiers MP, de Leeuw FE. 2010. Gait in elderly with cerebral small vessel disease. Stroke. 41(8):1652-8.

de Laat KF, Tuladhar AM, van Norden AG, Norris DG, Zwiers MP, de Leeuw FE. 2011. Loss of white matter integrity is associated with gait disorders in cerebral small vessel disease. Brain. 134(Pt 1):73-83.

de Medinaceli L, Freed WJ, Wyatt RJ. 1982. An index of the functional condition of rat sciatic nerve based on measurements made from walking tracks. Exp Neurol. 77(3):634-43.

Diamant M, Tushuizen ME, Sturk A, Nieuwland R. 2004. Cellular microparticles: new players in the field of vascular disease? Eur J Clin Invest. 34(6):392-401.

Dimitrijevic OB, Stamatovic SM, Keep RF, Andjelkovic AV. 2006. Effects of the chemokine CCL2 on blood-brain barrier permeability during ischemia-reperfusion injury. J Cereb Blood Flow Metab. 26(6):797-810.

Doeuvre L, Plawinski L, Toti F, Anglés-Cano E. 2009. Cell-derived microparticles: a new challenge in neuroscience.J Neurochem. 110(2):457-68.

Duan W, Gui L, Zhou Z, Liu Y, Tian H, Chen JF, Zheng J. 2009. Adenosine A2A receptor deficiency exacerbates white matter lesions and cognitive deficits induced by chronic cerebral hypoperfusion in mice. J Neurol Sci. 285(1-2):39-45.

Farkas E, de Vos RA, Donka G, Jansen Steur EN, Mihály A, Luiten PG. 2006. Age-related microvascular degeneration in the human cerebral periventricular white matter. Acta Neuropathol. 111(2):150-7.

Farkas E, Donka G, de Vos RA, Mihály A, Bari F, Luiten PG. 2004. Experimental cerebral hypoperfusion induces white matter injury and microglial activation in the rat brain. Acta Neuropathol. 108(1):57-64.

Farkas E, Luiten PG, Bari F. 2007. Permanent, bilateral common carotid artery occlusion in the rat: a model for chronic cerebral hypoperfusion-related neurodegenerative diseases. Brain Res Rev. 54(1):162-80.

Feng Y, Venema VJ, Venema RC, Tsai N, Behzadian MA, Caldwell RB. 1999. VEGF-induced permeability increase is mediated by caveolae. Invest Ophthalmol Vis Sci. 40(1):157-67.

Fernando MS, Simpson JE, Matthews F, Brayne C, Lewis CE, Barber R, Kalaria RN, Forster G, Esteves F, Wharton SB, Shaw PJ, O'Brien JT, Ince PG; MRC Cognitive Function and Ageing Neuropathology Study Group. 2006. White matter lesions in an unselected cohort of the elderly: molecular pathology suggests origin from chronic hypoperfusion injury. Stroke. 37(6):1391-8.

Fisher CM. 1968. The arterial lesions underlying lacunes. Acta Neuropathol. 12(1):1-15.

Fujita Y, Lin JX, Takahashi R, Tomimoto H. 2008**.** Cilostazol alleviates cerebral small-vessel pathology and white-matter lesions in stroke-prone spontaneously hypertensive rats. Brain Res. 1203:170-6.

Fukuda S, Fini CA, Mabuchi T, Koziol JA, Eggleston LL Jr, del Zoppo GJ. 2004. Focal cerebral ischemia induces active proteases that degrade microvascular matrix. Stroke. 35(4):998-1004.

Gao C, Li R, Liu Y, Ma L, Wang S. 2012. Rho-kinase-dependent F-actin rearrangement is involved in the release of endothelial microparticles during IFN-α-induced endothelial cell apoptosis. J Trauma Acute Care Surg. 73(5):1152-60.

Garcia JG, Davis HW, Patterson CE. 1995. Regulation of endothelial cell gap formation and barrierdysfunction: role of myosin light chain phosphorylation. J Cell Physiol. 163:510–522.

Gnant MF, Turner EM, Alexander HR Jr. 2000. Effects of hyperthermia and tumour necrosis factor on inflammatory cytokine secretion and procoagulant activity in endothelial cells. Cytokine. 12(4):339-47.

Gorelick PB, Scuteri A, Black SE, Decarli C, Greenberg SM, Iadecola C, Launer LJ, Laurent S, Lopez OL, Nyenhuis D, Petersen RC, Schneider JA, Tzourio C, Arnett DK, Bennett DA, Chui HC, Higashida RT, Lindquist R, Nilsson PM, Roman GC, Sellke FW, Seshadri S; American Heart Association Stroke Council, Council on Epidemiology and Prevention, Council on Cardiovascular Nursing, Council on Cardiovascular Radiology and Intervention, and Council on Cardiovascular Surgery and Anesthesia. 2011. Vascular contributions to cognitive impairment and dementia: a statement for healthcare professionals from the american heart association/american stroke association. Stroke. 42(9):2672-713.

Gouw AA, Seewann A, van der Flier WM, Barkhof F, Rozemuller AM, Scheltens P, Geurts JJ. 2011. Heterogeneity of small vessel disease: a systematic review of MRI and histopathology correlations. J Neurol Neurosurg Psychiatry. 82(2):126-35.

Gray F, Polivka M, Viswanathan A, Baudrimont M, Bousser MG, Chabriat H. 2007. Apoptosis in cerebral autosomal-dominant arteriopathy with subcortical infarcts and leukoencephalopathy. J Neuropathol Exp Neurol. 66(7):597-607.

Gruol DL, Nelson TE. 1997. Physiological and pathological roles of interleukin-6 in the central nervous system. Mol Neurobiol. 15, 307-339.

Guldiken B, Guldiken S, Turgut B, Turgut N, Demir M, Celik Y, Arikan E, Tugrul A. 2008. The roles of oxidized low-density lipoprotein and interleukin-6 levels in acute atherothrombotic and lacunar ischemic stroke. Angiology. 59(2):224-9.

Hachinski V. 2008. World Stroke Day 2008: "little strokes, big trouble". Stroke. 39(9):2407-20.

Hainsworth AH, Markus HS. 2008. Do *in vivo* experimental models reflect human cerebral small vessel disease? A systematic review. J Cereb Blood Flow Metab. 28(12):1877-91.

Hamann GF, Liebetrau M, Martens H, Burggraf D, Kloss CU, Bültemeier G, Wunderlich N, Jäger G, Pfefferkorn T. 2002. Microvascular basal lamina injury after experimental focal cerebral ischemia and reperfusion in the rat. J Cereb Blood Flow Metab. 22(5):526-33.

Hamann GF, Okada Y, Fitridge R, del Zoppo GJ. 1995. Microvascular basal lamina antigens disappear during cerebral ischemia and reperfusion. Stroke. 26(11):2120-6.

Han SW, Song TJ, Bushnell CD, Lee SS, Kim SH, Lee JH, Kim GS, Kim OJ, Koh IS, Lee JY, Suk SH, Lee SI, Nam HS, Kim WJ, Lee KY, Park JH, Kim JY, Park JH. 2014. Cilostazol decreases cerebral arterial pulsatility in patients with mild white matter hyperintensities: subgroup analysis from the Effect of Cilostazol in Acute Lacunar Infarction Based on Pulsatility Index of Transcranial Doppler (ECLIPse) study. Cerebrovasc Dis. 38(3):197-203.

Haorah J, Ramirez SH, Schall K, Smith D, Pandya R, Persidsky Y. 2007. Oxidative stress activates protein tyrosine kinase and matrix metalloproteinases leading to blood-brain barrier dysfunction. JNeurochem. 101(2):566-76.

Hassan A, Hunt BJ, O'Sullivan M, Parmar K, Bamford JM, Briley D, Brown MM, Thomas DJ, Markus HS. 2003. Markers of endothelial dysfunction in lacunar infarction and ischemic leukoaraiosis. Brain. 126(Pt 2):424-32.

He MM, Smith AS, Oslob JD, Flanagan WM, Braisted AC, Whitty A, Cancilla MT, Wang J, Lugovskoy AA, Yoburn JC, Fung AD, Farrington G, Eldredge JK, Day ES, Cruz LA, Cachero TG, Miller SK, Friedman JE, Choong IC, Cunningham BC. 2005. Small-molecule inhibition of TNF-alpha. Science. 310(5750):1022-5.

Hiratsuka M, Hinai Y, Sasaki T, Konno Y, Imagawa K, Ishikawa M, Mizugaki M. 2007. Characterization of human cytochrome p450 enzymes involved in the metabolism of cilostazol. Drug Metab Dispos. 35(10):1730-2.

Hong KW, Kim KY, Shin HK, Lee JH, Choi JM, Kwak YG, Kim CD, Lee WS, Rhim BY. 2003. Cilostazol prevents tumor necrosis factor-alpha-induced cell death by suppression of phosphatase and tensin homolog deleted from chromosome 10

phosphorylation and activation of Akt/cyclic AMP response element-binding protein phosphorylation. J Pharmacol Exp Ther. 306: 1182-1190.

Horai S, Nakagawa S, Tanaka K, Morofuji Y, Couraud PO, Deli MA, Ozawa M, Niwa M. 2013. Cilostazol strengthens barrier integrity in brain endothelial cells. Cell Mol Neurobiol. 33(2):291-307.

Hoshi T, Kitagawa K, Yamagami H, Furukado S, Hougaku H, Hori M. 2005. Relations of serum high-sensitivity C-reactive protein and interleukin-6 levels with silent brain infarction. Stroke. 36:768 -772.

Hu WH, Johnson H, Shu HB. 1999. Tumor necrosis factor-related apoptosis-inducing ligand receptors signal NF-kappaB and JNK activation and apoptosis through distinct pathways. J Biol Chem. 274(43):30603-10.

Huang J, Upadhyay UM, Tamargo RJ. 2006. Inflammation in stroke and focal cerebral ischemia. Surg Neurol. 66(3):232-45.

Ihara M, Tomimoto H, Kinoshita M, Oh J, Noda M, Wakita H, Akiguchi I, Shibasaki H. 2001. Chronic cerebral hypoperfusion induces MMP-2 but not MMP-9 expression in the microglia and vascular endothelium of white matter. J Cereb Blood Flow Metab. 21:828-34.

Inzitari D, Pracucci G, Poggesi A, Carlucci G, Barkhof F, Chabriat H, Erkinjuntti T, Fazekas F, Ferro JM, Hennerici M, Langhorne P, O'Brien J, Scheltens P, Visser MC, Wahlund LO, Waldemar G, Wallin A, Pantoni L; LADIS Study Group. 2009. Changes in white matter as determinant of global functional decline in older independent outpatients: three year follow-up of LADIS (leukoaraiosis and disability) study cohort. BMJ. 339:b2477.

Italiano JE Jr, Mairuhu AT, Flaumenhaft R. 2010. Clinical relevance of microparticles from platelets and megakaryocytes. Curr Opin Hematol. 17(6):578-84.

Jellinger KA. 2008. Morphologic diagnosis of "vascular dementia" - a critical update. J Neurol Sci. 270(1-2):1-12.

Jellinger KA. Pathology and pathogenesis of vascular cognitive impairment-a critical update. 2013. Front Aging Neurosci. 5:17.

Jellinger KA. Pathogenesis and treatment of vascular cognitive impairment. 2014. Neurodegener Dis Manag. 4(6):471-90.

Jiwa NS, Garrard P, Hainsworth AH. 2010. Experimental models of vascular dementia and vascular cognitive impairment: a systematic review. J Neurochem. 115(4):814-28.

Johnston GR, Webster NR. 2009. Cytokines and the immunomodulatory function of the vagus nerve. Br J Anaesth. 102(4):453-62.

Joutel A, Monet-Leprêtre M, Gosele C, Baron-Menguy C, Hammes A, Schmidt S, Lemaire-Carrette B, Domenga V, Schedl A, Lacombe P, Hubner N. 2010. Cerebrovascular dysfunction and microcirculation rarefaction precede white matter lesions in a mouse genetic model of cerebral ischemic small vessel disease. J Clin Invest.120:433–45.

Juma WM, Lira A, Marzuk A, Marzuk Z, Hakim AM, Thompson CS. 2011. C-reactive protein expression in a rodent model of chronic cerebral hypoperfusion. Brain Res. 1414:85-93.

Jung KH, Chu K, Lee ST, Park HK, Bahn JJ, Kim DH, Kim JH, Kim M, Kun Lee S, Roh JK. 2009. Circulating endothelial microparticles as a marker of cerebrovascular disease. Ann Neurol. 66(2):191-9.

Kaiser D, Weise G, Möller K, Scheibe J, Pösel C, Baasch S, Gawlitza M, Lobsien D, Diederich K, Minnerup J, Kranz A, Boltze J, Wagner DC. 2014. Spontaneous white matter damage, cognitive decline and neuroinflammation in middle-aged hypertensive rats: an animal model of early-stage cerebral small vessel disease. Acta Neuropathol Commun. 2(1):169.

Kalaria RN, Kenny RA, Ballard CG, Perry R, Ince P, Polvikoski T. 2004. Towards defining the neuropathological substrates of vascular dementia. J Neurol Sci. 226(1-2):75-80.

Kamada N, Yamada K, Odomi M, Mukai T, Nishibayashi T, Ogawara K, Kimura T, Higaki K. 2011. Sex differences in pharmacokinetics of cilostazol in rats. Xenobiotica. 41(10):903-13.

Khan U, Porteous L, Hassan A, Markus HS. 2007. Risk factor profile of cerebral small vessel disease and its subtypes. J Neurol Neurosurg Psychiatry. 78(7):702-6.

Kim MJ, Lee JH, Park SY, Hong KW, Kim CD, Kim KY, Lee WS. 2006. Protection from apoptotic cell death by cilostazol, phosphodiesterase type III inhibitor, via cAMP-dependent protein kinase activation. Pharmacol Res. 54(4):261-7.

Kimura Y, Tani T, Kanbe T, Watanabe K. 1985. Effect of cilostazol on platelet aggregation and experimental thrombosis. Arzneimittelforschung. 35(7A):1144-9.

Kondo R, Matsumoto Y, Furui E, Itabashi R, Sato S, Yazawa Y, Shimizu H, Fujiwara S, Takahashi A, Tominaga T. 2013. Effect of cilostazol in the treatment of acute ischemic stroke in the lenticulostriate artery territory. Eur Neurol. 69(2):122-8.

Kuhlmann CR, Tamaki R, Gamerdinger M, Lessmann V, Behl C, Kempski OS, Luhmann HJ. 2007. Inhibition of the myosin light chain kinase prevents hypoxia-induced blood-brain barrier disruption. J Neurochem. 102(2):501-7.

Kuriyama N, Nagakane Y, Hosomi A, Ohara T, Kasai T, Harada S, Takeda K, Yamada K, Ozasa K, Tokuda T, Watanabe Y, Mizuno T, Nakagawa M. 2010. Evaluation of factors associated with elevated levels of platelet-derived microparticles in the acute phase of cerebral infarction. Clin Appl Thromb Hemost. 16(1):26-32.

Kwak PA, Lim SC, Han SR, Shon YM, Kim YI. 2012. Supra-additive neuroprotection by renexin, a mixed compound of ginkgo biloba extract and cilostazol, against apoptotic white matter changes in rat after chronic cerebral hypoperfusion. J Clin Neurol. 8(4):284-92.

Lammie GA. 2000. Pathology of small vessel stroke. Br Med Bull. 56(2):296-306.

Lammie GA. 2002. Hypertensive cerebral small vessel disease and stroke. Brain Pathol. 12(3):358-70.

Lavallée PC, Labreuche J, Faille D, Huisse MG, Nicaise-Roland P, Dehoux M, Gongora-Rivera F, Jaramillo A, Brenner D,Deplanque D, Klein IF, Touboul PJ, Vicaut E, Ajzenberg N; Lacunar-B.I.C.H.A.T. Investigators. 2013. Circulating markers of endothelial dysfunction and platelet activation in patients with severe symptomatic cerebral small vessel disease. Cerebrovasc Dis. 36(2):131-8.

Lee YJ, Jy W, Horstman LL, Janania J, Reyes Y, Kelley RE, Ahn YS. 1993. Elevated platelet microparticles in transient ischemic attacks, lacunar infarcts, and multiinfarct dementias. Thromb Res. 72(4):295-304.

Lee JH, Kim KY, Lee YK, Park SY, Kim CD, Lee WS, Rhim BY, Hong KW. 2004. Cilostazol prevents focal cerebral ischemic injury by enhancing casein kinase 2 phosphorylation and suppression of phosphatase and tensin homolog deleted from chromosome 10 phosphorylation in rats. J Pharmacol Exp Ther. 308(3):896-903.

Lee JH, Park SY, Shin YW, Hong KW, Kim CD, Sung SM, Kim KY, Lee WS. 2006. Neuroprotection by cilostazol, a phosphodiesterase type 3 inhibitor, against apoptotic white matter changes in rat after chronic cerebral hypoperfusion. Brain Res. 1082(1):182-91.

Lee JH, Park SY, Shin YW, Kim CD, Lee WS, Hong KW. 2007. Concurrent administration of cilostazol with donepezil effectively improves cognitive dysfunction with increased neuroprotection after chronic cerebral hypoperfusion in rats. Brain Res. 1185:246-55.

Lee JH, Park SY, Shin HK, Kim CD, Lee WS, Hong KW. 2008. Protective effects of cilostazol against transient focal cerebral ischemia and chronic cerebral hypoperfusion injury. CNS Neurosci Ther. 14(2):143-52.

Lee JM, Zhai G, Liu Q, Gonzales ER, Yin K, Yan P, Hsu CY, Vo KD, Lin W. 2007. Vascular permeability precedes spontaneous intracerebral hemorrhage in stroke-prone spontaneously hypertensive rats. Stroke. 38(12):3289-91.

Li Q, Huang XJ, He W, Ding J, Jia JT, Fu G, Wang HX, Guo LJ. 2009. Neuroprotective potential of fasudil mesylate in brain ischemia-reperfusion injury of rats. Cell Mol Neurobiol. 29(2):169-80.

Lim JH, Woo JS, Shin YW. 2009. Cilostazol protects endothelial cells against lipopolysaccharide-induced apoptosis through ERK1/2- and P38 MAPK-dependent pathways. Korean J Intern Med. 24(2): 113-22.

Lin S, Cox HJ, Rhodes PG, Cai Z. 2006. Neuroprotection of alpha-phenyl-n-tert-butyl-nitrone on the neonatal white matter is associated with anti-inflammation. Neurosci Lett. 405(1-2):52-6.

Lopez-Ramirez MA, Fischer R, Torres-Badillo CC, Davies HA, Logan K, Pfizenmaier K, Male DK, Sharrack B, Romero IA. 2012. Role of caspases in cytokine-induced barrier breakdown in human brain endothelial cells. J Immunol. 189(6):3130-9.

Losy J & Zaremba J. 2001. Monocyte chemoattractant protein-1 is increased in the cerebrospinal fluid of patients with ischemic stroke. Stroke. 32, 2695-2696.

Lovren F, Verma S. 2013. Evolving role of microparticles in the pathophysiology of endothelial dysfunction. Clin Chem. 59(8):1166-74.

Ma T, Liu L, Wang P, Xue Y. 2012. Evidence for involvement of ROCK signaling in bradykinin-induced increase in murine blood-tumor barrier permeability. J Neurooncol. 106(2):291-301.

Maguire S, Strittmatter R, Chandra S, Barone FC. 2004. Stroke-prone rats exhibit prolonged behavioral deficits without increased brain injury: an indication of disrupted post-stroke brain recovery of function. Neurosci Lett. 354(3):229-33.

Mark KS, Davis TP. 2002. Cerebral microvascular changes in permeability and tight junctions induced by hypoxia-reoxygenation. Am J Physiol Heart Circ Physiol. 282(4):H1485-94.

Markus HS. 2008. Genes, endothelial function and cerebral small vessel disease in man. Exp Physiol. 93(1):121-7.

Mause SF, Weber C. 2010. Microparticles: protagonists of a novel communication network for intercellular information exchange. Circ Res. 107(9):1047-57.

McCoy MK, Tansey MG. 2008. TNF signaling inhibition in the CNS: implications for normal brain function and neurodegenerative disease. J Neuroinflammation. 5:45.

Minagar A, Alexander JS. 2003. Blood-brain barrier disruption in multiple sclerosis. Mult Scler. 9(6):540-9.

Minami M, Satoh M. 2003. Chemokines and their receptors in the brain: pathophysiological roles in ischemic brain injury. Life Sci. 74(2-3):321-7.

Mok V, Kim JS. 2015. Prevention and Management of Cerebral Small Vessel Disease. J Stroke. 17(2):111-22.

Müllberg J, Durie FH, Otten-Evans C, Alderson MR, Rose-John S, Cosman D, Black RA, Mohler KM. 1995. A metalloprotease inhibitor blocks shedding of the IL-6 receptor and the p60 TNF receptor. J Immunol. 155(11):5198-205.

Nag S, Kapadia A, Stewart DJ. 2011. Review: molecular pathogenesis of blood-brain barrier breakdown in acute brain injury. Neuropathol Appl Neurobiol. 37(1):3-23.

Nag S, Venugopalan R, Stewart DJ. 2007. Increased caveolin-1 expression precedes decreased expression of occludin and claudin-5 during blood-brain barrier breakdown. Acta Neuropathol. 114(5):459-69.

Nakaji K, Ihara M, Takahashi C, Itohara S, Noda M, Takahashi R, Tomimoto H. 2006. Matrix metalloproteinase-2 plays a critical role in the pathogenesis of white matter lesions after chronic cerebral hypoperfusion in rodents. Stroke. 37:2816-23.

Nakase T, Yamazaki T, Ogura N, Suzuki A, Nagata K. 2008. The impact of inflammation on the pathogenesis and prognosis of ischemic stroke. J Neurol Sci. 271(1-2):104-9.

Nomura S, Shouzu A, Omoto S, Hayakawa T, Kagawa H, Nishikawa M, Inada M, Fujimura Y, Ikeda Y, Fukuhara S. 1998. Effect of cilostazol on soluble adhesion molecules and platelet-derived microparticles in patients with diabetes. Thromb Haemost. 80(3):388-92.

Nonaka Y, Tsuruma K, Shimazawa M, Yoshimura S, Iwama T, Hara H. 2009. Cilostazol protects against hemorrhagic transformation in mice transient focal cerebral ischemia-induced brain damage. Neurosci Lett. 452(2):156-61.

O'Brien JT, Erkinjuntti T, Reisberg B, Roman G, Sawada T, Pantoni L, Bowler JV, Ballard C, DeCarli C, Gorelick PB, Rockwood K, Burns A, Gauthier S, DeKosky ST. 2003. Vascular cognitive impairment. Lancet Neurol. 2(2):89-98.

Ohta H, Nishikawa H, Kimura H, Anayama H, Miyamoto M. 1997. Chronic cerebral hypoperfusion by permanent internal carotid ligation produces learning impairment without brain damage in rats. Neuroscience. 79(4):1039-50.

Omote Y, Deguchi K, Tian F, Kawai H, Kurata T, Yamashita T, Ohta Y, Abe K. 2012. Clinical and pathological improvement in stroke-prone spontaneous hypertensive rats related to the pleiotropic effect of cilostazol. Stroke. 43(6):1639-46.

Oshima T, Laroux FS, Coe LL, Morise Z, Kawachi S, Bauer P, Grisham MB, Specian RD, Carter P, Jennings S, Granger DN, Joh T, Alexander JS. 2001. Interferon-gamma and interleukin-10 reciprocally regulate endothelial junction integrity and barrier function. Microvasc Res. 61:130-143.

O'Sullivan M, Lythgoe DJ, Periera AC, Summers PE, Jarosz JM, Williams SCR & Markus HS. 2002. Patterns of cerebral blood flow reduction in patients with ischemic leukoaraiosis. Neurology. 59(3):321-6.

Owens AP 3rd, Mackman N. 2011. Microparticles in hemostasis and thrombosis. Circ Res. 108(10):1284-97.

Pantoni L. 2010. Cerebral small vessel disease: from pathogenesis and clinical characteristics to therapeutic challenges. Lancet Neurol. 9(7):689-701.

Pantoni L, Garcia JH. 1997. Pathogenesis of leukoaraiosis: a review. Stroke. 28(3):652-9.

Peng J, He F, Zhang C, Deng X, Yin F. 2011. Protein kinase C-α signals P115RhoGEF phosphorylation and RhoA activation in TNF-α-induced mouse brain microvascular endothelial cell barrier dysfunction. J Neuroinflammation. 8:28.

Peterson DB, Sander T, Kaul S, Wakim BT, Halligan B, Twigger S, Pritchard KA Jr, Oldham KT, Ou JS. 2008. Comparative proteomic analysis of PAI-1 and TNF-alpha-derived endothelial microparticles. Proteomics. 8(12):2430-46.

Plaschke K, Grant M, Weigand MA, Züchner J, Martin E, Bardenheuer HJ. 2001. Neuromodulatory effect of propentofylline on rat brain under acute and long-term hypoperfusion. Br J Pharmacol. 133(1):107-16.

Plateel M, Teissier E, Cecchelli R. 1997. Hypoxia dramatically increases the nonspecific transport of blood-borne proteins to the brain. J Neurochem. 68(2):874-7.

Rautou PE, Vion AC, Amabile N, Chironi G, Simon A, Tedgui A, Boulanger CM. 2011. Microparticles, vascular function, and atherothrombosis. Circ Res. 109(5):593-606.

Rondina MT, Weyrich AS. Targeting phosphodiesterases in anti-platelet therapy. 2012. Handb Exp Pharmacol. (210):225-38.

Rosenberg GA. 2002. Matrix metalloproteinases in neuroinflammation. Glia. 39:279-291.

Rosenberg GA, Sullivan N, Esiri MM. 2001. White matter damage is associated with matrix metalloproteinases in vascular dementia. Stroke. 32:1162-8.

Sakurai-Yamashita Y, Shigematsu K, Yamashita K, Niwa M. 2006. Expression of MCP-1 in the hippocampus of SHRSP with ischemia-related delayed neuronal death. Cell Mol Neurobiol. 26(4-6):823-31.

Sapet C, Simoncini S, Loriod B, Puthier D, Sampol J, Nguyen C, Dignat-George F, Anfosso F. 2006. Thrombin-induced endothelial microparticle generation: identification of a novel pathway involving ROCK-II activation by caspase-2. Blood. 108(6):1868-76.

Sarti C, Pantoni L, Bartolini L, Inzitari D. 2002. Persistent impairment of gait performances and working memory after bilateral common carotid artery occlusion in the adult Wistar rat. Behav Brain Res. 136(1):13-20.

Sawant DA, Tharakan B, Wilson RL, Stagg HW, Hunter FA, Childs EW. 2013. Regulation of tumor necrosis factor-α-induced microvascular endothelial cell

hyperpermeability by recombinant B-cell lymphoma-extra large. J Surg Res. 184(1):628-37.

Schmidtke K, Hüll M. 2005. Cerebral small vessel disease: how does it progress? J Neurol Sci. 229-230:13-20.

Schneider J, Chromik AM, Uhl W, Mügge A, Bulut D. 2012. Apoptosis in esophagus and pancreas carcinoma cells induced by circulating microparticles is related to phosphatidyl serine and microparticle-associated caspases. Med Oncol. 29(2):962-9.

Schock SC, Edrissi H, Burger D, Cadonic R, Hakim A, Thompson C. 2014. Microparticles generated during chronic cerebral ischemia deliver proapoptotic signals to cultured endothelial cells. Biochem Biophys Res Commun. 450(1):912-7.

Schreiber S, Bueche CZ, Garz C, Kropf S, Angenstein F, Goldschmidt J, Neumann J, Heinze HJ, Goertler M, Reymann KG, Braun H. 2012. The pathologic cascade of cerebrovascular lesions in SHRSP: is erythrocyte accumulation an early phase? J Cereb Blood Flow Metab. 32(2):278-90.

Schubert W, Frank PG, Razani B, Park DS, Chow CW, Lisanti MP. 2001. Caveolae-deficient endothelial cells show defects in the uptake and transport of albumin *in vivo*. J Biol Chem. 276(52):48619-22.

Seo JH, Park HP, Jeon YT, Lim YJ, Nam K, Hwang JW. 2013. Combined treatment with celecoxib and sevoflurane after global cerebral ischemia has no additive neuroprotective effects in rats. Br J Anaesth. 110(6):988-95.

Shen Q, Wu MH, Yuan SY. 2009. Endothelial contractile cytoskeleton and microvascular permeability. Cell Health Cytoskelet. 2009 (1):43-50.

Shibuya M, Hirai S, Seto M, Satoh S, Ohtomo E; Fasudil Ischemic Stroke Study Group. 2005. Effects of fasudil in acute ischemic stroke: results of a prospective placebo-controlled double-blind trial. J Neurol Sci. 238(1-2):31-9.

Shin JS, Hyun SY, Kim DH, Lee S, Jung JW, Choi JW, Ko KH, Kim JM, Ryu JH. 2008. Chronic hypoperfusion increases claudin-3 immunoreactivity in rat brain. Neurosci Lett. 445(2):144-8.

Shin HK, Kim YK, Kim KY, Lee JH, Hong KW. 2004. Remnant lipoprotein particles induce apoptosis in endothelial cells by NAD(P)H oxidase-mediated production of superoxide and cytokines via lectin-like oxidized low-density lipoprotein receptor-1 activation: prevention by cilostazol. Circulation. 109(8):1022-8.

Shoamanesh A, Preis SR, Beiser AS, Vasan RS, Benjamin EJ, Kase CS, Wolf PA, DeCarli C, Romero JR, Seshadri S. 2015. Inflammatory biomarkers, cerebral microbleeds, and small vessel disease: Framingham Heart Study. Neurology. 84(8):825-32.

Silbert LC, Nelson C, Howieson DB, Moore MM, Kaye JA. 2008. Impact of white matter hyperintensity volume progression on rate of cognitive and motor decline. Neurology. 71(2):108-13.

Silwedel C, Förster C. 2006. Differential susceptibility of cerebral and cerebellar murine brain microvascular endothelial cells to loss of barrier properties in response to inflammatory stimuli. J Neuroimmunol. 179:37-45.

Simak J, Gelderman MP, Yu H, Wright V, Baird AE. 2006. Circulating endothelial microparticles in acute ischemic stroke: a link to severity, lesion volume and outcome. J Thromb Haemost. 4(6):1296-302.

Simoncini S, Njock MS, Robert S, Camoin-Jau L, Sampol J, Harlé JR, Nguyen C, Dignat-George F, Anfosso F. 2009. TRAIL/Apo2L mediates the release of procoagulant endothelial microparticles induced by thrombin *in vitro*: a potential mechanism linking inflammation and coagulation. Circ Res. 104(8):943-51.

Simpson JE, Wharton SB, Cooper J, Gelsthorpe C, Baxter L, Forster G, Shaw PJ, Savva G, Matthews FE, Brayne C, Ince PG. 2010. Alterations of the blood-brain barrier in cerebral white matter lesions in the ageing brain. Neurosci Lett. 486(3):246-51.

Smallwood A, Oulhaj A, Joachim C, Christie S, Sloan C, Smith AD, Esiri M. 2012. Cerebral subcortical small vessel disease and its relation to cognition in elderly subjects: a pathological study in the Oxford Project to Investigate Memory and Ageing (OPTIMA) cohort. Neuropathol Appl Neurobiol. 38(4):337-43.

Sood R, Yang Y, Taheri S, Candelario-Jalil E, Estrada EY, Walker EJ, Thompson J, Rosenberg GA. 2009. Increased apparent diffusion coefficients on MRI linked with matrix metalloproteinases and edema in white matter after bilateral carotid artery occlusion in rats. J Cereb Blood Flow Metab. 29(2):308-16.

Stamatovic SM, Dimitrijevic OB, Keep RF, Andjelkovic AV. 2006. Protein kinase C alpha-RhoA cross-talk in CCL2-induced alterations in brain endothelial permeability. J Biol Chem. 281(13):8379-88.

Stamatovic SM, Shakui P, Keep RF, Moore BB, Kunkel SL, Van Rooijen N, Andjelkovic AV. 2005. Monocyte chemoattractant protein-1 regulation of blood-brain barrier permeability. J Cereb Blood Flow Metab. 25(5):593-606.

Stevens WD, Fortin T, Pappas BA. 2002. Retinal and optic nerve degeneration after chronic carotid ligation: time course and role of light exposure. Stroke. 33(4):1107-12.

Street CA, Bryan BA. 2011. Rho kinase proteins--pleiotropic modulators of cell survival and apoptosis. Anticancer Res. 31(11):3645-57.

Sugiura Y, Morikawa T, Takenouchi T, Suematsu M, Kajimura M. 2014. Cilostazol strengthens the endothelial barrier of postcapillary venules from the rat mesentery in situ. Phlebology. 29(9):594-9.

Suri A, Forbes WP, Bramer SL. 1998. Pharmacokinetics of multiple-dose oral cilostazol in middle-age and elderly men and women. J Clin Pharmacol. 38(2):144-50.

Takagi T, Mishiro K, Shimazawa M, Yoshimura S, Iwama T, Hara H. 2014. The phosphodiesterase III inhibitor cilostazol ameliorates ethanolinduced endothelial dysfunction. Curr Neurovasc Res. 11(4):302-11.

Tanaka K, Nogawa S, Ito D, Suzuki S, Dembo T, Kosakai A, Fukuuchi Y. 2001. Phosphorylation of cyclic adenosine monophosphate response element binding protein in oligodendrocytes in the corpus callosum after focal cerebral ischemia in the rat. J Cereb Blood Flow Metab. 21(10):1177-88.

Taupin V, Renno T, Bourbonnière L, Peterson AC, Rodriguez M, Owens T. 1997. Increased severity of experimental autoimmune encephalomyelitis, chronic macrophage/microglial reactivity, and demyelination in transgenic mice producing tumor necrosis factor-alpha in the central nervous system. Eur J Immunol. 27(4):905-13.

Tian XS, Guo XJ, Ruan Z, Lei Y, Chen YT, Zhang HY. 2014. Long-term vision and non-vision dominant behavioral deficits in the 2-VO rats are accompanied by time and regional glial activation in the white matter. PLoS One. 9(6):e101120.

Torii H, Kubota H, Ishihara H, Suzuki M. 2007. Cilostazol inhibits the redistribution of the actin cytoskeleton and junctional proteins on the blood-brain barrier under hypoxia/reoxygenation. Pharmacol Res. 55(2):104-10.

Totsukawa G, Yamakita Y, Yamashiro S, Hartshorne DJ, Sasaki Y, Matsumura F. 2000. Distinct roles of ROCK (Rho-kinase) and MLCK in spatial regulation of MLC phosphorylation for assembly of stress fibers and focal adhesions in 3T3 fibroblasts. J Cell Biol. 150(4):797-806.

Tushuizen ME, Diamant M, Sturk A, Nieuwland R. 2011. Cell-derived microparticles in the pathogenesis of cardiovascular disease: friend or foe? Arterioscler Thromb Vasc Biol. 31(1):4-9.

Uchiyama S, Shinohara Y, Katayama Y, Yamaguchi T, Handa S, Matsuoka K, Ohashi Y, Tanahashi N, Yamamoto H, Genka C, Kitagawa Y, Kusuoka H, Nishimaru K, Tsushima M, Koretsune Y, Sawada T, Hamada C. 2014. Benefit of cilostazol in patients with high risk of bleeding: subanalysis of cilostazol stroke prevention study 2. Cerebrovasc Dis. 37(4):296-303.

Ueno M, Tomimoto H, Akiguchi I, Wakita H, Sakamoto H. 2002. Blood-brain barrier disruption in white matter lesions in a rat model of chronic cerebral hypoperfusion. J Cereb Blood Flow Metab. 22(1):97-104.

Ueno Y, Zhang N, Miyamoto N, Tanaka R, Hattori N, Urabe T. 2009. Edaravone attenuates white matter lesions through endothelial protection in a rat chronic hypoperfusion model. Neuroscience. 162(2):317-27.

van Dijk EJ, Prins ND, Vermeer SE, Vrooman HA, Hofman A, Koudstaal PJ, Breteler MM. 2005. C-reactive protein and cerebral small-vessel disease: the Rotterdam Scan Study. Circulation. 112(6):900-5.

van Nieuw Amerongen GP, Beckers CM, Achekar ID, Zeeman S, Musters RJ, van Hinsbergh VW. 2007. Involvement of Rho kinase in endothelial barrier maintenance. Arterioscler Thromb Vasc Biol. 27(11):2332-9.

Vermeer SE, Longstreth WT Jr, Koudstaal PJ. 2007. Silent brain infarcts: a systematic review. Lancet Neurol. 6(7):611-9.

Villeda SA, Luo J, Mosher KI, Zou B, Britschgi M, Bieri G, Stan TM, Fainberg N, Ding Z, Eggel A, Lucin KM, Czirr E, Park JS, Couillard-Després S, Aigner L, Li G, Peskind ER, Kaye JA, Quinn JF, Galasko DR, Xie XS, Rando TA, Wyss-Coray T. 2011. The ageing systemic milieu negatively regulates neurogenesis and cognitive function. Nature. 477(7362):90-4.

Wakita H, Tomimoto H, Akiguchi I, Kimura J. 1994. Glial activation and white matter changes in the rat brain induced by chronic cerebral hypoperfusion: an immunohistochemical study. Acta Neuropathol. 87(5):484-92.

Wakita H, Tomimoto H, Akiguchi I, Kimura J. 1995. Protective effect of cyclosporin A on white matter changes in the rat brain after chronic cerebral hypoperfusion. Stroke. 26(8):1415-22.

Wakita H, Tomimoto H, Akiguchi I, Matsuo A, Lin JX, Ihara M, McGeer PL. 2002. Axonal damage and demyelination in the white matter after chronic cerebral hypoperfusion in the rat. Brain Res. 924(1):63-70.

Wang CX, Shuaib A. 2002. Involvement of inflammatory cytokines in central nervous system injury. Prog Neurobiol. 67(2):161-72.

Wang J, Zhang HY, Tang XC. 2010. Huperzine a improves chronic inflammation and cognitive decline in rats with cerebral hypoperfusion. J Neurosci Res. 88(4):807-15.

Watanabe T, Zhang N, Liu M, Tanaka R, Mizuno Y, Urabe T. 2006. Cilostazol protects against brain white matter damage and cognitive impairment in a rat model of chronic cerebral hypoperfusion. Stroke. 37(6):1539-45.

Wardlaw JM. 2005. What causes lacunar stroke? J Neurol Neurosurg Psychiatry. 76:617– 619.

Wardlaw JM. 2010. Blood-brain barrier and cerebral small vessel disease. J Neurol Sci. 299(1-2):66-71.

Wardlaw JM, Doubal F, Armitage P, Chappell F, Carpenter T, Muñoz Maniega S, Farrall A, Sudlow C, Dennis M, Dhillon B. 2009. Lacunar stroke is associated with diffuse blood-brain barrier dysfunction. Ann Neurol. 65(2):194-202.

Wardlaw JM, Doubal FN, Valdes-Hernandez M, Wang X, Chappell FM, Shuler K, Armitage PA, Carpenter TC, Dennis MS. 2013. Blood-brain barrier permeability and long-term clinical and imaging outcomes in cerebral small vessel disease. Stroke. 44(2):525-7.

Wardlaw JM, Farrall A, Armitage PA, Carpenter T, Chappell F, Doubal F, Chowdhury D, Cvoro V, Dennis MS. 2008. Changes in background blood-brain barrier integrity between lacunar and cortical ischemic stroke subtypes. Stroke. 39(4):1327-32.

Wardlaw JM, Sandercock PA, Dennis MS, Starr J. 2003. Is breakdown of the blood-brain barrier responsible for lacunar stroke, leukoaraiosis, and dementia? Stroke. 34(3):806-12.

Wardlaw JM, Smith C, Dichgans M. 2013. Mechanisms of sporadic cerebral small vessel disease: insights from neuroimaging. Lancet Neurol. 12(5):483-97.

Washida K, Ihara M, Nishio K, Fujita Y, Maki T, Yamada M, Takahashi J, Wu X, Kihara T, Ito H, Tomimoto H, Takahashi R. 2010. Nonhypotensive dose of telmisartan attenuates cognitive impairment partially due to peroxisome proliferator-activated receptor-gamma activation in mice with chronic cerebral hypoperfusion. Stroke. 41(8):1798-806.

Wassmer SC, Combes V, Candal FJ, Juhan-Vague I, Grau GE. 2006. Platelets potentiate brain endothelial alterations induced by Plasmodium falciparum. Infect Immun. 74(1):645-53.

Wheeler RD, Boutin H, Touzani O, Luheshi GN, Takeda K & Rothwell NJ. 2003. No role for interleukin-18 in acute murine stroke-induced brain injury. J Cereb Blood Flow Metab. 23, 531–535.

Wiggins-Dohlvik K, Merriman M, Shaji CA, Alluri H, Grimsley M, Davis ML, Smith RW, Tharakan B. 2014. Tumor necrosis factor-α disruption of brain endothelial cell barrier is mediated through matrix metalloproteinase-9. Am J Surg. 208(6):954-60.

Witt KA, Mark KS, Hom S, Davis TP. 2003. Effects of hypoxia-reoxygenation on rat blood-brain barrier permeability and tight junctional protein expression. Am J Physiol Heart Circ Physiol. 285(6):H2820-31.

Wright CB, Sacco RL, Rundek TR, Delman JB, Rabbani LE, Elkind MS. 2006. Interleukin-6 is associated with cognitive function: the Northern Manhattan Study. J Stroke Cerebrovasc Dis. 15(1):34-8.

Wu WB, Huang TF. 2003. Activation of MMP-2, cleavage of matrix proteins, and adherens junctions during a snake venom metalloproteinase-induced endothelial cell apoptosis. Exp Cell Res. 288(1):143-57.

Xue S, Cai X, Li W, Zhang Z, Dong W, Hui G. 2012. Elevated plasma endothelial microparticles in Alzheimer's disease. Dement Geriatr Cogn Disord. 34(3-4):174-80.

Yamada H, Yoneda M, Inaguma S, Watanabe D, Banno S, Yoshikawa K, Mizutani K, Iwaki M, Zako M. 2013. Infliximab counteracts tumor necrosis factor-α-enhanced induction of matrix metalloproteinases that degrade claudin and occludin in non-pigmented ciliary epithelium. Biochem Pharmacol. 85(12):1770-82.

Yamamoto H, Schmidt-Kastner R, Hamasaki DI, Yamamoto H, Parel JM. 2006. Complex neurodegeneration in retina following moderate ischemia induced by bilateral common carotid artery occlusion in Wistar rats. Exp Eye Res. 82(5):767-79.

Yang Y, Estrada EY, Thompson JF, Liu W, Rosenberg GA. 2007. Matrix metalloproteinase-mediated disruption of tight junction proteins in cerebral vessels

is reversed by synthetic matrix metalloproteinase inhibitor in focal ischemia in rat. J Cereb Blood Flow Metab. 27:697–709.

Yang Y, Rosenberg GA. 2011. Blood-brain barrier breakdown in acute and chronic cerebrovascular disease. Stroke. 42(11):3323-8.

Yong VW, Power C, Forsyth P, Edwards DR. 2001. Metalloproteinases in biology and pathology of the nervous system. Nat Rev Neurosci. 2:502-11.

Yoshizaki K, Adachi K, Kataoka S, Watanabe A, Tabira T, Takahashi K, Wakita H. 2008. Chronic cerebral hypoperfusion induced by right unilateral common carotid artery occlusion causes delayed white matter lesions and cognitive impairment in adult mice. Exp Neurol. 210(2):585-91.

Yu H, Wang P, An P, Yixue X. 2012. Recombinant human angiopoietin-1 ameliorates the expressions of ZO-1, occludin, VE-cadherin, and PKCα signaling after focal cerebral ischemia/reperfusion in rats. J Mol Neurosci. 46(1):236-47.

Yuan SY. 2002. Protein kinase signaling in the modulation of microvascular permeability. Vascul Pharmacol. 39(4-5):213-23.

Yuen CM, Chiu CA, Chang LT, Liou CW, Lu CH, Youssef AA & Yip HK. 2007. Level and value of interleukin-18 after acute ischemic stroke. Circ J. 71, 1691-1.

Zhang Q, Zhang JJ, Han ZM. 2015. Efficacy of Rho kinase inhibitor on cognitive impairment induced by chronic cerebral hypoperfusion in rats. Int J Clin Exp Med. 8(2):2435-40.

Zaremba J, Losy J. 2004. Cytokines in clinical and experimental ischemic stroke. Neurol Neurochir Pol. 38(1 Suppl 1):S57-62.

Zhu Y, Saito K, Murakami Y, Asano M, Iwakura Y, Seishima M. 2006. Early increase in mRNA levels of pro-inflammatory cytokines and their interactions in the mouse hippocampus after transient global ischemia. Neurosci Lett. 393(2-3):122-6.

# Appendix:

# Reprint of published figures

The following figures are reprinted from the following published article by permission: Schock SC, Edrissi H, Burger D, Cadonic R, Hakim A, Thompson C. 2014. Microparticles generated during chronic cerebral ischemia deliver proapoptotic signals to cultured endothelial cells. Biochem Biophys Res Commun. 450(1):912-7.

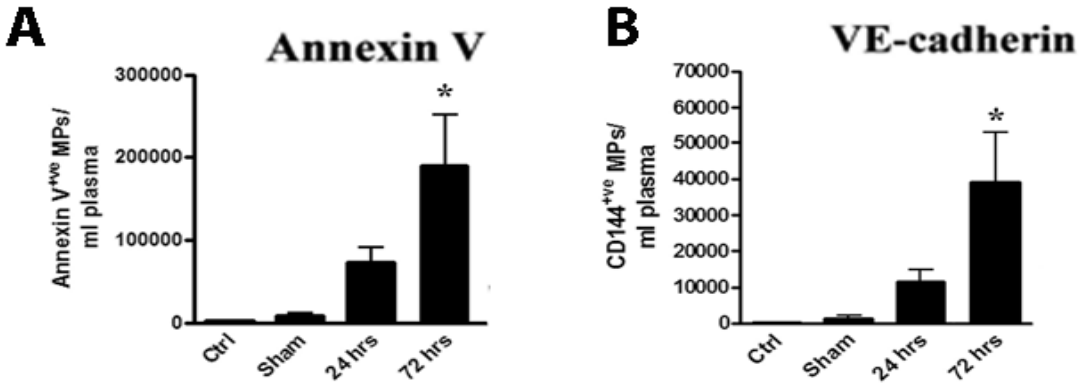


**Figure 1A**

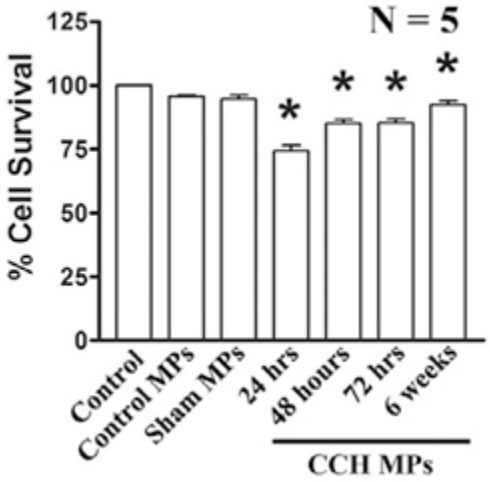


**Figure 1B**

**Figure 1. (A)** Increased numbers of circulating MPs at various time points in rats subjected to 2VO surgery as determined by flow cytometry. The numbers of annexin V +ve (representing total number of MPs) and VE-cadherin +ve (CD144) MPs (representing endothelial of MPs) are increased in the plasma. **(B)** Toxicity of circulating MPs (their potency to induce cell death in cultured RBMVECs) is highest 24h following BCCAO and decreases thereafter.

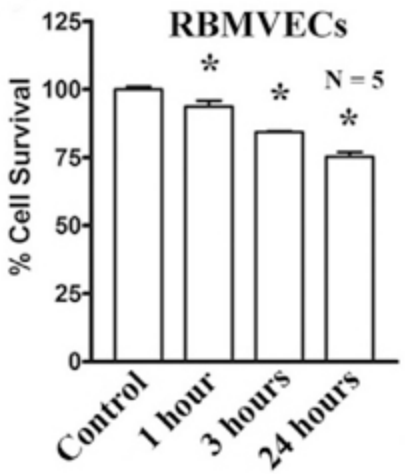


**Figure 2A**

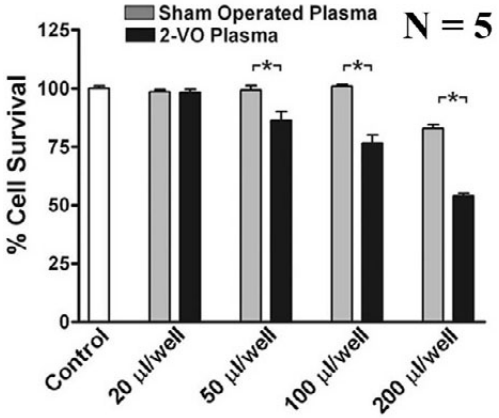


**Figure 2B**

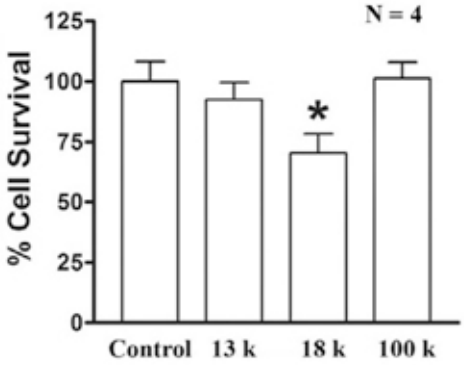


**Figure 2C**

**Figure 2. (A)** Exposure of cultured endothelial cells to MPs causes cell death in a time-dependent manner. **(B)** Exposure of cultured endothelial cells to MPs causes cell death in a concentration dependent manner. **(C)** Pellets containing MPs (centrifugation of plasma at 18000g) induced a significant amount of cell death compared to pellets containing apoptotic bodies (13000g) or exosomes (100000g), when they applied to cultured NRK (normal rat kidney) cells.

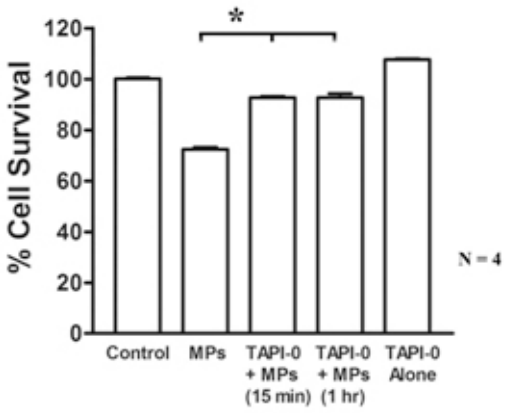


**Figure 3A**

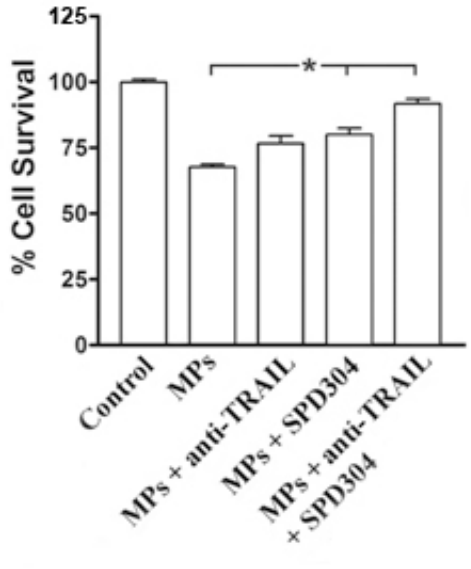


**Figure 3B**

**Figure 3. (A)** Pretreatment of MPs with a TACE inhibitor improved cell survival (n = 4). **(B)** Pretreatment of cultured NRKCs with SPD-304 or a neutralizing antibody against TRAIL or both improved cell survival (n = 5).